



TITAN-24 MT SURVEY
GEOPHYSICAL REPORT
EAST BULL LAKE PROJECT
(ONTARIO, CANADA)
ON BEHALF OF
MUSTANG MINERALS CORP.
(ONTARIO, CANADA)

EXECUTIVE SUMMARY

INTRODUCTION

A Titan-24 MT survey was undertaken on behalf of Mustang Minerals Corp. from February 23rd to March 1st, 2012, over the East Bull Lake Project,

The survey grid is located approximately 27 km North of Massey, Ontario, and includes acquisition of magnetotelluric data for frequencies ranging from 10kHz to 0.01Hz along six spreads of various orientation, with dipole length of 150m. Three MT profiles were defined from these six spreads, two oriented +27°, and one +129°, for a total coverage of 8850m.

SURVEY OBJECTIVES

The exploration objective of the Titan-24 MT survey at East Bull Lake Project was to detect zones and define structures related to the emplacement of Nickel mineralisation. The Titan-24 survey should provide the following benefits:

- Detecting and delineating zones and structures related to the emplacement of sulphide mineralisation from surface to depths of up to 1500m and greater with MT resistivity.
- Mapping the resistivity features related to mineralisation, alteration, faults and lithologies.

RESULTS

The MT data were inverted using 2D inversion algorithms and produced section showing resistivity distribution of subsurface.

The area defined by the conductive zones **L1_B** and **L1_D** on profile L100 has been already identified by Eaton et al (2011) as potential zone for Cu-Ni-PGE mineralisation. That area represents the principal zone of interest for follow up of this Titan-24 MT survey. The more conductive zone **L3_B** observed on profile L300 represents a second zone to consider for follow up. The orientation of profile L200 along the geological structures and the ZTEM anomaly limit the capability to resolve potential zone of interest.

Quantec recommend the full integration of all the Titan-24 MT results with existing VTEM and ZTEM results, as with other geophysical data (i.e., magnetic), and known geology information, to enhance the interpretation of the current results. Quantec recommend extension of the Titan-24 MT profiles L100 to the north to better characterize the north contact of the *East Bull Lake Intrusive*, and additional Titan-24 DC/IP/MT profiles across the *Marginal Zone* to better characterize the potential of that area for Cu-Ni-PGE mineralisation.

TABLE OF CONTENTS

List of Figures	4
List of Tables.....	4
1 Introduction	5
1.1 Survey Objectives	5
1.2 General Survey Information	5
1.3 Project Location Information	6
2 Previous Work & Geology	8
2.1 Geology of the area	8
2.2 Previous Geophysical work in the area	10
3 Results and Interpretation	16
3.1 Overview of Inversion Procedure.....	16
3.1.1 Audio-Magnetotelluric Inversions	16
3.2 Discussion of Results	18
3.2.1 Line L100.....	19
3.2.2 Line L300.....	21
3.2.3 Line L200.....	23
4 Conclusions and Recommendations	25
5 Statement of Qualifications	26
5.1 Benoît Tournerie	26
5.2 Mojtaba Daneshvar Nilu.....	27
6 Digital Archive	28
A Production Summary	29
B Survey Logistics	31
C MT Soundings Curves of Final Processed Data	37
D MT Pseudo-Sections of Final Processed Data	57
E MT (TE/TM) Pseudo-Sections along MT 2D profiles	63
F Parallel Sensor Test	67
G MT Remote Test – Unreferenced Data	89
H Instruments Specifications.....	93
I Geosoft Sections	99
J Introduction to the Magnetotelluric Method	103
K References.....	109

LIST OF FIGURES

Figure 1-1: General Project Location. 6

Figure 1-2: Surveyed Location Map with Claim map. 7

Figure 2-1: Generalized bedrock geology of the East Bull Lake intrusion (Dyer, 2008). 9

Figure 2-2: Titan-24 survey location with Geology map from Eaton et al (2011). 10

Figure 2-3: Simplified Geology over the East Bull Lake area with VTEM anomalies. 11

Figure 2-4: Plan map of ZTEM results over the East Bull Lake survey area. 11

Figure 2-5: Section of ZTEM results along profile L1020. 12

Figure 2-6: Section of ZTEM results along profile L1380. 12

Figure 2-7: Section of ZTEM results along profile L1270. 13

Figure 2-8: Section of ZTEM results along profile L2080. 13

Figure 2-9: Location of the Titan-24 MT2D profiles with ZTEM profiles. 14

Figure 2-10: Location of the Titan-24 MT2D profiles with ZTEM-merge anomaly map. 15

Figure 3-1: MT 2D resistivity colour bar. 18

Figure 3-2: MT 2D results along line L100 (spreads 1-2-3). 19

Figure 3-3: MT 2D results along line L300 (spread 6). 21

Figure 3-4: MT 2D results along line L200 (spreads 4-5). 23

LIST OF TABLES

Table 2-1: Approximate correspondence between Titan-24 and ZTEM station numbering. 14

1 INTRODUCTION

This report presents the logistics and the results of the analysis of the Titan-24 MT data acquired from 2012/02/23 to 2012/03/01 over the East Bull Lake Project, on behalf of Mustang Minerals Corp.

The first part of this report presents the inversion results, their geophysical interpretation, and some recommendations for future follow-up on the property.

The second part of the report presents the logistics of the survey, including the survey parameters and methodology, and the survey results (data) in digital documents.

1.1 SURVEY OBJECTIVES

The Titan 24 **D**istributed **A**cquisition **S**ystem (**DAS**; Sheard, 1998) employs a combination of multiplicity of sensors, 24-bit digital sampling, and advanced signal processing. It provides three in-dependent datasets capable of measuring subsurface resistivity's (structure, alteration & lithology) and chargeability (mineralization) to depth.

The exploration objective of the Titan 24 MT survey at East Bull Lake Project was to detect zones and define structures related to the emplacement of nickel mineralisation. Titan 24 should provide the following benefits:

- Detecting and delineating zones and structures related to the emplacement of sulphide mineralisation from surface to depths of up to 1500m and greater with MT resistivity.
- Mapping the resistivity features related to mineralisation, alteration, faults and lithologies.

The MT resistivity provides additional resistivity information from surface to depths beyond 1km. The MT resistivity is useful for mapping geological contacts with resistivity contrasts and deep conductors that may potentially represent alteration or mineralization.

1.2 GENERAL SURVEY INFORMATION

Quantec Project No.:	CA00927T
Client:	Mustang Minerals Corp.
Client Address	65 Queen Street West, Suite 530, P.O. 12, Toronto, Ontario M5H 2M5 Canada
Client representative:	David B. Stevenson Phone: (416) 955 4773 Email: dbs@mustangminerals.com
Project Name:	East Bull Lake Project
Survey Type:	Titan-24 MT
Project Survey Period:	2012/02/23 to 2012/03/01

1.3 PROJECT LOCATION INFORMATION

General Location:	27 km North of Massey, Ontario
Province	Ontario
Nearest Settlement:	Massey
Datum & Projection:	WGS84/17T
Latitude & Longitude:	Approx. 082°11'00"N, 046°26'00"W
UTM position:	Approx. 409000 m E, 5143000 m N
List of Claims Surveyed¹:	1226700 ; 1227909 ; 1227911 ; 1134489 ; 1134490 ; 1134478 ; 1229206 ; 1229207 ; 1229204

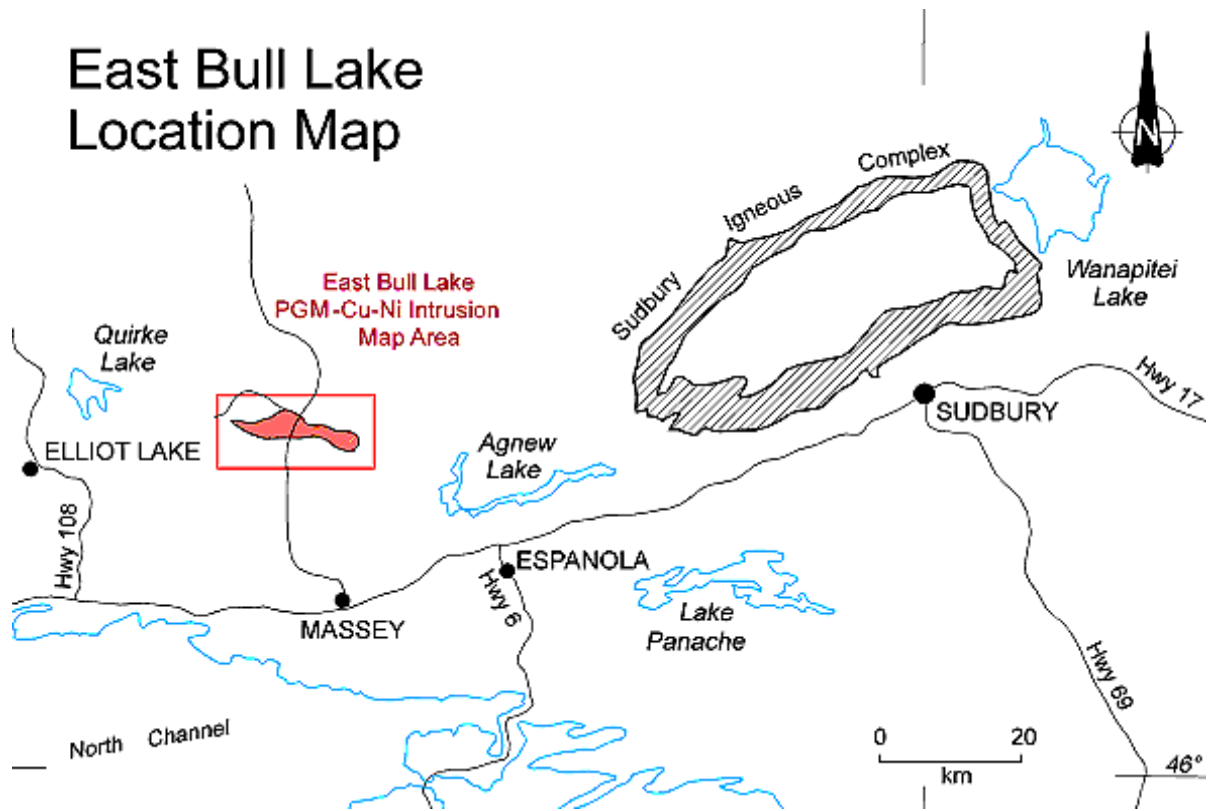


Figure 1-1: General Project Location².

¹ Geology Ontario – CLAIMaps (III) web site:
<http://www.geologyontario.mndmf.gov.on.ca/website/claimapsiii/viewer.asp>

² Image downloaded from Mustang Mineral web site.

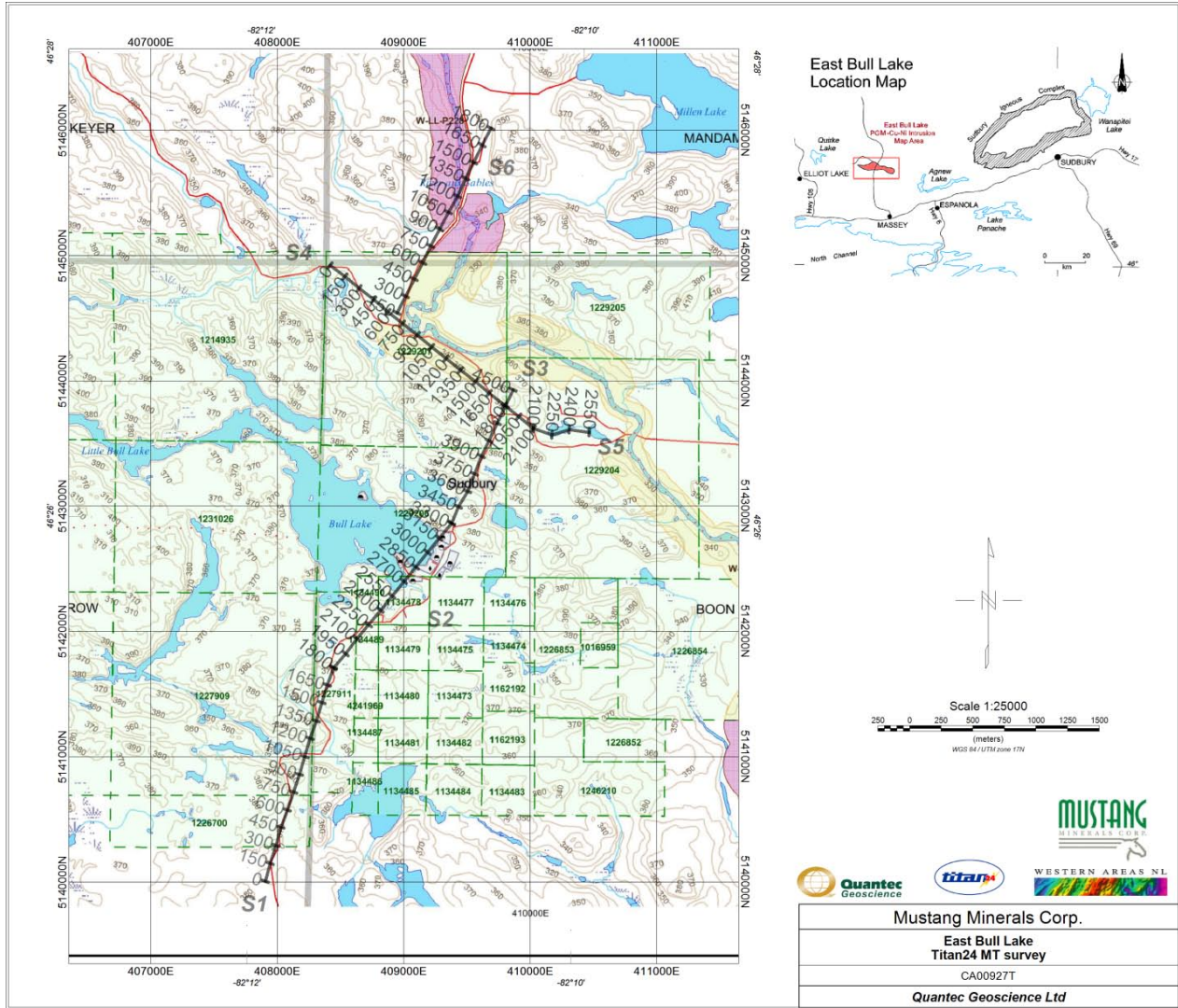


Figure 1-2: Surveyed Location Map with Claim map³

³ Claim map download from Geology Ontario – CLAIMaps (III) web site:
<http://www.geologyontario.mndmf.gov.on.ca/website/claimapsiii/viewer.asp>

2 PREVIOUS WORK & GEOLOGY

2.1 GEOLOGY OF THE AREA

A review of the geology over the survey area has been recently presented in documents published by Ontario Geological Survey:

Dyer, R.D. 2008. East Bull Lake Intrusion Copper-Nickel-Platinum Group Element Dispersion Case Study, Northeastern Ontario; in Summary of Field Work and Other Activities 2008, Ontario Geological Survey, Open File Report 6226, p.27-1 to 27-7.

Easton, R.M., Josey, S.D., Murphy, E.I. and James, R.S. 2011. Geological compilation, East Bull Lake and Agnew intrusions; Ontario Geological Survey, Preliminary Map P.3596, scale 1:50 000.

Geological information presented in that section are from these documents.

“The East Bull Lake intrusive suite rocks are of Paleoproterozoic age and consist of a number of layered plutons that occur near the Archean Superior Province–Proterozoic Southern Province and Proterozoic Southern Province–Grenville Province boundary areas, in the Sudbury region of Ontario. In general, these plutons are gabbroic in composition (gabbroic to gabbroic anorthosite) and the 3 largest are known as the East Bull Lake, Agnew and River Valley intrusions”.

“The main focus for platinum group metals (PGM) exploration within East Bull Lake intrusive suite rocks is what is known as “contact-type” mineralization, which is present throughout the Lower and underlying Marginal Zone, but is best developed within inclusion-bearing gabbroic, within a few tens of metres of the sidewall or footwall contacts at the margins of the plutons (Easton, Jobin-Bevans and James 2004). This mineralization occurs as PGE-rich disseminated sulphides, typically with an average sulphide mineral content of 1 to 2%. The sulphide minerals usually consist of approximately equal amounts of coarse chalcopyrite and pyrrhotite, and subordinate, finer grained pentlandite (Easton, Jobin-Bevans and James 2004). Secondary exploration focus are hydrothermally altered breccia zones within deformed rocks at or near the margins of the plutons (i.e., Parisien Lake deformation zone). Such hydrothermally enriched zones typically contain up to 10% sulphide minerals (chalcopyrite-pyrrhotite-pentlandite), up to 10 g/t combined Pt+Pd and are generally enclosed by broader lower grade mineralization with Pt+Pd concentrations in the background range of 20 to 50 ppb (Easton, Jobin-Bevans and James 2004).”

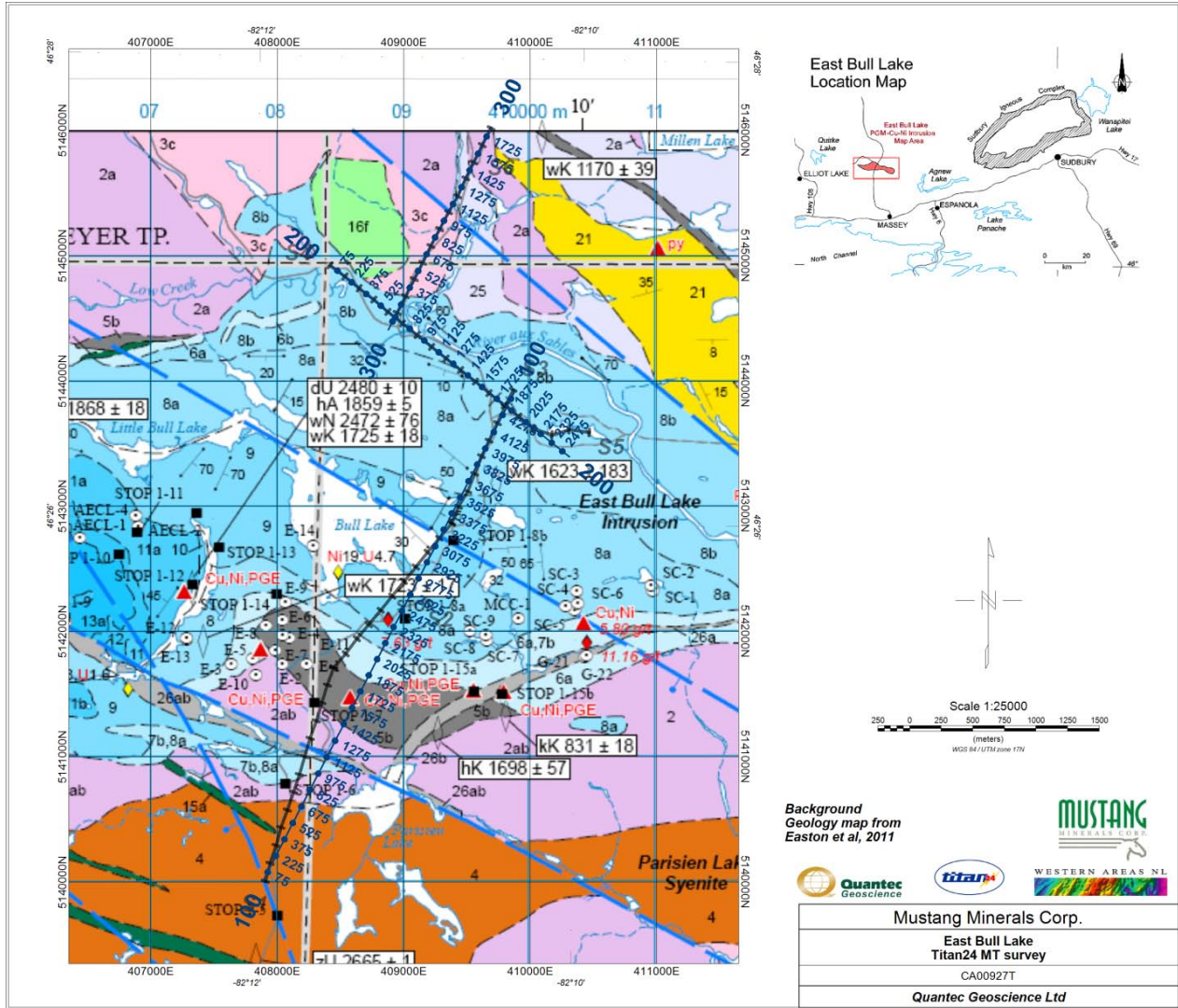


Figure 2-2: Titan-24 survey location with Geology map from Eaton et al (2011).

2.2 PREVIOUS GEOPHYSICAL WORK IN THE AREA

A VTEM and a ZTEM surveys⁴ have been completed over the survey area. Summary of the VTEM anomalies are presented with a simplified geology map on Figure 2-3. The ZTEM survey results are presented as a plan map (Figure 2-4), and along selected sections (Figure 2-5: L1020; Figure 2-7: 1270; Figure 2-6: L1380; Figure 2-8: L2080). Note that the approximate location of the ZTEM profiles with the Titan-24 profiles is provided on Figure 2-9. We note that none of the ZTEM profiles is co-linear with the Titan-24 profiles. So, in order to compare the results, Table 2-1 presents an approximate correspondence between the Titan-24 MT station and the ZTEM station.

⁴ Information provided by Mustang Minerals.

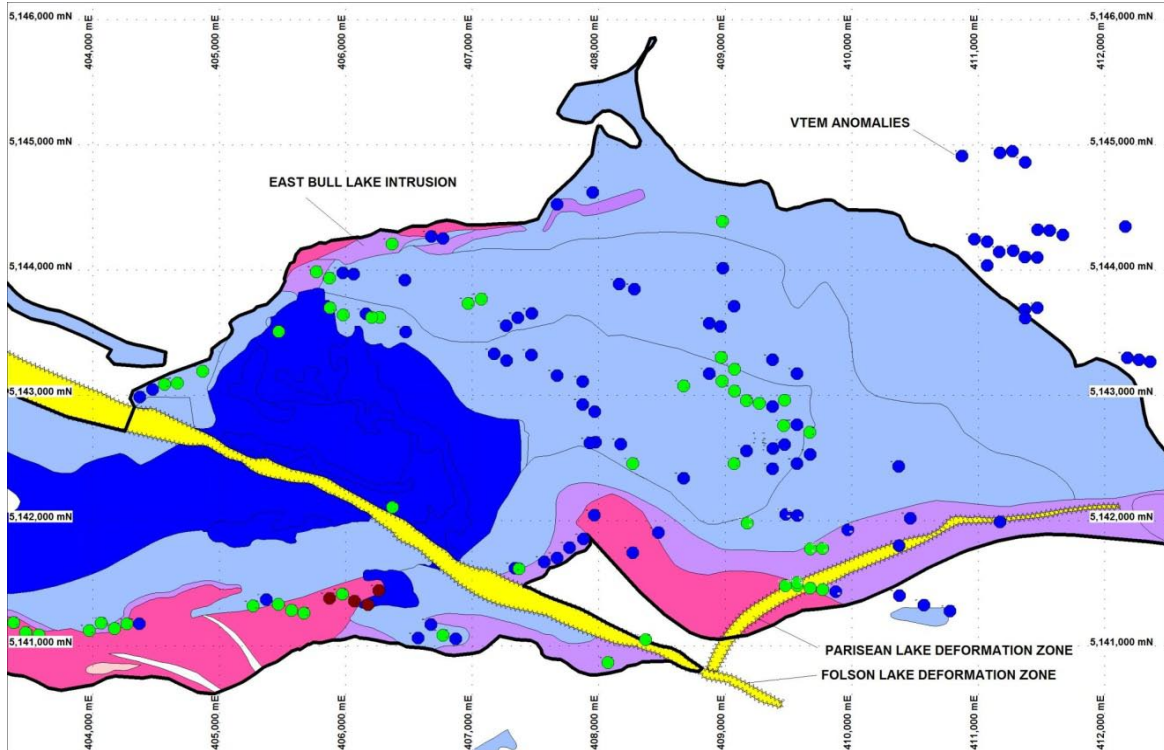


Figure 2-3: Simplified Geology over the East Bull Lake area with VTEM anomalies.

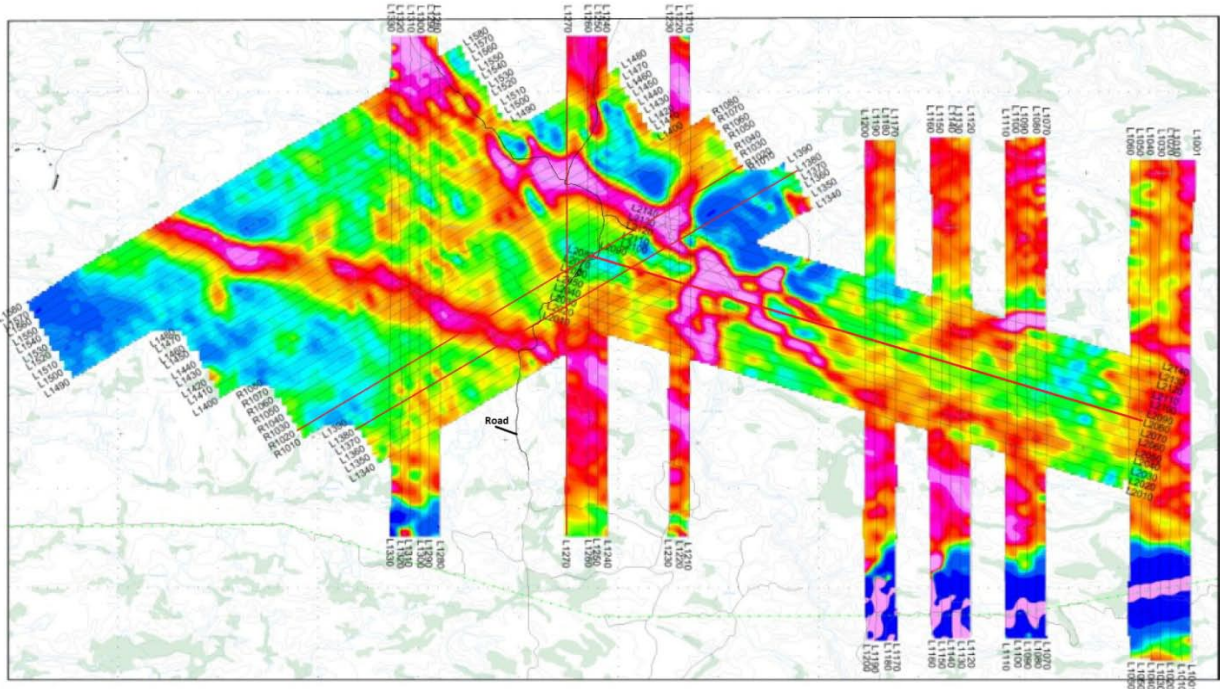
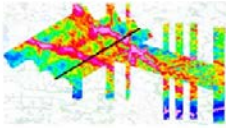


Figure 2-4: Plan map of ZTEM results over the East Bull Lake survey area.



2D INVERSION PARAMETERS
 Inversion code: Geotech AV2DTP0
 Model Mesh: 440 wide x 112 vertical
 Average cell width: 27.18 m
 2 cells between sites
 Input Data: In-Phase & Quadrature,
 Tzx In-line (only)
 Average sampling rate: 4.180 points,
 Total data points: 2304
 Frequency (Hz): 30 45 90 180 360 720
 Input error(%): 1.00 1.00 1.00 1.00 1.00
 Half-space resistivity: 5000 ohm-m,
 Output error: 0.977 RMS in 5 iterations

Flight Path of Line 1020 over IP 109Hz DT image



Mustang Minerals Corporation East Bull Lake Elliot Lake, Ontario
Geotech ZTEM System Resistivity-Depth Image Project 11154, Line 1020 Flight 2, 2010/09/28
Flown and processed by Geotech Ltd. 245 Industrial Parkway North Aurora, Ontario, Canada L4G 4C4 www.geotech.ca
2011/7/27

L1020, East Bull Lake, ZTEM 2D Inversion, 5000 ohm-m start

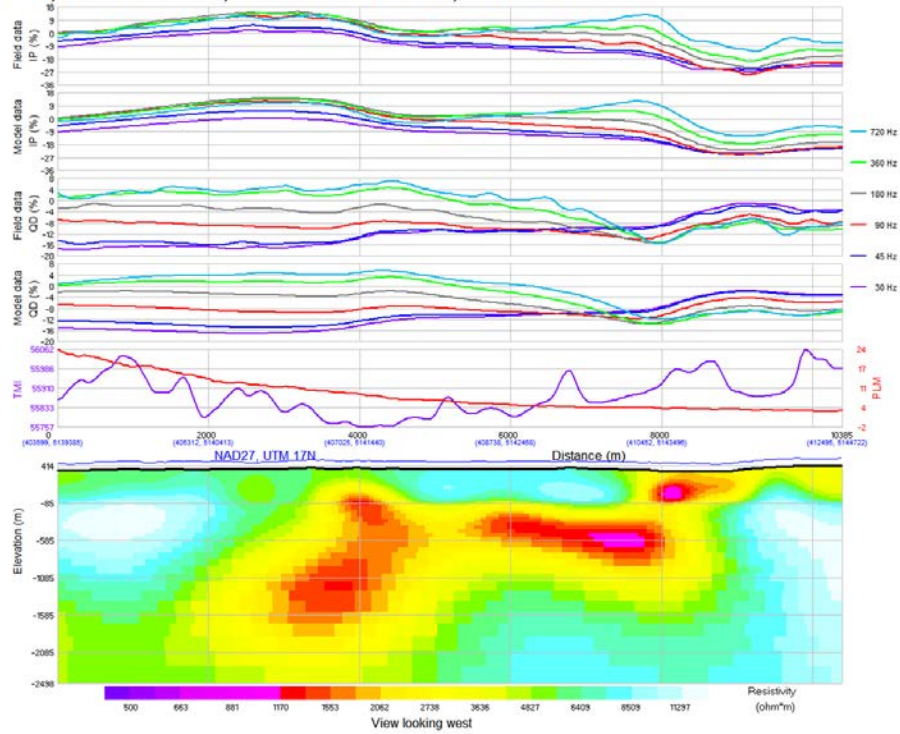
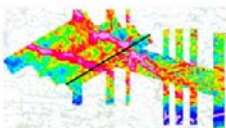


Figure 2-5: Section of ZTEM results along profile L1020.



2D INVERSION PARAMETERS
 Inversion code: Geotech AV2DTP0
 Model Mesh: 440 wide x 112 vertical
 Average cell width: 26.66 m
 2 cells between sites
 Input Data: In-Phase & Quadrature,
 Tzx In-line (only)
 Average sampling rate: 5.050 points,
 Total data points: 2304
 Frequency (Hz): 30 45 90 180 360 720
 Input error(%): 1.41 1.41 1.41 1.41 1.41 1.41
 Half-space resistivity: 5000 ohm-m,
 Output error: 0.994 RMS in 5 iterations

Flight Path of Line 1380 over IP 109Hz DT image



Mustang Minerals Corporation East Bull Lake Elliot Lake, Ontario
Geotech ZTEM System Resistivity-Depth Image Project 11154, Line 1380 Flight 2, 2011/05/13
Flown and processed by Geotech Ltd. 245 Industrial Parkway North Aurora, Ontario, Canada L4G 4C4 www.geotech.ca
2011/7/26

L1380, East Bull Lake, ZTEM 2D Inversion, 5000 ohm-m start

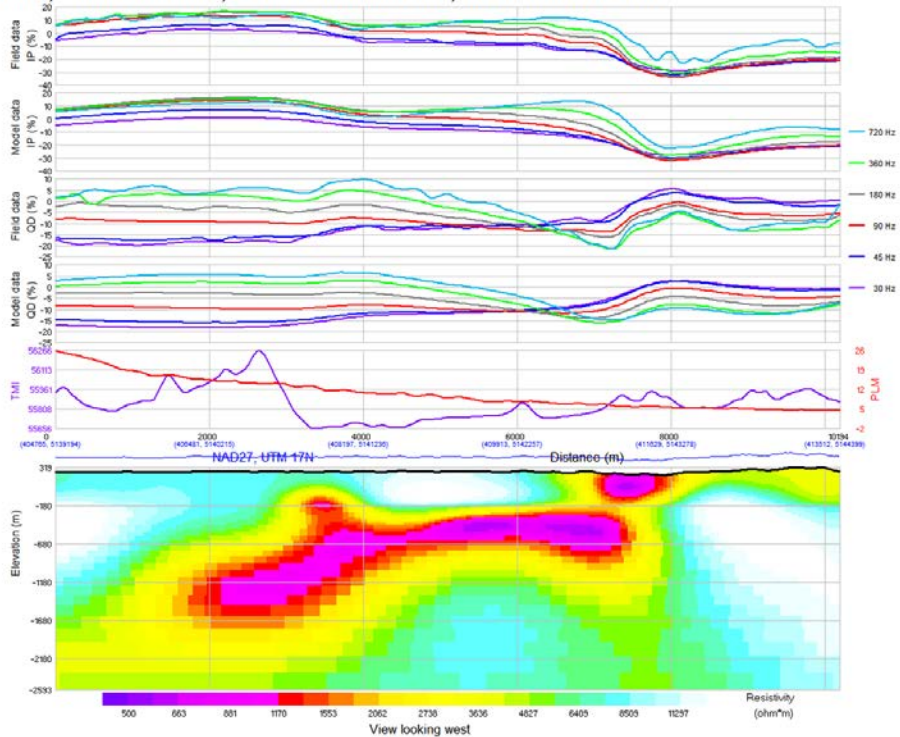
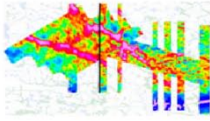


Figure 2-6: Section of ZTEM results along profile L1380.



2D INVERSION PARAMETERS
 Inversion code: Geotech AVZDPOPO
 Model Mesh: 440 wide x 112 vertical
 Average cell width: 26.40 m
 2 cells between sites
 Input Data: In-Phase & Quadrature, Tzz In-line (only)
 Average sampling rate: 5.080 points,
 Total data points: 2304
 Frequency (Hz): 30 45 90 180 360 720
 Input error(%): 3.10 3.10 3.10 3.10 3.10 3.10
 Half-space resistivity: 5000 ohm-m,
 Output error: 0.993 RMS in 5 iterations

Flight Path of Line 1270 over IP 109Hz DT image



Mustang Minerals Corporation East Bull Lake Elliot Lake, Ontario
Geotech ZTEM System Resistivity-Depth Image Project 11154, Line 1270 Flight 6, 2011/05/20
Flown and processed by Geotech Ltd. 245 Industrial Parkway North Aurora, Ontario, Canada L4G 4C4 www.geotech.ca 2011/7/26

L1270, East Bull Lake, ZTEM 2D Inversion, 5000 ohm-m start

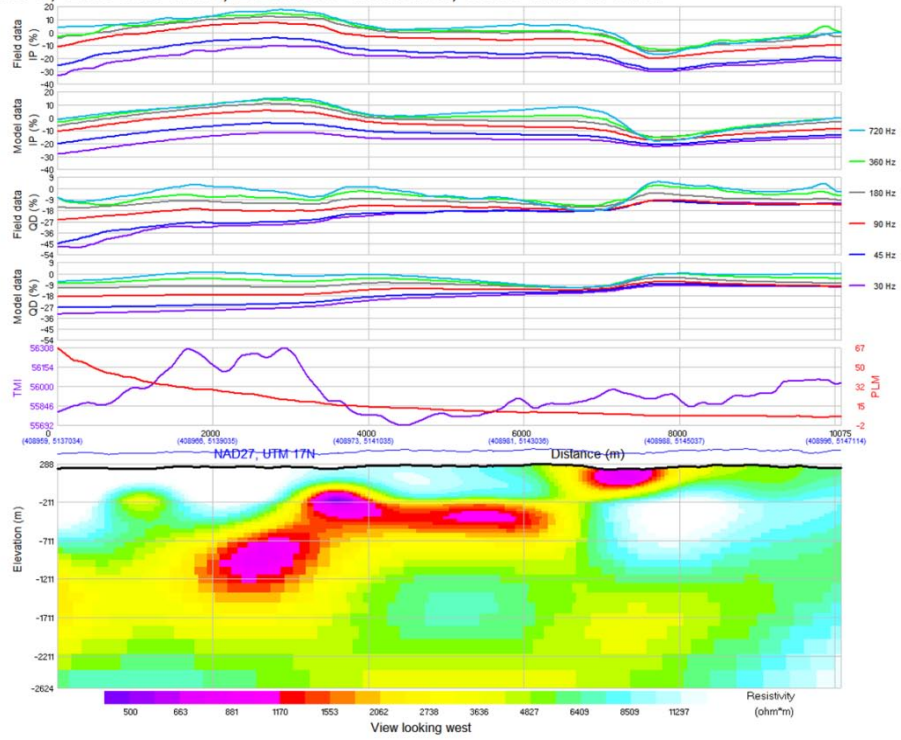
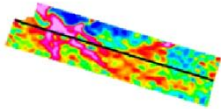


Figure 2-7: Section of ZTEM results along profile L1270.



2D INVERSION PARAMETERS
 Inversion code: Geotech Avert2D
 Model Mesh: 440 wide x 62 vertical,
 Average cell width: 29.65m
 2 cells between sites
 Input Data: 6 frequencies (30-720 Hz)
 In-Phase & Quadrature, Tzz In-line (only)
 Sampling: Average sampling rate: 5.47 points,
 Total number of points: 2304
 Input error: 1.13% to In-Phase & Quadrature
 (1-times error to 30Hz data)
 Output error: 0.997 RMS in 4 iterations
 Half-space resistivity: 5000 ohm-m

Flight Path of Line 2080 over IP 90Hz DT image



Mustang Minerals Corp. East Bull Lake east Block Elliot Lake, Ontario
Geotech ZTEM System Resistivity-Depth Image Project10214, Line 2080 Flight 1 - Sept. 27, 2010
Flown and processed by Geotech Ltd. 245 Industrial Parkway North Aurora, Ontario, Canada L4G 4C4 www.geotech.ca October, 2010

L2080, East Bull Lake east, ZTEM 2D Inversion, 5000 ohm-m start

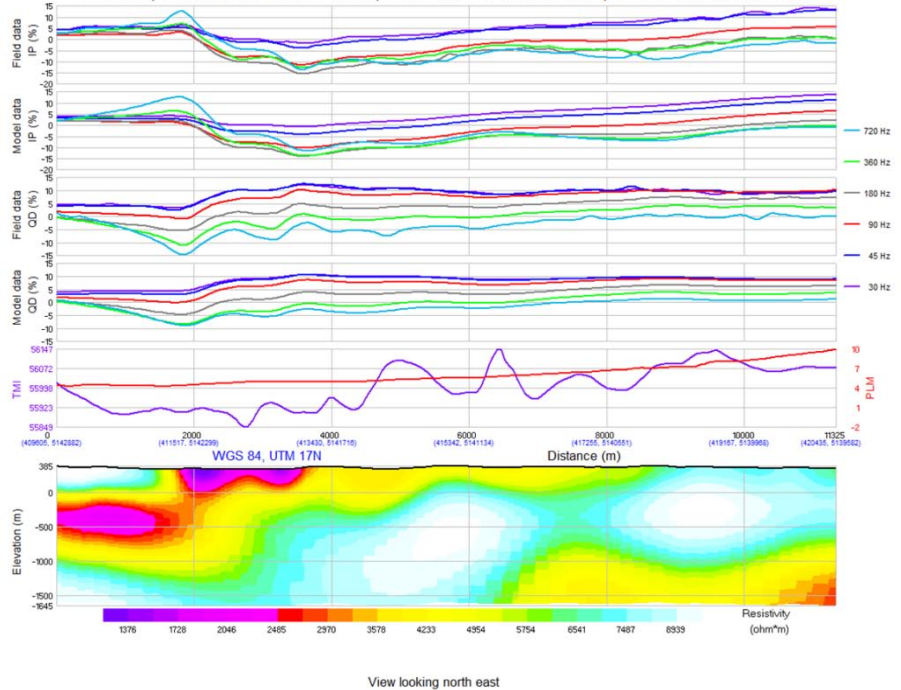


Figure 2-8: Section of ZTEM results along profile L2080.

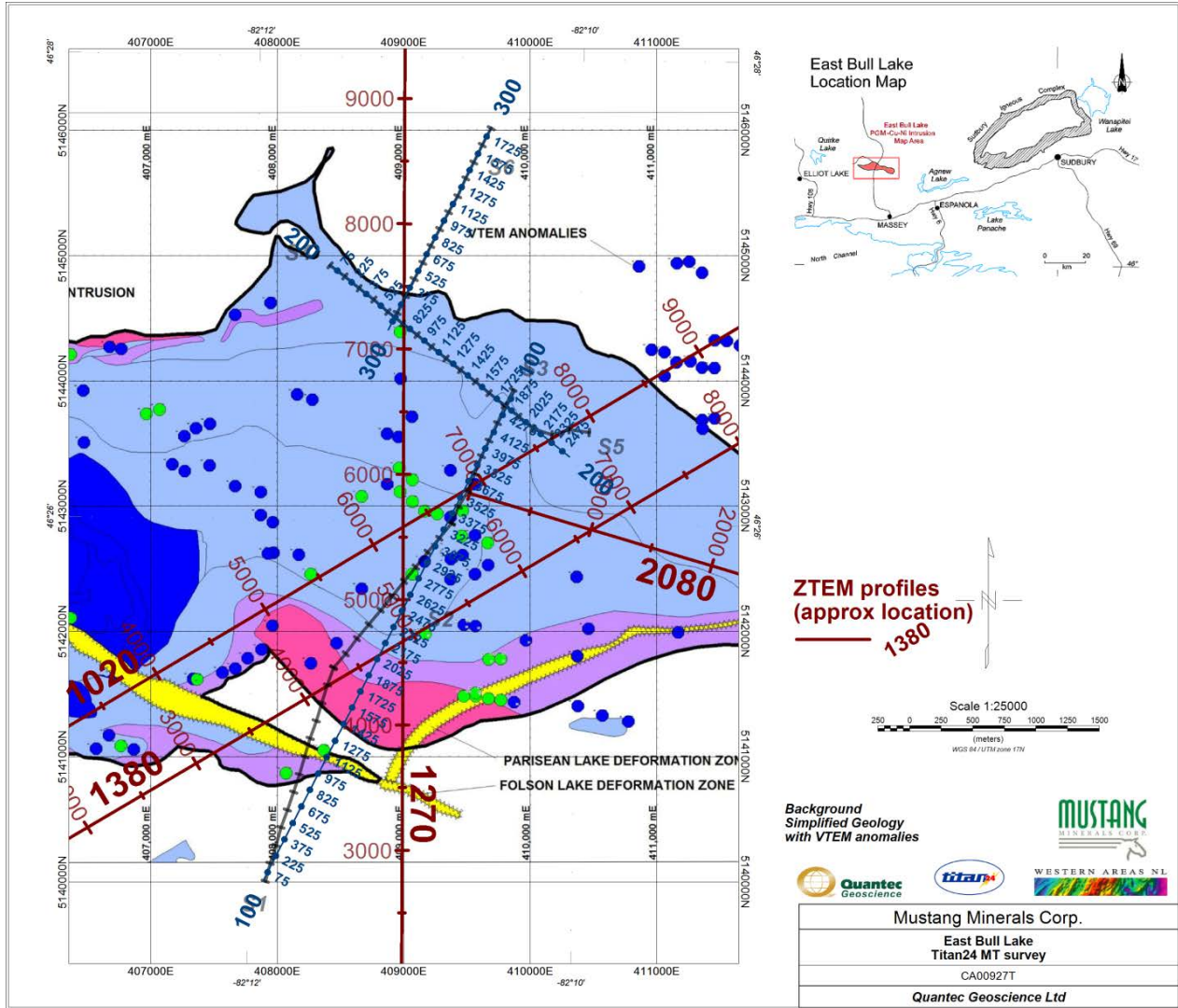


Figure 2-9: Location of the Titan-24 MT2D profiles with ZTEM profiles.

Table 2-1: Approximate correspondence between Titan-24 and ZTEM station numbering.

Titan-24 Profile	MT station	ZTEM Profile	ZTEM stations that approximately cover the Titan-24 profiles
100	75 to 4425	1380	3000 to 6800
		1020	4000 to 7600
200	75 to 2475	1270	7800 to 6200 (note reserve direction)
300	75 to 1725	1270	7200 to 8800

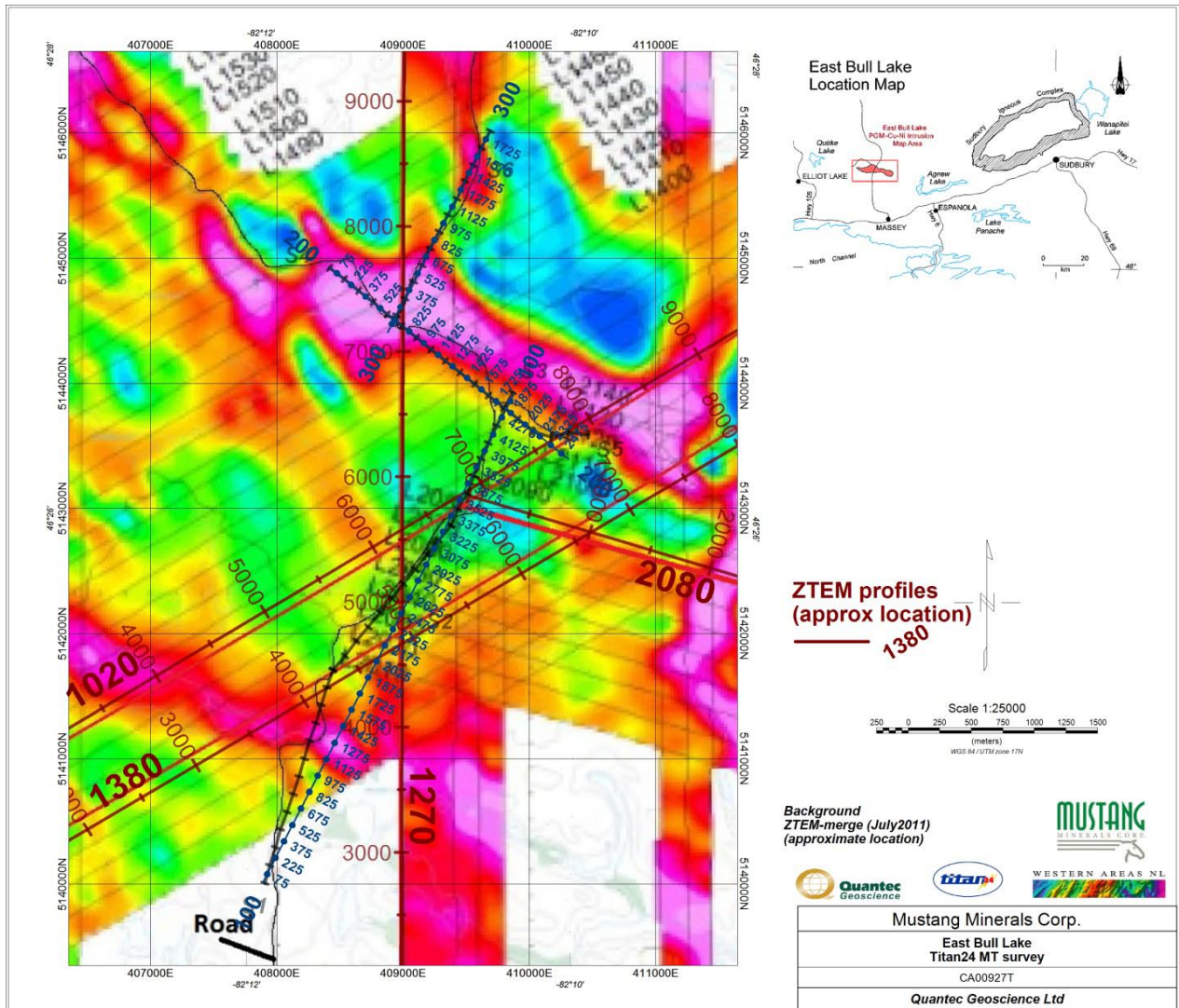


Figure 2-10: Location of the Titan-24 MT2D profiles with ZTEM-merge anomaly map.

3 RESULTS AND INTERPRETATION

This section presents the results of the 2D inversion of the Titan-24 data and interpretation in context with the survey objectives and significance to future exploration at East Bull Lake Project.

The Titan-24 system acquires three types of geophysical data – magnetotelluric (MT), direct current resistivity (DC), and induced polarization (IP).

The MT and DC methods are used to resolve the resistivity distribution of the subsurface by measuring the electric potential (DC) and the variation of natural source electric and magnetic fields (MT). Resistivity can be an indicator of metallic mineralization, but is more often than not controlled by rock porosity and is therefore an indirect indicator of alteration and mineral grain fabric.

In the induced polarization method, electrical capacitance or chargeability of the subsurface is measured. Chargeability is a near-direct indicator of the presence of sulphide mineralization, in both massive and disseminated forms. Chargeable mineralization is most commonly various sulphides and graphite, but also includes clay-type minerals potentially making it a useful tool for base-metals exploration.

For the context of this survey, only magnetotelluric data had been acquired.

For each line surveyed, electric data were acquired using 150m dipoles oriented along the spreads, plus another set of 150m dipoles oriented perpendicular to the spreads at every second site. One set of high-frequency and one set of low frequency magnetic sensors was used on each spread. A remote site with the same magnetic sensor configuration was used to improve processing of the MT data.

Detailed information on the survey logistics, acquisition parameters and screen capture of the acquired data for the survey are provided in appendices at the end of this report.

The final inversion models are presented graphically in Geosoft plot format along with an interpretation overlay and comments on the most significant results and recommended targets. Scaled sections of all the resistivity models are also provided at the end of this report.

Detail results, i.e. observed MT data and equivalent calculated responses for each model, are presented on a line per line basis in PowerPoint (PDF) documents delivered in the digital archive (DVD) attached to this report.

3.1 OVERVIEW OF INVERSION PROCEDURE

3.1.1 AUDIO-MAGNETOTELLURIC INVERSIONS

The Audio-Magnetotelluric (AMT) method is a natural source method that measures the variation of both the electric (E) and magnetic (H) field on the surface of the earth in order to determine the distribution at depth of the resistivity of the underlying rocks. A complete review of the method is presented in Vozoff (1972) and Orange (1989).

The measured MT impedance Z , defined by the ratio between the E and H fields, is a tensor of complex numbers. This tensor is generally represented by its two off-diagonal elements. In a 1D earth model, i.e. the resistivity varies only with depth, there is no strike direction and the two off-diagonal impedances

are equal. In the 2D case, i.e. when the resistivity varies with depth and perpendicularly to the strike, and when the profile is set perpendicular to the strike direction, the two off-diagonal elements are not equal but reflect the variation of the resistivity along two directions, one parallel and the other perpendicular to the strike, i.e., the TE (Transverse Electric; E parallel to the strike) and the TM (Transverse Magnetic; E perpendicular to the strike) modes.

Both TE and TM impedances are represented by an apparent resistivity (a parameter proportional to the modulus of Z) and a phase (argument of Z). The variation of those parameters with frequency relates the variations of the resistivity with depth, the high frequencies sampling the sub-surface and the low frequencies the deeper part of the earth. However the apparent resistivity and the phase have an opposite behaviour. An increase of the phase indicates a more conductive zone than the host rocks, and is associated with a decrease of the apparent resistivity. The objective of the inversion of MT data is to compute a distribution of the resistivity of the surface that explains the variations of the MT parameters, i.e. the response of the model that fits the observed data. The solution however is not unique and different inversions must be performed (different programs, different conditions) in order to test and compare solutions for artefacts versus a target anomaly.

The primary tool for evaluating the Spartan MT data is 1D, 2D, and 3D inversion.

The depth of investigation is determined primarily by the frequency content of the measurement. Depth estimates from any individual sounding may easily exceed 20 km. However, the data can only be confidently interpreted when the aperture of the array is comparable to the depth of investigation.

The inversion model is dependent on the data, but also on the associated data errors and the model norm. The inversion models are not unique, may contain artefacts of the inversion process and may not therefore accurately reflect all of the information apparent in the actual data. Inversion models need to be reviewed in context with the observed data, model fit. They must have an understanding of the model norm used and if the model is geologically plausible.

For this study, 1D and 2D inversions were performed on the data.

A 1D model at each MT site and for each mode (TE, TM, and DET-determinant⁵) has been calculated as a QA/QC tool using the Occam layered inversion program. This inversion calculates a 1D resistivity earth model (i.e., the resistivity varies only with depth) that best fits the data.

The 2D inversions presented in this report were carried out using the Quantec proprietary Phil Wannamaker inversion algorithm (PWm). The inversions were performed using the resistivity and phase data from 10kHz to 0.01Hz, interpolated at 6 frequencies per decade, assuming 5% error for the resistivity and 3 degrees error for the phase. For each MT2D profile, we assume the strike direction is perpendicular to the profile for all sites: the TM mode is then defined by the inline E-field (and cross line H-field), and the TE mode is defined by the cross line E-field (and inline H-field) data. Consequently, MT data used on lines L100 (spreads 1 to 3) and L300 (spread 6) where rotated to strike direction of -63°, i.e., a direction perpendicular to the pre-defined line azimuth of +27°, while MT data for line L200 (spreads 4 and 5) where rotated to strike direction of +39°, i.e. a direction perpendicular to the pre-defined line azimuth of +129°.

The topography variation along on each profile is small (±50m), and so it was not included in the PWm 2D inversions, but presentation of the 2D section include the topography. Finally, each 2D inversion started from a half space model of 1000 Ohm-m.

⁵ The determinant of the impedances is defined as: $Z_{det} = \sqrt{Z_{xy}Z_{yx} - Z_{xx}Z_{yy}}$.

A second inversion algorithm was used to invert same MT data: the Randy Mackie inversion code (RLM). Results are presented in the appendices. From previous work, we noticed that the PWm code has a tendency to accentuate anomalies with sharp vertical boundaries and to locate these anomalies at a greater depth than the RLM code. In contrast, the RLM code has a tendency to accentuate anomalies with a layered (horizontal) aspect resulting in a smooth lateral variation and lower depth to top of the anomalous bodies.

3.2 DISCUSSION OF RESULTS

This section presents and discusses the significant geophysical anomalies and potential targets interpreted from the final Titan-24 MT inversion models.

For clarity of the discussion, labels on sections are defined by the line number (first digit) and a letter, i.e., **L1_A**, and all the sections are using the same range of resistivity as the ZTEM sections, i.e., from 500 Ohm-m to 10,000 Ohm-m (see Figure 3-1).

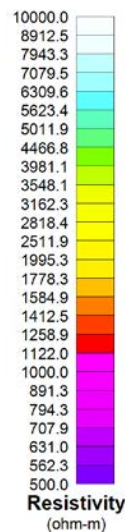


Figure 3-1: MT 2D resistivity colour bar.

3.2.1 LINE L100

The profile L100 is defined from data of spreads 1 to 3. Data on this profile had been all rotated to an X direction perpendicular to the line azimuth, i.e., with $X = -63^\circ$, and location of the MT station had been projected onto the MT2D profile. Note that line azimuth of $+27^\circ$ correspond closely to the azimuth of spreads 1 and 3, and so it minimize variation to a uniform distribution of the MT sites along the line.

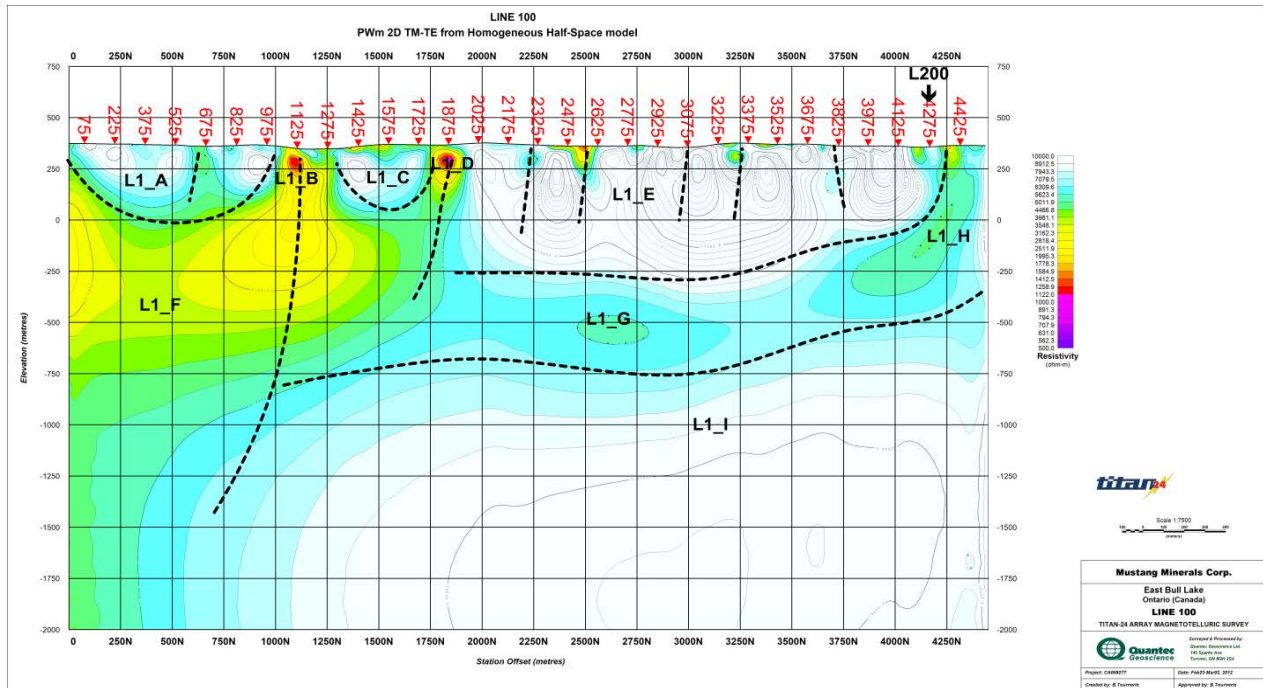


Figure 3-2: MT 2D results along line L100 (spreads 1-2-3).

Figure 3-2 presents MT results along the profile L100. In the following discussion, the reference to geological unit numbers is from the geological map from Eaton, et al (2011) presented on Figure 2-2.

The first 500m of the section is characterized by several more resistive units near the surface, i.e., **L1_A**, **L1_C**, and **L1_E**, and by two main more sub-vertical conductive zones **L1_B** and **L1_D**.

The sub-vertical zone **L1_B** is located near the MT site 1125, and it is well correlated very well with the *Folson Lake deformation zone*. This conductive zone seems to present some deep extension. South of this conductive zone **L1_B**, we have identified a more resistive unit **L1_A**. That unit presents a small gradient of the resistivity at station 675; that variation seems to correlate with the contact between the *Intermediate Intrusive* (unit "2ab") and the *Parisien Lake Syenite* (unit "4").

The sub-vertical zone **L1_D** is located near the MT site 1875, and it seems to correlate with the contact between the *Marginal Zone* (unit "5"), identified here as the resistive unit **L1_C**, and the *East Bull Lake Intrusive*, identified as the resistive unit **L1_E**. It is possible that the conductive zone **L1_D** merges with the other sub-vertical zone **L1_B** at depth, to delineate a more conductive south zone (**L1_F**) and a more resistive north zone (**L1_G-H & L1_I**) below 400m depth.

The local variation observed within the **L1_E** resistive unit might coincide with geological contact between different units within the intrusive. However, resolution of the lateral variation within this unit will be limited to the length of the one to two dipoles (i.e., 150-300m).

At depth, we observed a more conductive zone **L1_F** that seems to extend up to the sub-vertical zone **L1_D**, i.e., site 1875. A less resistive zone is also observed at depth below the more resistive unit **L1_E**

and the deep resistive zone **L1_I**. This less resistive zone seems to be characterized by two distinct units, **L1_G** and **L1_H**. We observe a lateral variation of the resistivity between these two units, which might indicate that they are representing two distinct geological units.

Finally, we note that the general geometry of the conductive zone observed at depth on the ZTEM profiles 1020 (Figure 2-5) and 1380 (Figure 2-6) correlates with the Titan-24 less resistive unit defined by the units **L1_G** & **L1_H**. However, the Titan-24 MT results are presenting a higher resolution image of the resistivity near the surface, and especially of the first 400m.

3.2.2 LINE L300

The profile L300 is defined from data of spread 6. This line has the same azimuth as Line L100, but it is located approximately 1km west of line L100. Data on this profile had been all rotated to an X direction perpendicular to the line azimuth (+27°), i.e., with X = -63. That profile might be considered to map the northern boundaries of the *East Bull Lake Intrusive*, i.e., as a north extension of line L100; however, correlation between lines L100 and L300 might be weak because of the 1km offset.

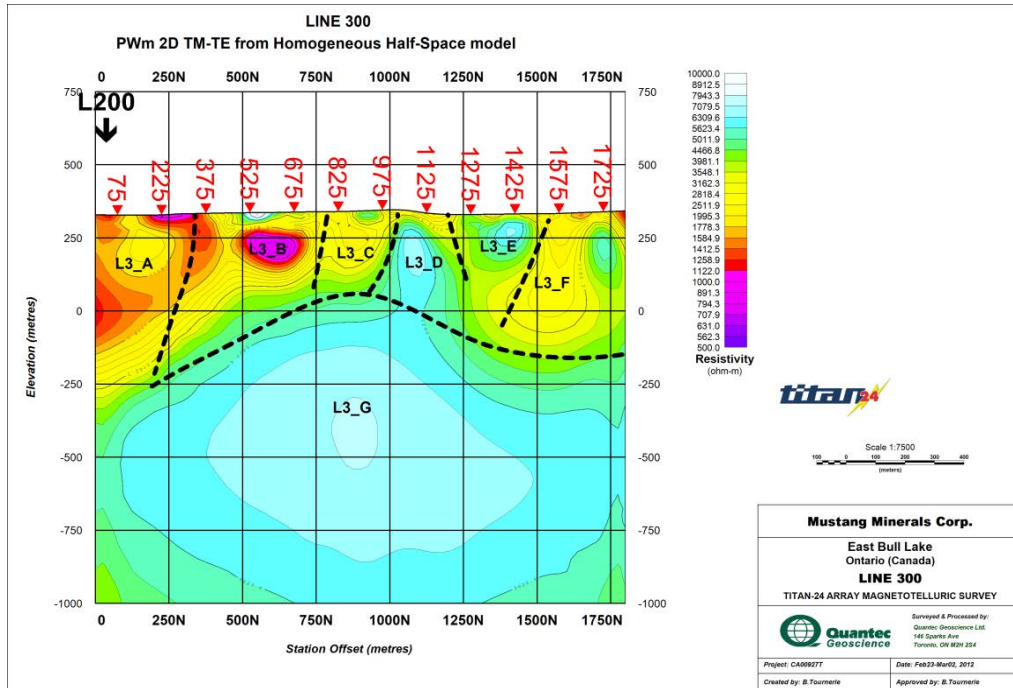


Figure 3-3: MT 2D results along line L300 (spread 6).

Figure 3-3 presents MT results along the profile L300. In the following discussion, the reference to geological unit numbers is from the geological map from Eaton, et al (2011) presented on Figure 2-2.

The profile is mainly characterized by a more conductive unit above a more resistive zone (**L3_G**). We note however lateral variation within the top conductive zone, highlighted on Figure 3-3 by the units **L3_A** to **L3_F**.

The inferred contact between the unit **L3_A** and the more conductive **L3_B** near site 375 seem to correlate with the contact between the *East Bull Lake Intrusive* (unit "8b") and the *Felsic Intrusive rocks* (unit "3c"). The conductive nature of the unit **L3_A** seems to correlate with the more conductive zone **L1_H** observed on the northern end of L100, and might indicate an increase of alteration or weathering of the formation at the contact. The more conductive zone **L3_B** could represent local variation within the *Felsic Intrusive rocks* (unit "3c"), but it might represent also an edge effect (may be alteration) associated with the granite (unit "16f") observed west of sites 575-675.

The contact between the conductive zone **L3_C** and the more resistive zone **L3_D** located near 1050 seems to correlate with an inferred fault identified on Figure 2-2.

Finally, the contact near 1500 between the resistive unit **L3_E** and the more conductive zone **L3_F** correlates with the contact between the *Mafic Intrusive Rocks* (unit "25"; **L3_E**), and the *Intermediate Intrusive* (unit "2a"; **L3_F**) observed on Figure 2-2. The conductive nature of **L3_F** might indicate an increase of alteration or weathering of the formation.

There is here also a relative good correlation between the general distribution of the resistivity along the ZTEM profile 1270, from approximately 7200 to 8800 and the Titan-24 MT results. The ZTEM section 1270, station located between 7200 to 8800, presents a more conductive zone approximately 500m thick near the surface. That conductive zone correlates well with the top first conductive unit observed in the Titan-24 MT section. We can observe also that both surveys present the more resistive unit at depth. Nevertheless, the Titan-24 MT image presents here more details within the top conductive unit.

3.2.3 LINE L200

The profile L200 is defined from data of spreads 4 and 5. The line azimuth was set to +129° which correspond to the azimuth of spread 4. Consequently, data on this profile had been all rotated to an X direction perpendicular to the line azimuth, i.e., with X = +39°, and location of the MT station of spread 5 had been projected onto that MT2D profile.

Note that inversion results along profile L200 need to be taken with care as the orientation of the profile is almost parallel to the main contact and geological structures (see Figure 2-2), and along a ZTEM anomaly (Figure 2-10), so the TE/TM definition applied on this profile (XY=TE) is not following the observed general geological strike, and so final result might not represent correct resistivity distribution along the profile.

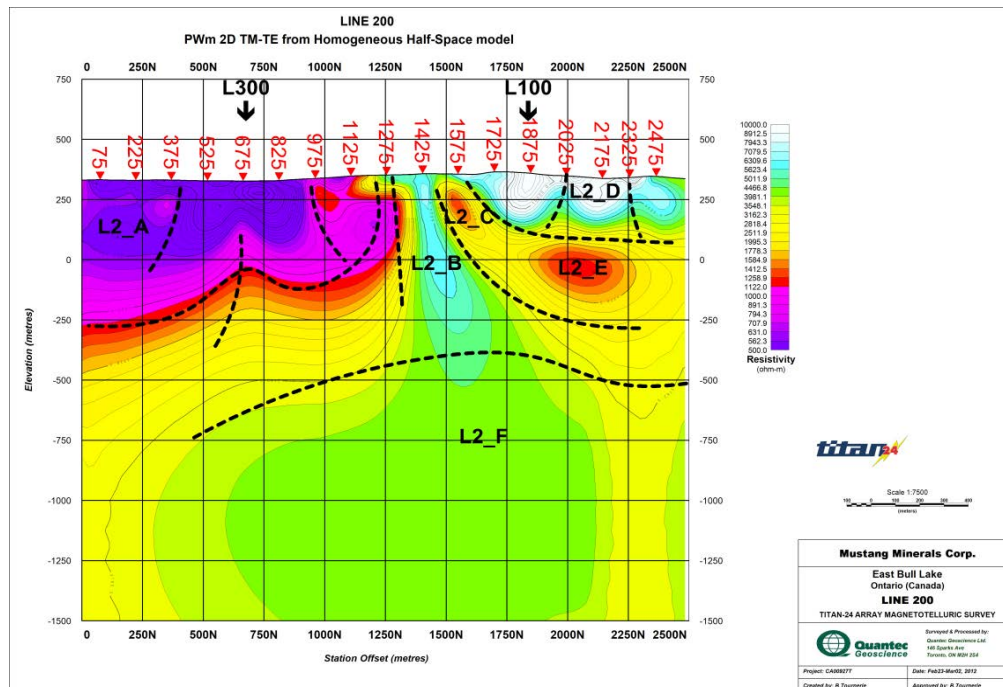


Figure 3-4: MT 2D results along line L200 (spreads 4-5).

Figure 3-4 presents MT results along the profile L200. Starting point of L300 and crossing point with line L100 are located at sites 675 and 1875 respectively. In the following discussion, the reference to geological unit numbers is from the geological map from Eaton, et al (2011) presented on Figure 2-2.

The profile is mainly characterized by two conductive units, **L2_A** and **L2_C-L2_E** separated by a more resistive zone **L2_B**. The conductive zone defined by the units **L2_C & L2_E** is dipping to the north, below the more resistive zone **L2_D**. That those units overlain a more resistive zone **L2_F** at depth.

There is no clear evidence of correlation between the near surface variation of the resistivity observed on L200 and the geology units described on the geological map (Figure 2-2) as the profile is located on the same geological unit (*East Bull Lake Intrusive* unit "8b").

However, we can notice a relative correlation between the conductive zone **L2_A** and the more conductive zone **L3_A** observed on profile L300. Following that observation, the unit **L2_A** might represent an image of the contact between the *East Bull Lake Intrusive* (unit "8b") and the *Felsic Intrusive rocks* (unit "3c"), or the image of the ZTEM anomaly that extend between site 75 to 1425. Note that the break on the ZTEM anomaly observed near UTM 410000E / 5144000N corresponds to the more

resistive zone **L2_B**.

Similarly, we note some correlation between the vertical sequence **L2_D-L2_E** observed on L200 and the units **L1_E – L1_H** identified on L100. The unit **L2_D** and its small lateral variation of the resistivity might be attributed to the *East Bull Lake Intrusive* (unit “8b”) formation, and its deformation (layering). The conductive unit **L2_E** seem to outcrop near site 1575 (**L2_C**). That structure (i.e., **L2_C/L2_E**) with the more resistive zone **L2_B** might represent the signature of a fault.

4 CONCLUSIONS AND RECOMMENDATIONS

This report presents the results of the analysis of the Titan-24 MT data acquired from February 23rd to March 1st, 2012, over the East Bull Lake Project, on behalf of Mustang Minerals Corp.

The survey grid is located approximately 27 km North of Massey, Ontario, and includes acquisition of magnetotelluric data for frequencies ranging from 10kHz to 0.01Hz along six spreads of various orientation, with dipole length of 150m. Three MT profiles were defined from these six spreads, two oriented +27°, and one +129°, for a total coverage of 8850m.

The MT data were inverted using 2D inversion algorithms and produced section showing resistivity distribution of subsurface.

The area defined by the conductive zones **L1_B** and **L1_D** on profile L100 has been already identified by Eaton et al (2011) as potential zone for Cu-Ni-PGE mineralisation. That area represents the principal zone of interest for follow up of this Titan-24 MT survey. The more conductive zone **L3_B** observed on profile L300 represents a second zone to consider for follow up. The orientation of profile L200 along the geological structures and the ZTEM anomaly limit the capability to resolve potential zone of interest.

Quantec recommend the full integration of all the Titan-24 MT results with existing VTEM and ZTEM results, as with other geophysical data (i.e., magnetic), and known geology information, to enhance the interpretation of the current results. Quantec recommend extension of the Titan-24 MT profiles L100 to the north to better characterize the north contact of the *East Bull Lake Intrusive*, and additional Titan-24 DC/IP/MT profiles across the *Marginal Zone* to better characterize the potential of that area for Cu-Ni-PGE mineralisation.

Respectfully Submitted

Toronto, ON, the 03/04/2012,

Benoît Tournerie, DSc, PGeo

Quantec Geoscience Ltd

5 STATEMENT OF QUALIFICATIONS

5.1 BENOÎT TOURNERIE

I, Benoît Tournerie, declare that:

I am a Geophysicist with residence in Toronto, Ontario and am presently employed in this capacity with Quantec Geoscience Ltd., Toronto, Ontario;

I obtained a License (equivalent to B.Sc.) in 1989, a DEA (equivalent to M.Sc.) in 1991, and a Doctorate with Honours (equivalent to Ph.D.) in December 1995, in Earth Sciences, option geophysics, from the University of Rennes 1, Rennes, France;

I am a registered geophysicist, since 2008, with license to practice in the Province of Ontario (APGO member # 1609); a registered geoscientist, since 2008 with a license to practice in the Province of Quebec (OGQ #1322); a registered geoscientist, since 2009 with a license to practice in the Province British Columbia (APEG-BC #33786);

I have practiced my profession continuously since April, 1996 in North and South America, in Europe, and in Oceania;

I am a member of the Society of Exploration Geophysicists (SEG), the European Association of Geoscientist and Engineers (EAGE), and the Canadian Exploration Geophysics Society (KEGS);

I have no interest, nor do I expect to receive any interest in the properties or securities of **Mustang Minerals Corp.**, its subsidiaries or its joint-venture partners;

I am the Professional Geophysicist responsible for this project and have authored this Geophysical Report.

I was in charge of the Quality Control and Assurance of the acquired data; I have reviewed the survey results and the logistics sections of the report, and can attest that these accurately and faithfully reflect the data acquired on site;

I undertook the 1D, and 2D MT inversions of the data, and have compiled the final processed data, inversions and interpretation results contained in the Geophysical Report.

The statements made in this report represent my professional opinion in consideration of the information available to me at the time of writing this report.

Toronto, Ontario, the 03/04/2012

Benoît Tournerie, D. Sc., P.Geol.
Quantec Geoscience Ltd.

5.2 MOJTABA DANESHVAR NILU

I, Mojtaba Daneshvar, declare that:

I am a data processor with residence in Toronto, Ontario and am presently employed in this capacity with Quantec Geoscience Ltd., Toronto, Ontario;

I obtained a Bachelor of Science Degree (B.Sc.), with Honours, in Earth Science/Geophysics Specialization in 2010 from the University of Waterloo, Waterloo, Ontario.

I have practiced my profession continuously since Sep, 2010 in Canada;

I have no interest, nor do I expect to receive any interest in the properties or securities of **Mustang Minerals Corp.**, its subsidiaries or its joint-venture partners;

I was the data processor on site, responsible for the quality control of data acquired throughout the survey. I compiled and edited the logistics report. The statements made in this report represent my professional opinion based on my consideration of the information available to me at the time of writing this report.

Toronto, Ontario, the 03/04/2012

Mojtaba Daneshvar, B.Sc.

Quantec Geoscience Ltd.

6 DIGITAL ARCHIVE

The DVD attached to this report contains a copy of all the inversion results, final processed data, including the survey files, the daily processing (and field) notes, and an electronic copy of this report (with all appendices).

Folder	Sub level 1	Sub level 2	Description
Contract and Client Info			Contract, technical reports, images, and other documents
Fields Results			Final field results EDI, survey Files, and Processing Notes
Presentation of Results			Power Points, PDF, and documents presented or emailed to client
Geosoft			Geosoft Files
		Base Maps	Base maps, location, etc
		Sections	2D sections (MT), including interpretation sections
invMT			MT inversions
			Data, 1D and 2D models are included in the Geotools db's

A PRODUCTION SUMMARY

DATE	Field Activities and Observations	Line & Spread	Receiver		READ TODAY?	MT read	Spreads Completed
			Starting	Ending			
23/02/2012	Mob to Massey						
24/02/2012	Set up remote MT. PST. Prep electrodes on line L100.						
25/02/2012	Redo PST for HF coils; Finish setting up spread & read MT	sp1	0	1800	MT	1800	1
		sp2	1800	3150	MT	1350	1
26/02/2012	Picked up equipment and prep next spreads.						
27/02/2012	Picked up; Set up & read MT	sp2	2550	3300	MT	750	
		sp3	3300	4500	MT	1200	1
28/02/2012	Picked up; Set up & read MT	sp6	0	1800	MT	1800	1
29/02/2012	Picked up; Set up & read MT	sp4	0	2100	MT	2100	1
		sp5	2100	2550	MT	450	1
01/03/2012	Packed up gear						
02/03/2012	Demob to Toronto						
TOTAL coverage (km), including overlap						9.45	
TOTAL Number of Spreads							6

B SURVEY LOGISTICS

B.1 ACCESS

Base of Operation: East Bull Lake Wilderness Resort
10 East Bull Lake
Massey, Ontario
POP1P0

Mode of Access to Grid: Trucks

Mode of Access to Lines: Trucks, Snowmobile, by foot

B.2 SURVEY GRID AREA

Established by: Mustang Minerals Corp.

Coordinate Reference System: Grid referenced to UTM Coordinates

Datum & Projection: WGS84/ Zone 17NH

Grid Azimuth:

Spread 1:	17°
Spread 2:	38°
Spread 3:	23°
Spread 4:	130°
Spread 5:	93°
Spread 6:	26°

Magnetic Declination: 11° West

Station Interval: 150 m

Method of Chaining: Metric, pickets GPS surveyed

Surveyed Line-start and -end point coordinates.

Line	Grid Coordinate		UTM Coordinate Start		UTM Coordinate End	
	Start	End	Easting	Northing	Easting	Northing
Spread1	0	1800	407904	5140008	408443	5141713
Spread2	1800	3300	408443	5141713	409377	5142865
Spread3	3300	4500	409377	5142865	409864	5143930
Spread4	0	2100	408417	5144924	410023	5143621
Spread5	2100	2550	410023	5143621	410466	5143590
Spread6	0	1800	408877	5144408	409690	5146018

B.3 PRODUCTION AND COVERAGE

Survey Period/days: February 23rd to March 2nd, 2012
9 days

Survey Days (read time): 7 days

Mob/Demob: 2 days

Safety Inductions: 0 days

Parallel Sensor Test: 2 days

Weather/Down Days: 0 days

Number of Lines surveyed: 6 Spreads

MT Survey Coverage: 8.85 km

MT Survey Coverage (Electrode to Electrode).

Spread	Min Extent (m)	Max Extent (m)	Coverage (km)
1	0	1800	1.8
2	1800	3300	1.5
3	3300	4500	1.2
4	0	2100	2.1
5	2100	2550	0.45
6	0	1800	1.8
TOTAL			8.85km

B.4 PERSONNEL

Project Manager: David Macgillivray

Responsible Geophysicist: Benoît Tournerie

Data Processing (in field): Mojtaba Daneshvar Nilu

Crew Chief: Jeff Violette

MT operator: Joey Plouffe
Ethan Peterson

Remote Operator: Connor McLellan

Field Technicians: Wade Lee
Mike Belben
Jeff Violette
Dustin Kirk
John Spezeski

B.5 INSTRUMENTATION

Receiver System:

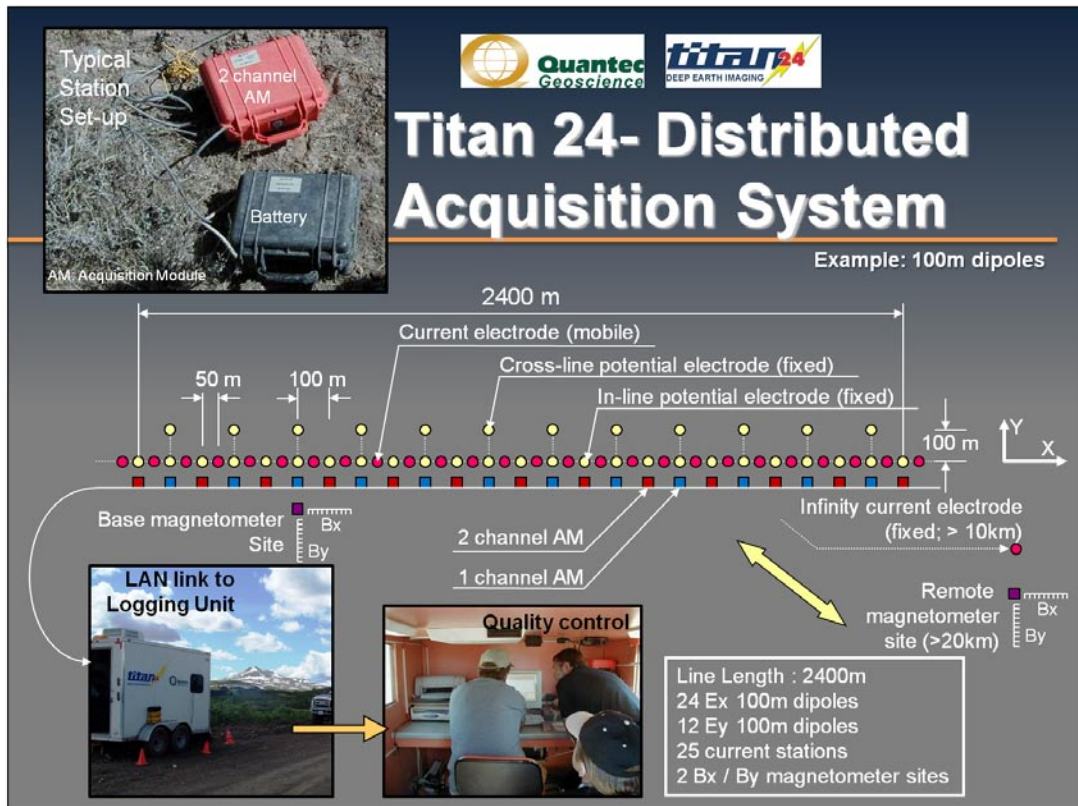
- Quantec Distributed Array Acquisition System:
- 61 channels max. per system (55ch operationally with internal A/D conversion (24bit @120db / dual speed @120-48kHz), and buffer memory (6Mb).
 - 24 x 2-channel Acquisition Modules (AMs)
 - 13 x 1-channel Acquisition Modules (AMs)
 - AM data transmission using LAN cabling
 - 2 Central Recording Units (CRU; 140 Gb data storage) at base & at MT remote reference (MT survey)
 - 2 GPS synchronization clocks (10nsec precision /12.3MHz clock-speed), at base & at MT remote reference (MT survey)
 - 2 PC-based Central Processing Units (CPU) at base & at MT remote reference (MT survey)

Receiver Electrodes:

Ground contacts using stainless steel rods

Receiver Coils (MT Surveys):

- Low Frequency Range (0.0001Hz to 1kHz):
- 4 Magnetometers (P50)
 - {2 at base & 2 at remote}
 - Mid to High Frequency Range (1Hz to 25kHz)
 - 4 Magnetometers (GHF model)
 - {2 at base & 2 at remote}



Titan-24 DCIP and MT Schematic Survey Layout.

B.6 MT SURVEY SPECIFICATION

B.6.1 GEOMETRY

Technique:	Tensor soundings, remote-referenced
Line Configuration:	23-24 Ex = Continuous In-line voltages, 12-13 Ey = Alternating (2-stations) cross-line E-fields 1 pair Low Frequency coils 1 pair High Frequency coils
Remote Configuration:	1 Ex = in line E-fields 1 Ey = cross-line E fields 1 pair Low Frequency coils 1 pair High Frequency coils
Spread Length:	0.45 to 2.1 km
Number of spreads per line:	1 to 3
Dipole size:	Ex = 150 metres (100 metres at remote) Ey = 150 metres(100 metres at remote)
Sampling Interval:	Ex = 150 metres Ey = 300 metres
Ex/Ey sampling Ratio:	2/1
E/H sampling Ratio:	Ex: 23-24/2 Ey: 12-13/2
Remote Reference Position:	405804m E, 5160727m N (WGS84/Zone 17NH)

B.6.2 ACQUISITION & PROCESSING

Data Acquisition:	Full-waveform time-series acquisition Data processing/output in frequency-domain.
Remote-Base Synchronization:	GPS clocks (10µsec time-accuracy)
Frequency Bandwidth:	<u>Operating:</u> 0.01 to 48000 Hz <u>Effective:</u> 0.1 to 20000 Hz
Time-series Sampling:	<u>High Range:</u> 48000 samples/sec <u>Mid-Range:</u> 12000 samples/sec <u>Low Range:</u> 120 samples/sec
Time-Series Stacking:	<u>High Range:</u> 1,534,999 samples <u>Mid-Range:</u> 2 ²⁰ (1,048,576) samples <u>Low Range:</u> 2 ¹⁹ (524,288) samples
Sample/Record Time:	<u>High Range:</u> min. 2 events @ 30 seconds per event <u>Mid Range:</u> min. 2 events @ 2.0 minutes per event <u>Low Range:</u> 2 - 3 events @ 80 minutes for a full event (total recording and retrieving time approx. 7 hrs)

Post-Processing: using Quantec proprietary QuickLay v.4.1
 1) Coherent noise rejection using remote-reference
 2) Proprietary digital filtering (scrubbing)
 3) Coherency sorting
 4) Impedance estimate stacking

B.6.3 DATA PRESENTATION

Parallel Sensor Test: Result of the test of the equipment (PST) is presented in detail in Appendix Parallel Sensor Test.

Data Error: Apparent Resistivity = $<1/20^{\text{TH}}$ decade average.
 Phase = <3 degrees average

Sounding Curves: Apparent resistivity and phase (XY and YX) sounding curves versus the frequency (8 pts. per decade) using Geotools™ viewer.

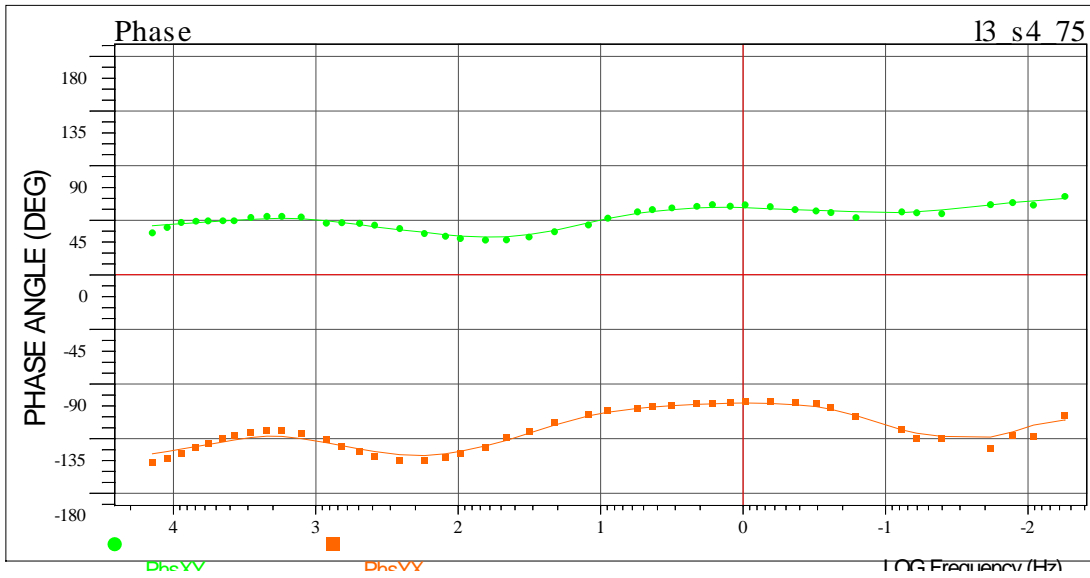
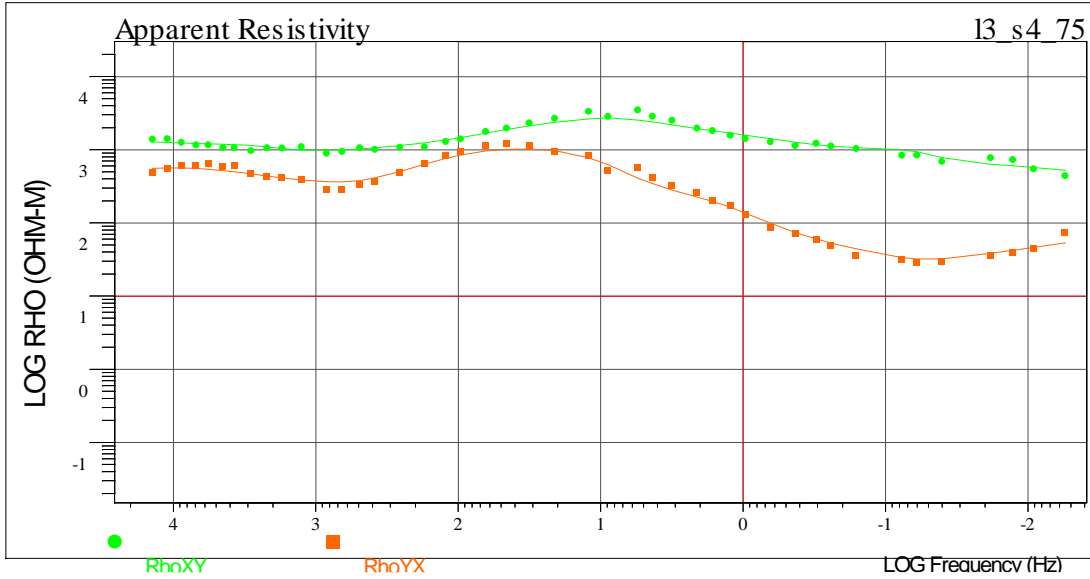
Pseudo-Section Plots: MT Apparent Resistivity and Phase Pseudo-Sections (XY, and YX) posted, contoured (equal area zoning) and plotted in grid units using Geotools™ viewer.

Raw Data (digital): (external Hard Drive)
 Base and Remote Raw Event Log File Folders (i.e. Base-Eventxxx.dat; Remote-Eventxxxx.dat). Also contains AU.txt and Event.log files, which contain information on the location and time of the event in QuickLay digital format (external Hard Drive). (Raw data output to Matlab format upon request)

Processed Data (digital): MT DATA in EDI (Electronic Data Interchange) file created in Geotools™ containing Auto and Cross-power Spectral estimates for individual stations (sites) and profiles (site-sets); Spectra are in Right Hand positive down co-ordinate system, and for profiles, EDI files are created with X as the profile direction.

For this study, final EDI for spreads 1 to 6 have X at 17°, 38°, 23°, 130°, 93°, 26° respectively (i.e., ROTSPEC= 17, 38, 23, 26, 130 and 93)

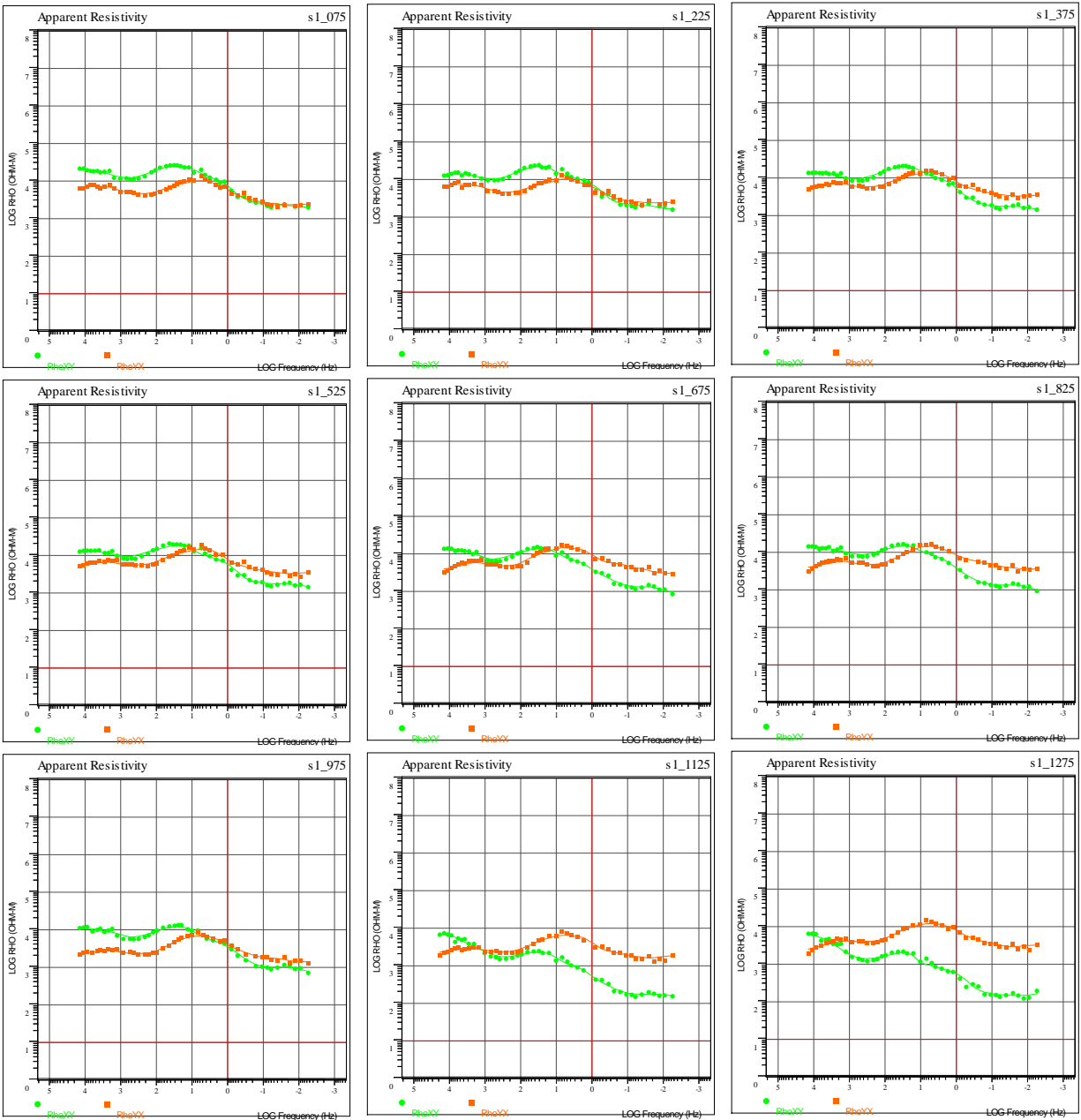
EDI is a format conforming to SEG standard for the storage of magnetotelluric (MT) data (Wight, D. E., 1987).



Example of Apparent Resistivity and Phase (XY and YX) Sounding Curves.

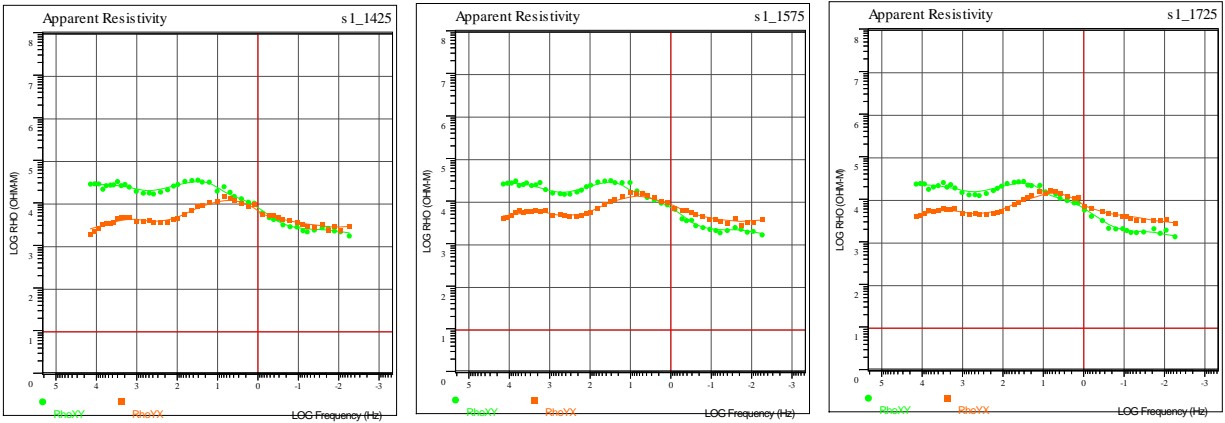
C MT SOUNDINGS CURVES OF FINAL PROCESSED DATA

C.1 SPREAD 1 WITH X @ 17°



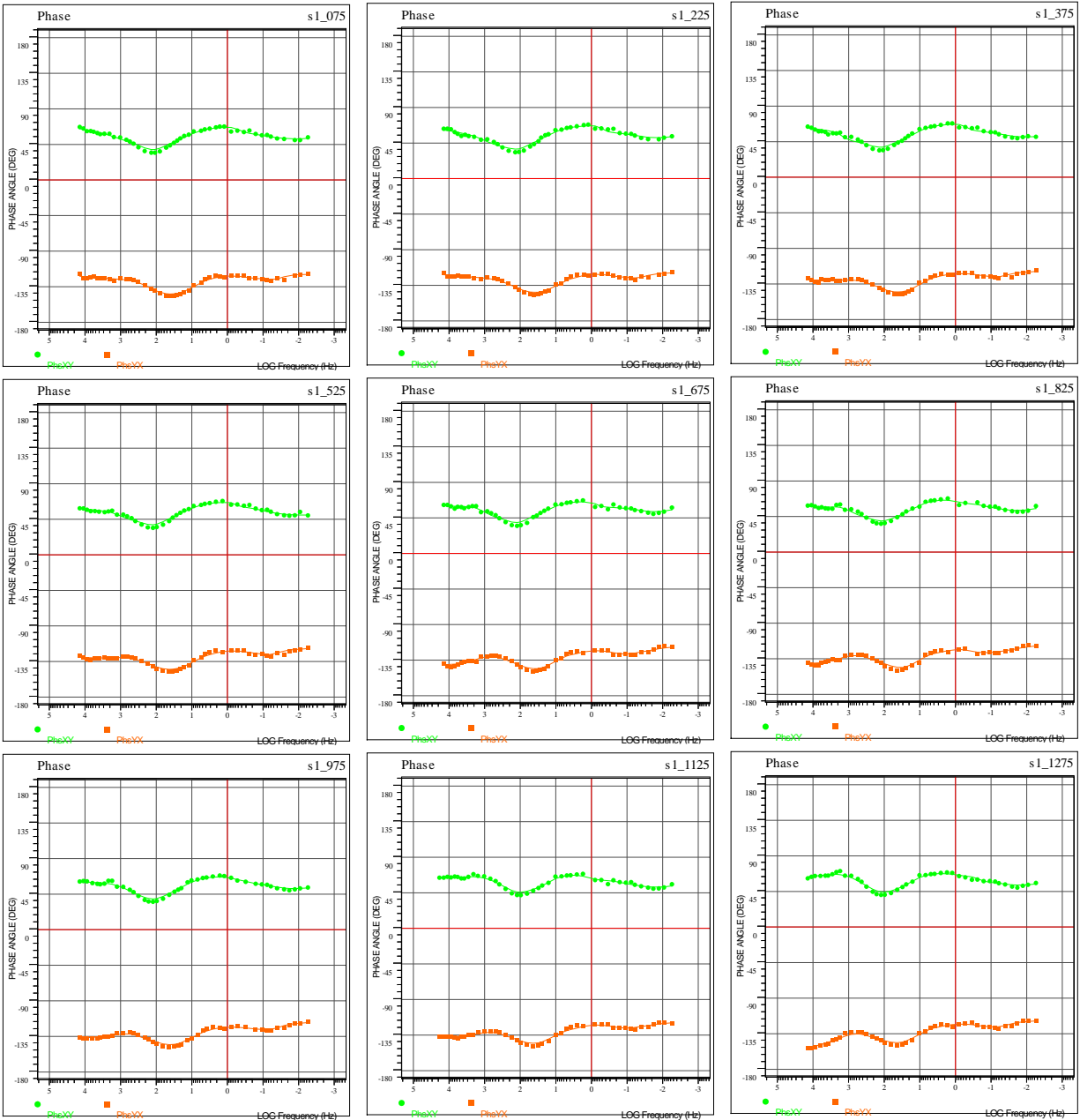
Spread 1 (X @ 17°) – Apparent Resistivity Sounding Curves vs Frequency (1 of 2).

MODE XY (GREEN) DENOTES ELECTRICAL (**EX**) FIELD AND ORTHOGONAL MAGNETIC (**HY**) FIELD (=EX/HY)
MODE YX (ORANGE) DENOTES ELECTRICAL (**EY**) FIELD AND ORTHOGONAL MAGNETIC (**HX**) FIELD (=EY/HX)



Spread 1 (X @ 17°) – Apparent Resistivity Sounding Curves vs Frequency (2 of 2).

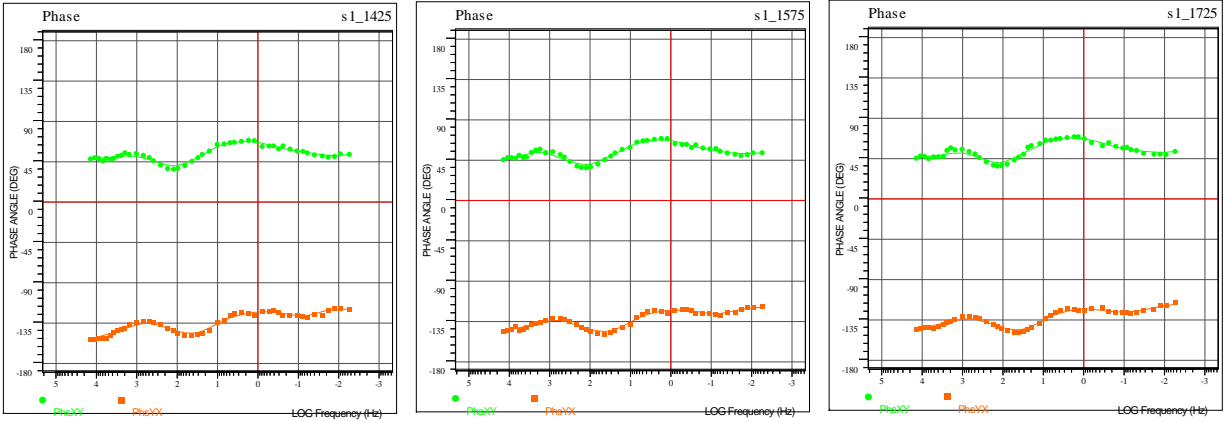
MODE XY (GREEN) DENOTES ELECTRICAL (**Ex**) FIELD AND ORTHOGONAL MAGNETIC (**Hy**) FIELD (=Ex/Hy)
MODE YX (ORANGE) DENOTES ELECTRICAL (**Ey**) FIELD AND ORTHOGONAL MAGNETIC (**Hx**) FIELD (=Ey/Hx)



Spread 1 (X @ 17°) – Phase Sounding Curves vs Frequency (1 of 2).

MODE XY (GREEN) DENOTES ELECTRICAL (**Ex**) FIELD AND ORTHOGONAL MAGNETIC (**Hy**) FIELD (=Ex/Hy)

MODE YX (ORANGE) DENOTES ELECTRICAL (**Ey**) FIELD AND ORTHOGONAL MAGNETIC (**Hx**) FIELD (=Ey/Hx)

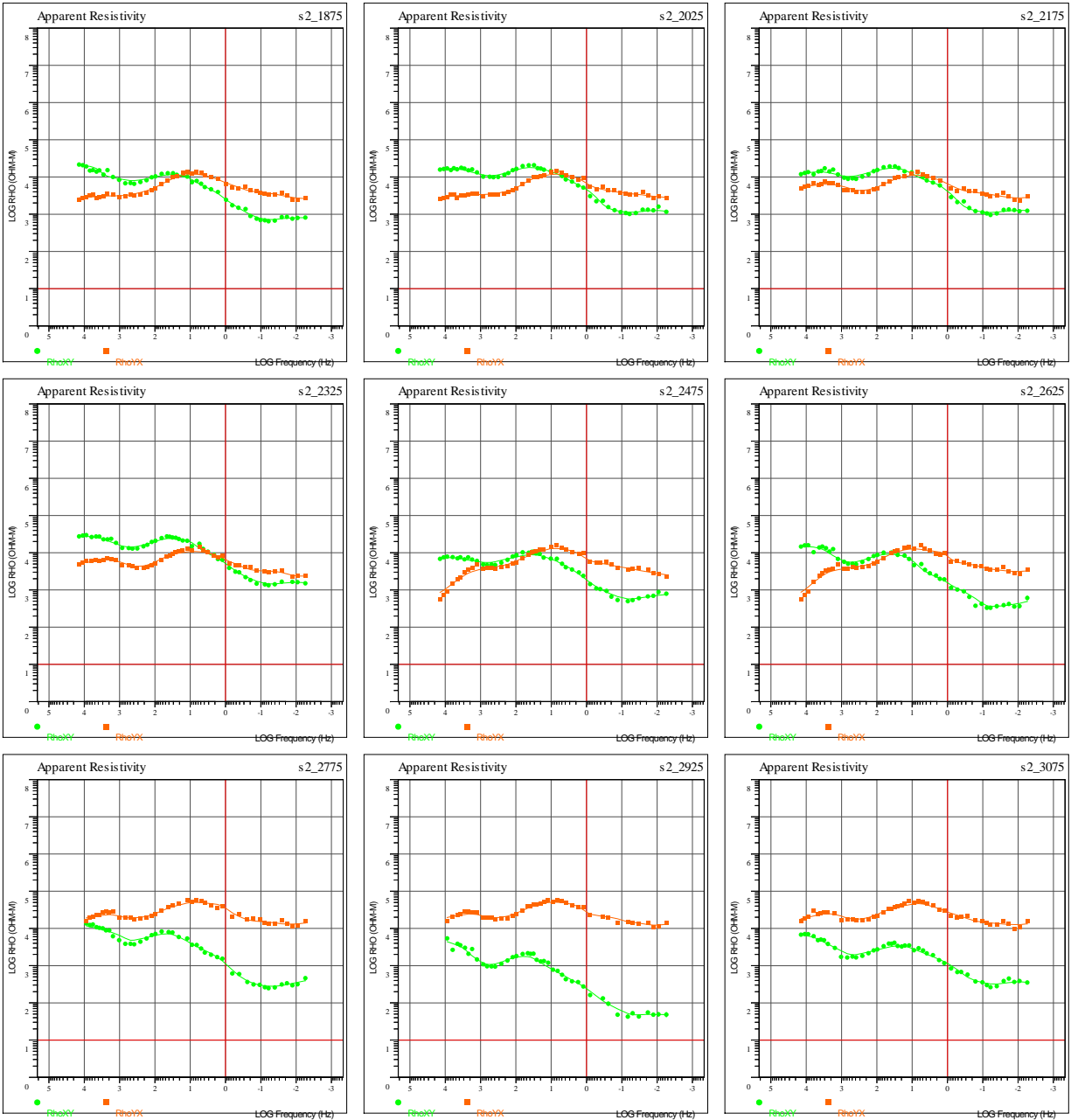


Spread 1 (X @ 17°) – Phase Sounding Curves vs Frequency (2 of 2).

MODE XY (GREEN) DENOTES ELECTRICAL (**Ex**) FIELD AND ORTHOGONAL MAGNETIC (**Hy**) FIELD (=Ex/Hy)

MODE YX (ORANGE) DENOTES ELECTRICAL (**Ey**) FIELD AND ORTHOGONAL MAGNETIC (**Hx**) FIELD (=Ey/Hx)

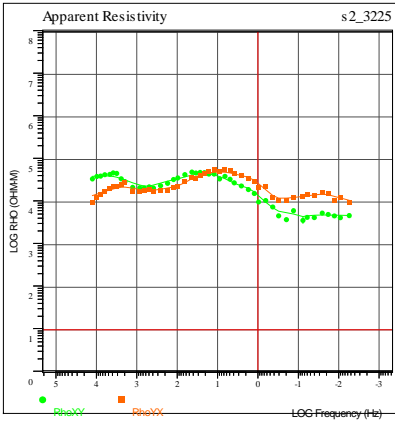
C.2 SPREAD 2 WITH X @ 38°



Spread 2 (X @ 38°) – Apparent Resistivity Sounding Curves vs Frequency (1 of 2).

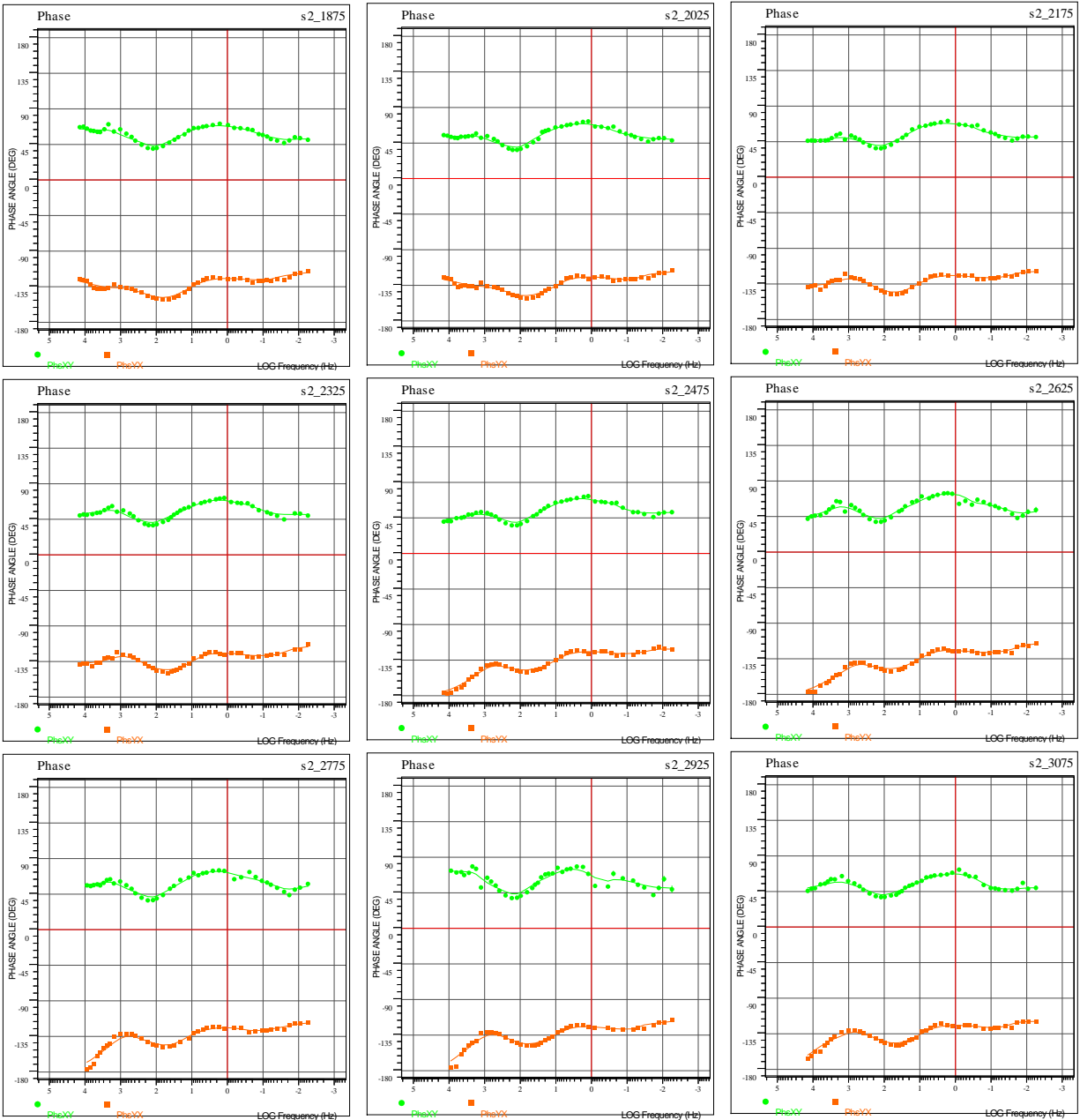
MODE XY (GREEN) DENOTES ELECTRICAL (**EX**) FIELD AND ORTHOGONAL MAGNETIC (**HY**) FIELD (=EX/HY)

MODE YX (ORANGE) DENOTES ELECTRICAL (**EY**) FIELD AND ORTHOGONAL MAGNETIC (**HX**) FIELD (=EY/HX)



Spread 2 (X @ 38°) – Apparent Resistivity Sounding Curves vs Frequency (2 of 2).

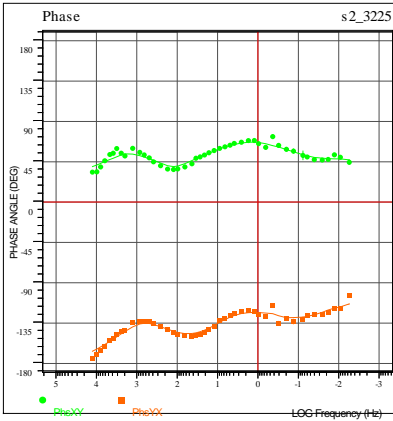
MODE XY (GREEN) DENOTES ELECTRICAL (**EX**) FIELD AND ORTHOGONAL MAGNETIC (**HY**) FIELD (=EX/HY)
MODE YX (ORANGE) DENOTES ELECTRICAL (**EY**) FIELD AND ORTHOGONAL MAGNETIC (**HX**) FIELD (=EY/HX)



Spread 2 (X @ 38°) – Phase Sounding Curves vs Frequency (1 of 2).

MODE XY (GREEN) DENOTES ELECTRICAL (EX) FIELD AND ORTHOGONAL MAGNETIC (HY) FIELD (=EX/HY)

MODE YX (ORANGE) DENOTES ELECTRICAL (EY) FIELD AND ORTHOGONAL MAGNETIC (HX) FIELD (=EY/HX)

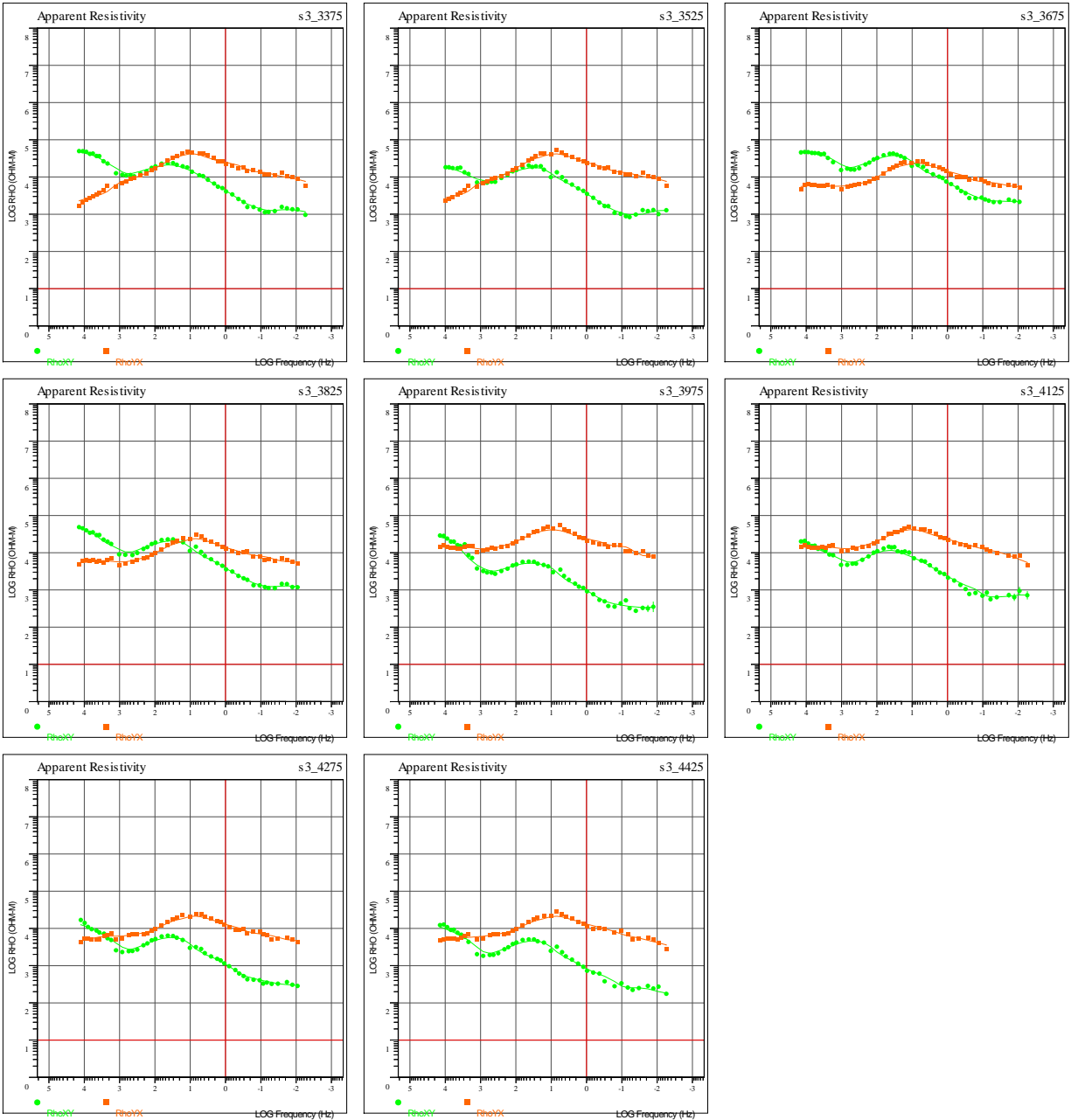


Spread 2 (X @ 38°) – Phase Sounding Curves vs Frequency (2 of 2).

MODE XY (GREEN) DENOTES ELECTRICAL (**EX**) FIELD AND ORTHOGONAL MAGNETIC (**HY**) FIELD (=EX/HY)

MODE YX (ORANGE) DENOTES ELECTRICAL (**EY**) FIELD AND ORTHOGONAL MAGNETIC (**HX**) FIELD (=EY/HX)

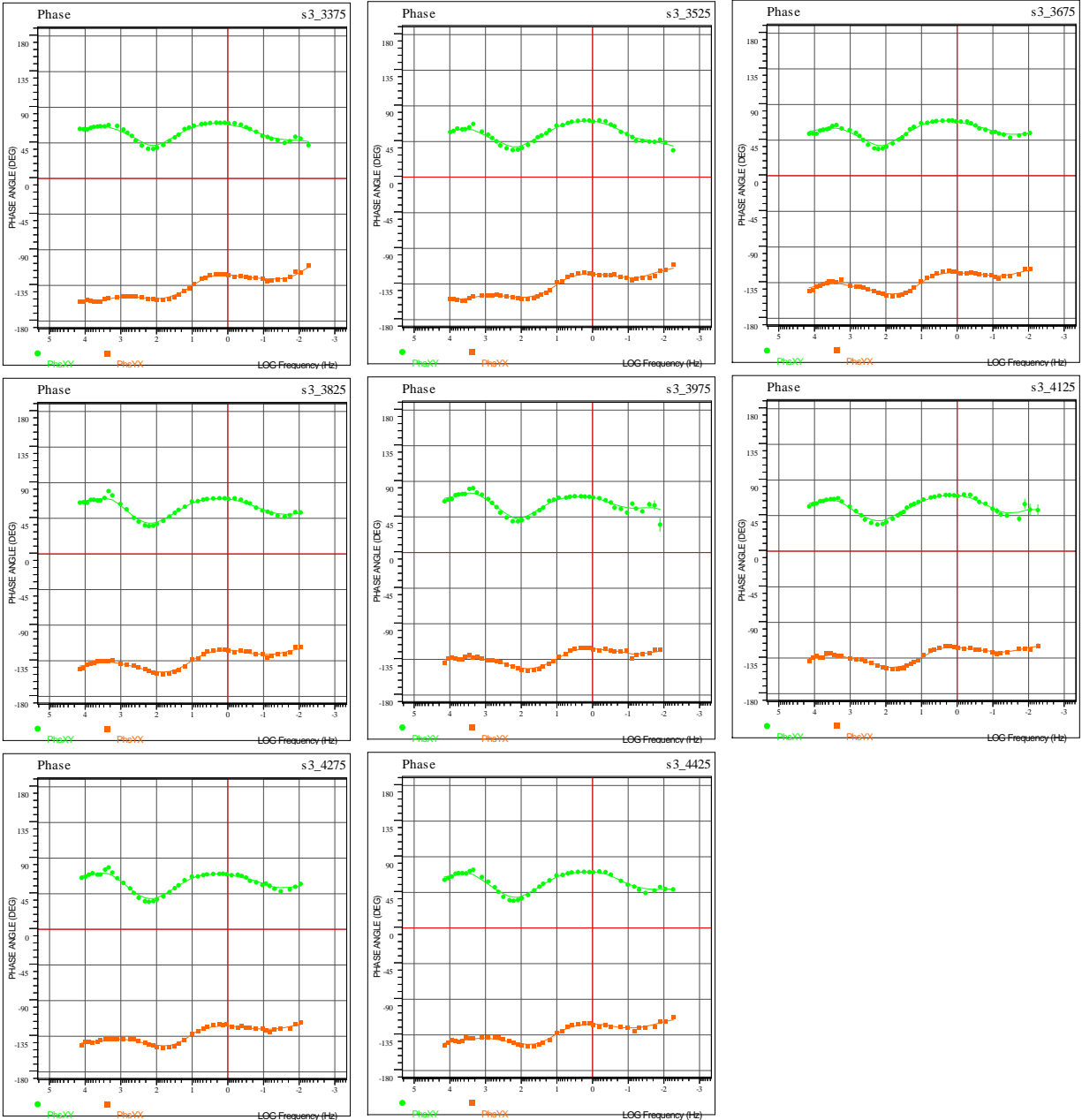
C.3 SPREAD 3 WITH X @ 23°



Spread 3 (X @ 23°) – Apparent Resistivity Sounding Curves vs Frequency.

MODE XY (GREEN) DENOTES ELECTRICAL (**EX**) FIELD AND ORTHOGONAL MAGNETIC (**HY**) FIELD (=EX/HY)

MODE YX (ORANGE) DENOTES ELECTRICAL (**EY**) FIELD AND ORTHOGONAL MAGNETIC (**HX**) FIELD (=EY/HX)

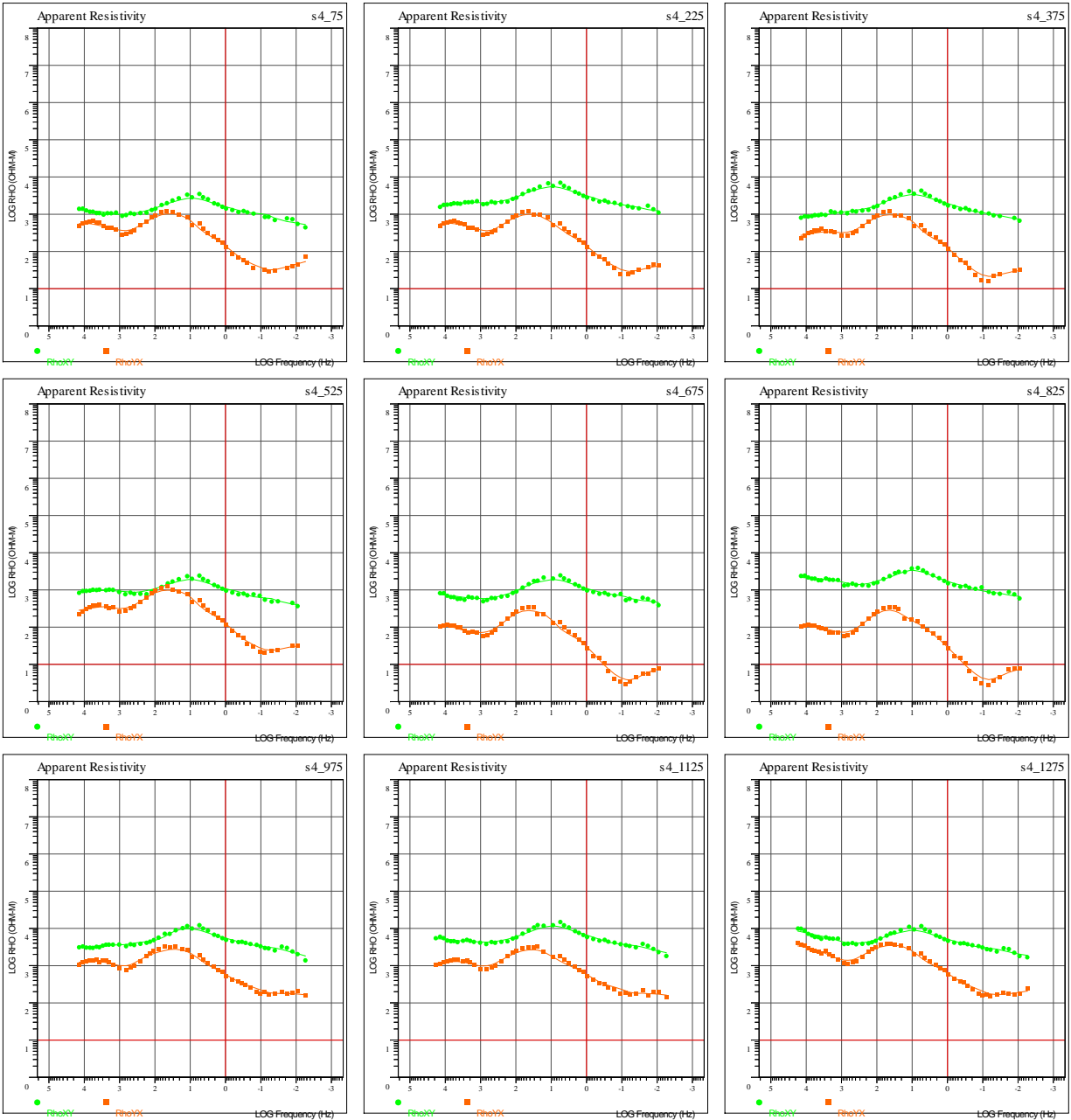


Spread 3 (X @ 23°) – Phase Sounding Curves vs Frequency.

MODE XY (GREEN) DENOTES ELECTRICAL (**EX**) FIELD AND ORTHOGONAL MAGNETIC (**HY**) FIELD (=EX/HY)

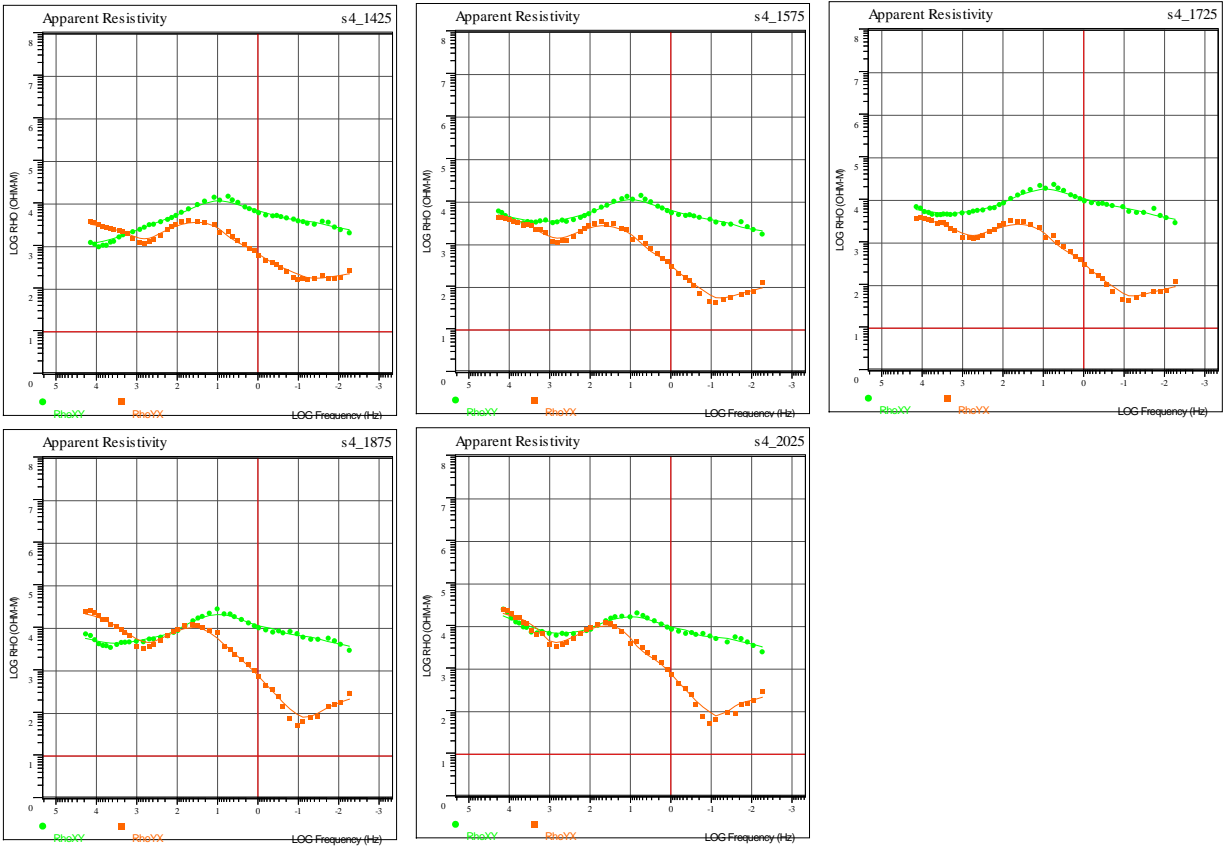
MODE YX (ORANGE) DENOTES ELECTRICAL (**EY**) FIELD AND ORTHOGONAL MAGNETIC (**HX**) FIELD (=EY/HX)

C.4 SPREAD 4 WITH X @ 130°



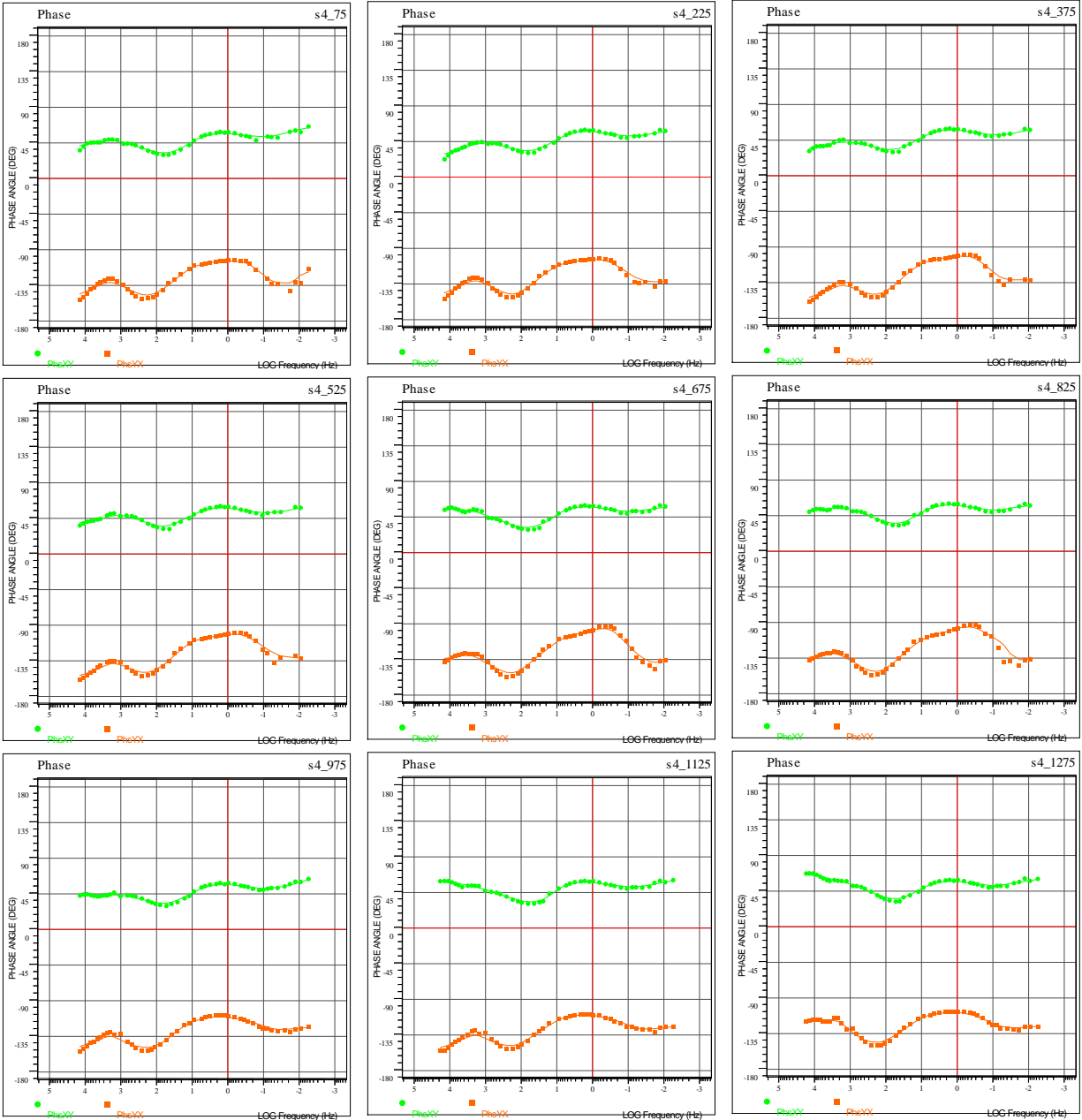
Spread 4 (X @ 130°) – Apparent Resistivity Sounding Curves vs Frequency (1 of 2).

MODE XY (GREEN) DENOTES ELECTRICAL (**EX**) FIELD AND ORTHOGONAL MAGNETIC (**HY**) FIELD (=EX/HY)
MODE YX (ORANGE) DENOTES ELECTRICAL (**EY**) FIELD AND ORTHOGONAL MAGNETIC (**HX**) FIELD (=EY/HX)



Spread 4 (X @ 130°) – Apparent Resistivity Sounding Curves vs Frequency (2 of 2).

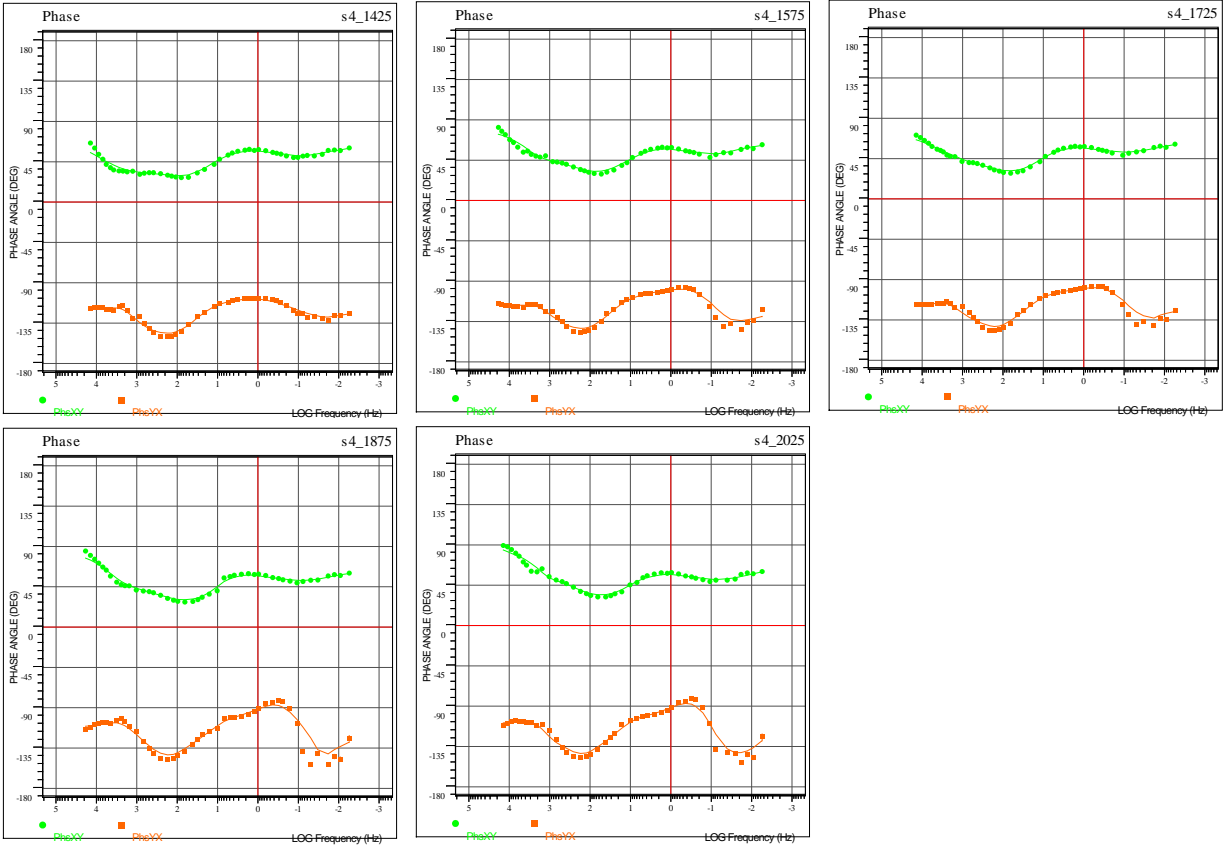
MODE XY (GREEN) DENOTES ELECTRICAL (**EX**) FIELD AND ORTHOGONAL MAGNETIC (**HY**) FIELD (=EX/HY)
MODE YX (ORANGE) DENOTES ELECTRICAL (**EY**) FIELD AND ORTHOGONAL MAGNETIC (**HX**) FIELD (=EY/HX)



Spread 4 (X @ 130°) – Phase Sounding Curves vs Frequency (1 of 2).

MODE XY (GREEN) DENOTES ELECTRICAL (**Ex**) FIELD AND ORTHOGONAL MAGNETIC (**Hy**) FIELD (=Ex/Hy)

MODE YX (ORANGE) DENOTES ELECTRICAL (**Ey**) FIELD AND ORTHOGONAL MAGNETIC (**Hx**) FIELD (=Ey/Hx)

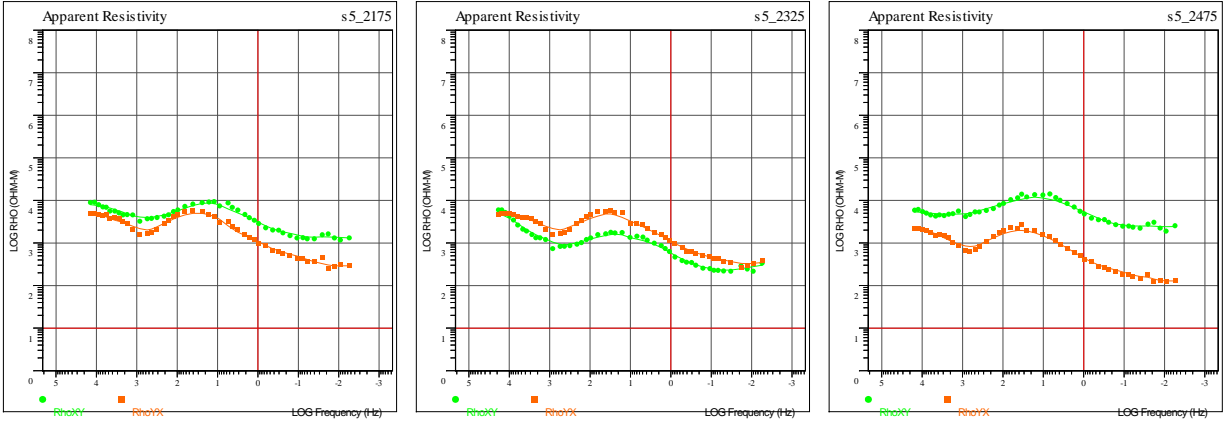


Spread 4 (X @ 130°) – Phase Sounding Curves vs Frequency (2 of 2).

MODE XY (GREEN) DENOTES ELECTRICAL (**EX**) FIELD AND ORTHOGONAL MAGNETIC (**HY**) FIELD (=EX/HY)

MODE YX (ORANGE) DENOTES ELECTRICAL (**EY**) FIELD AND ORTHOGONAL MAGNETIC (**HX**) FIELD (=EY/HX)

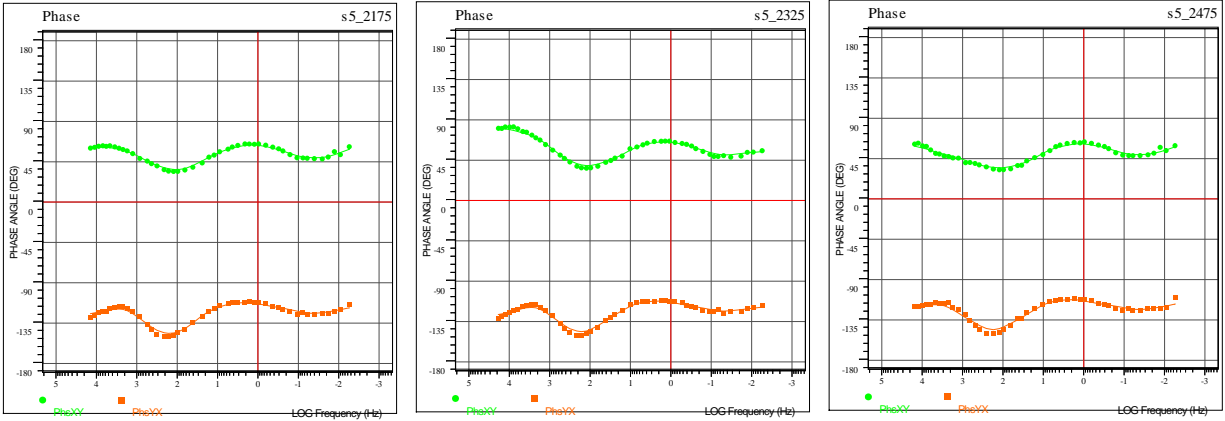
C.5 SPREAD 5 WITH X @ 93°



Spread 5 (X @ 93°) – Apparent Resistivity Sounding Curves vs Frequency.

MODE XY (GREEN) DENOTES ELECTRICAL (**Ex**) FIELD AND ORTHOGONAL MAGNETIC (**Hy**) FIELD (=Ex/Hy)

MODE YX (ORANGE) DENOTES ELECTRICAL (**Ey**) FIELD AND ORTHOGONAL MAGNETIC (**Hx**) FIELD (=Ey/Hx)

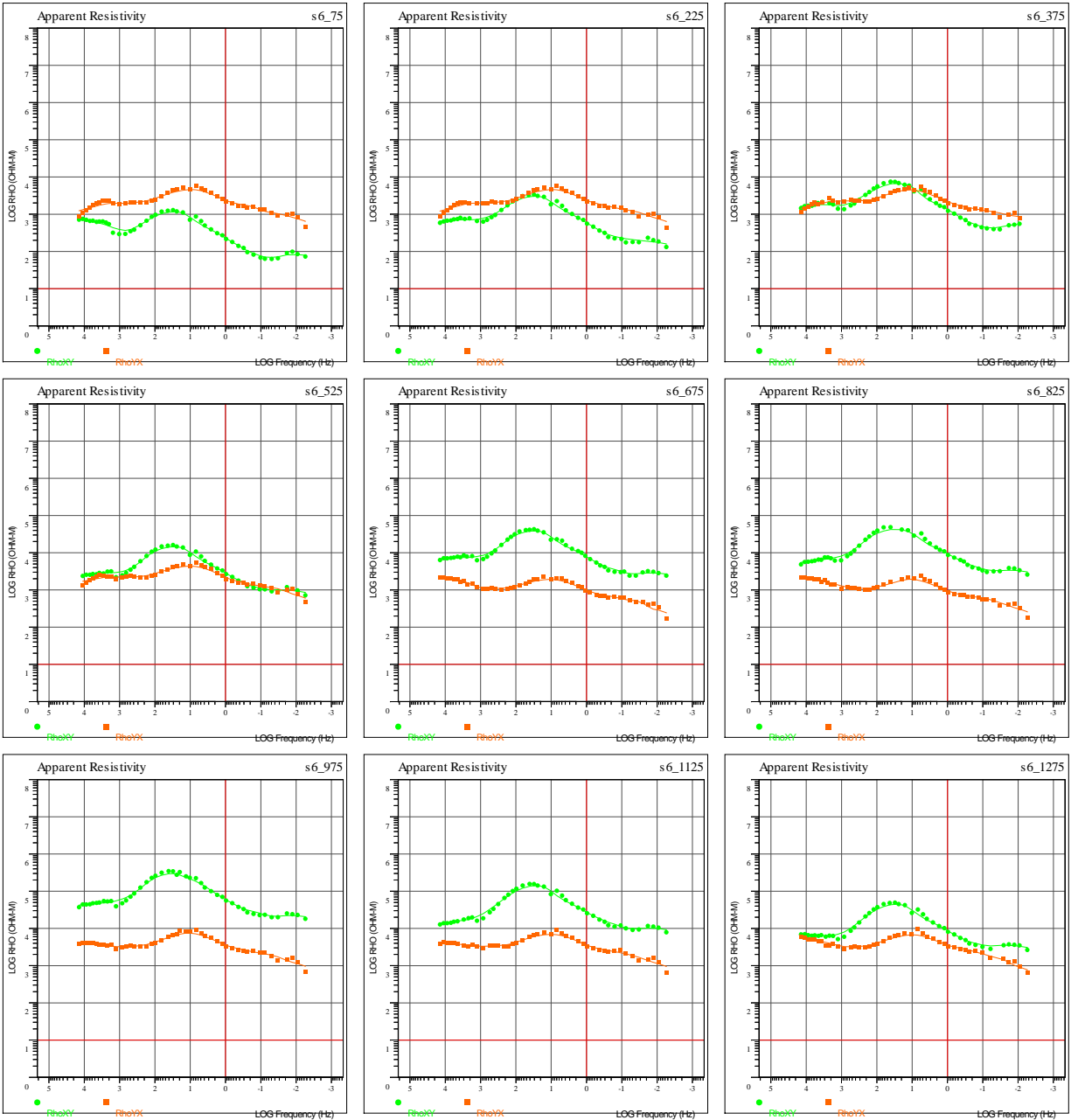


Spread 5 (X @ 93°) – Phase Sounding Curves vs Frequency.

MODE XY (GREEN) DENOTES ELECTRICAL (**Ex**) FIELD AND ORTHOGONAL MAGNETIC (**Hy**) FIELD (=Ex/Hy)

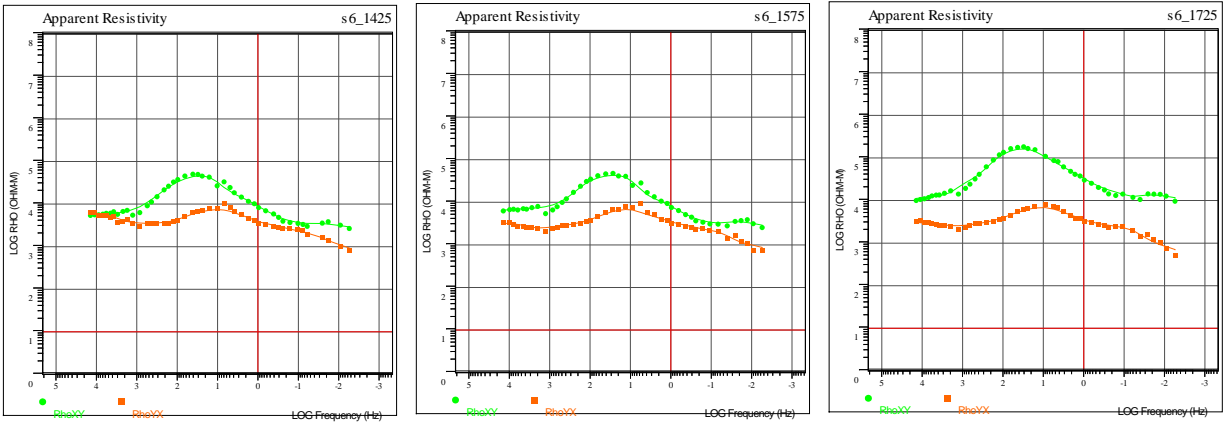
MODE YX (ORANGE) DENOTES ELECTRICAL (**Ey**) FIELD AND ORTHOGONAL MAGNETIC (**Hx**) FIELD (=Ey/Hx)

C.6 SPREAD 6 WITH X @ 26°



Spread 6 (X @ 26°) – Apparent Resistivity Sounding Curves vs Frequency (1 of 2).

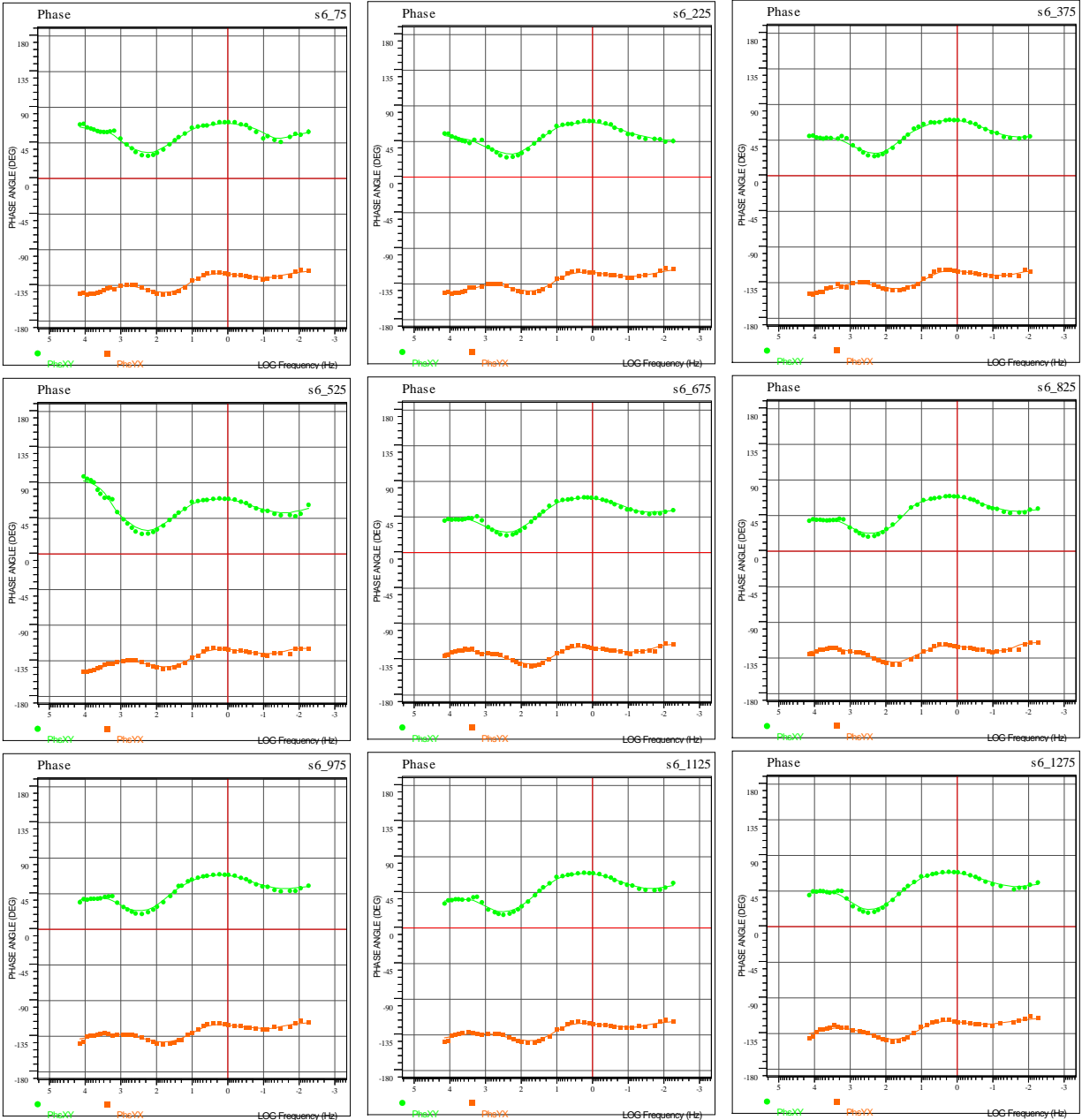
MODE XY (GREEN) DENOTES ELECTRICAL (**EX**) FIELD AND ORTHOGONAL MAGNETIC (**HY**) FIELD (=EX/HY)
MODE YX (ORANGE) DENOTES ELECTRICAL (**EY**) FIELD AND ORTHOGONAL MAGNETIC (**HX**) FIELD (=EY/HX)



Spread 6 (X @ 26°) – Apparent Resistivity Sounding Curves vs Frequency (2 of 2).

MODE XY (GREEN) DENOTES ELECTRICAL (**Ex**) FIELD AND ORTHOGONAL MAGNETIC (**Hy**) FIELD (=Ex/Hy)

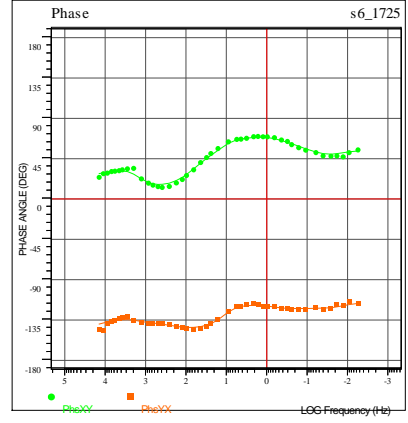
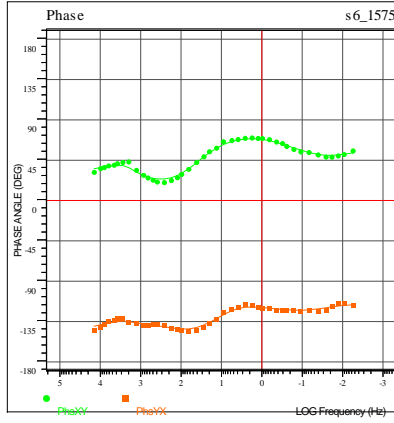
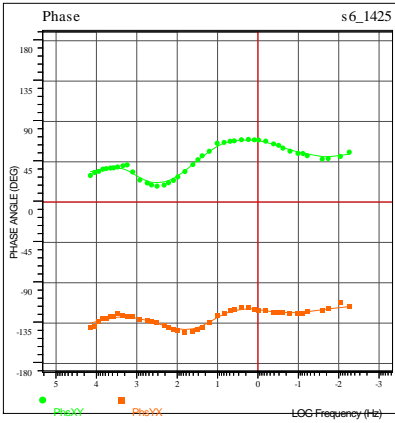
MODE YX (ORANGE) DENOTES ELECTRICAL (**Ey**) FIELD AND ORTHOGONAL MAGNETIC (**Hx**) FIELD (=Ey/Hx)



Spread 6 (X @ 26°) – Phase Sounding Curves vs Frequency (1 of 2).

MODE XY (GREEN) DENOTES ELECTRICAL (EX) FIELD AND ORTHOGONAL MAGNETIC (HY) FIELD (=EX/HY)

MODE YX (ORANGE) DENOTES ELECTRICAL (EY) FIELD AND ORTHOGONAL MAGNETIC (HX) FIELD (=EY/HX)



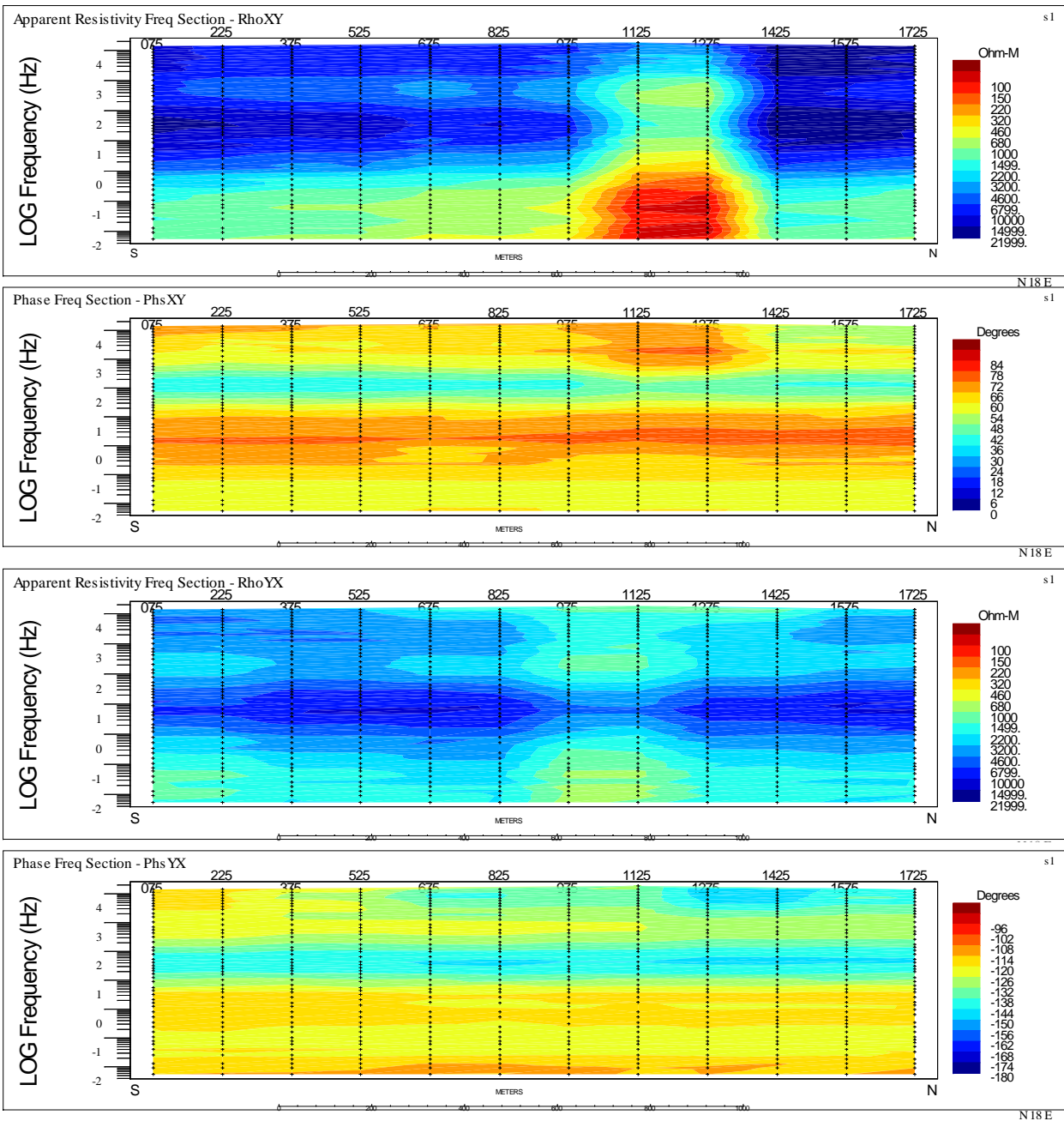
Spread 6 (X @ 26°) – Phase Sounding Curves vs Frequency (2 of 2).

MODE XY (GREEN) DENOTES ELECTRICAL (**EX**) FIELD AND ORTHOGONAL MAGNETIC (**HY**) FIELD (=EX/HY)

MODE YX (ORANGE) DENOTES ELECTRICAL (**EY**) FIELD AND ORTHOGONAL MAGNETIC (**HX**) FIELD (=EY/HX)

D MT PSEUDO-SECTIONS OF FINAL PROCESSED DATA

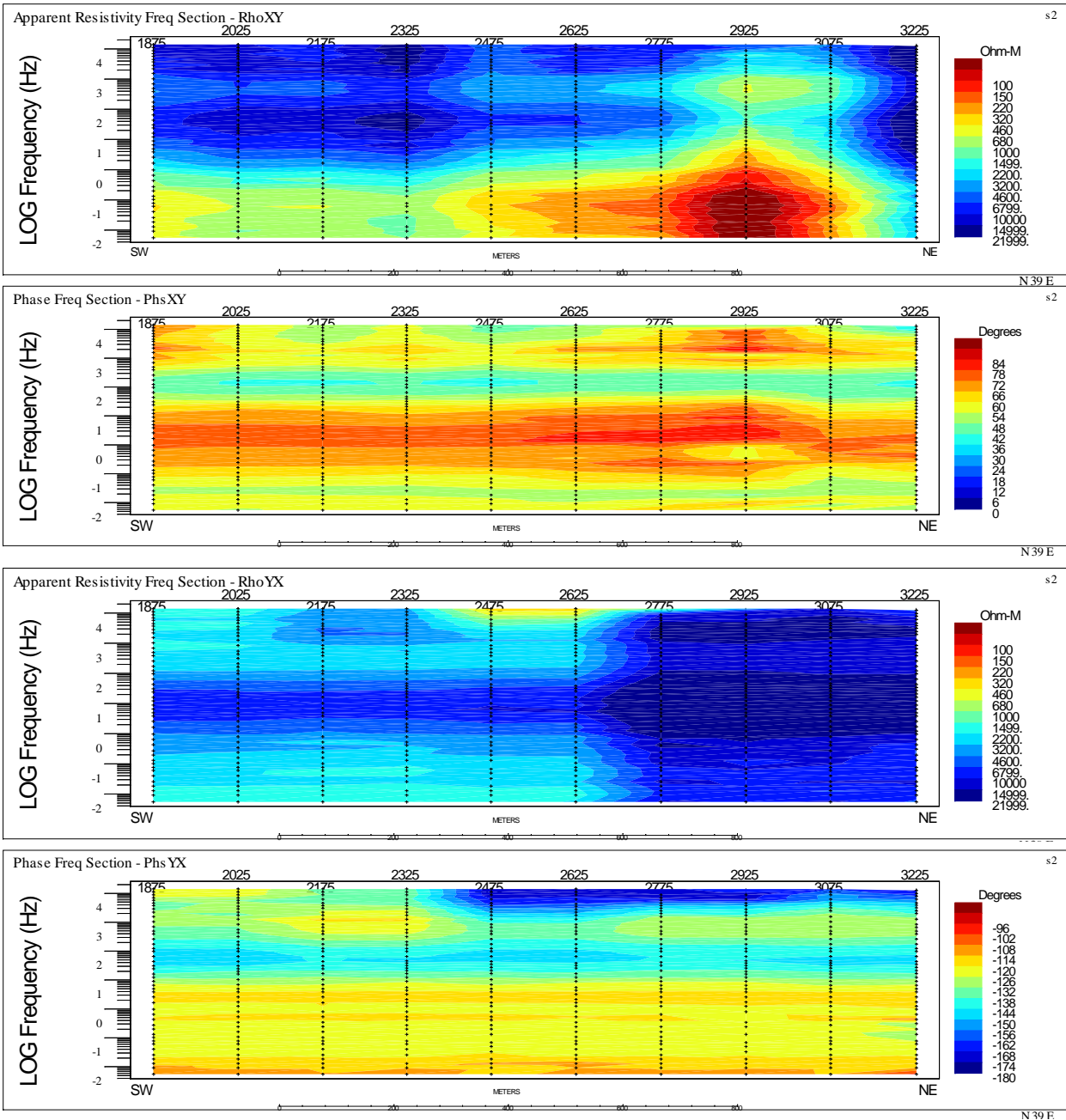
D.1 SPREAD 1 WITH X @ 17°



Spread 1 – Apparent Resistivity and Phase (XY & YX) Pseudo-Section.

STRIP 1 (TOP): RHO XY – STRIP 2: PHASE XY – STRIP 3: RHO YX – STRIP 4 (BOTTOM): PHASE YX
WHERE XY DENOTES ELECTRICAL (EX) FIELD AND ORTHOGONAL MAGNETIC (HY) FIELD (=EX/HY)
AND YX DENOTES ELECTRICAL (EY) FIELD AND ORTHOGONAL MAGNETIC (HX) FIELD (=EY/HX)

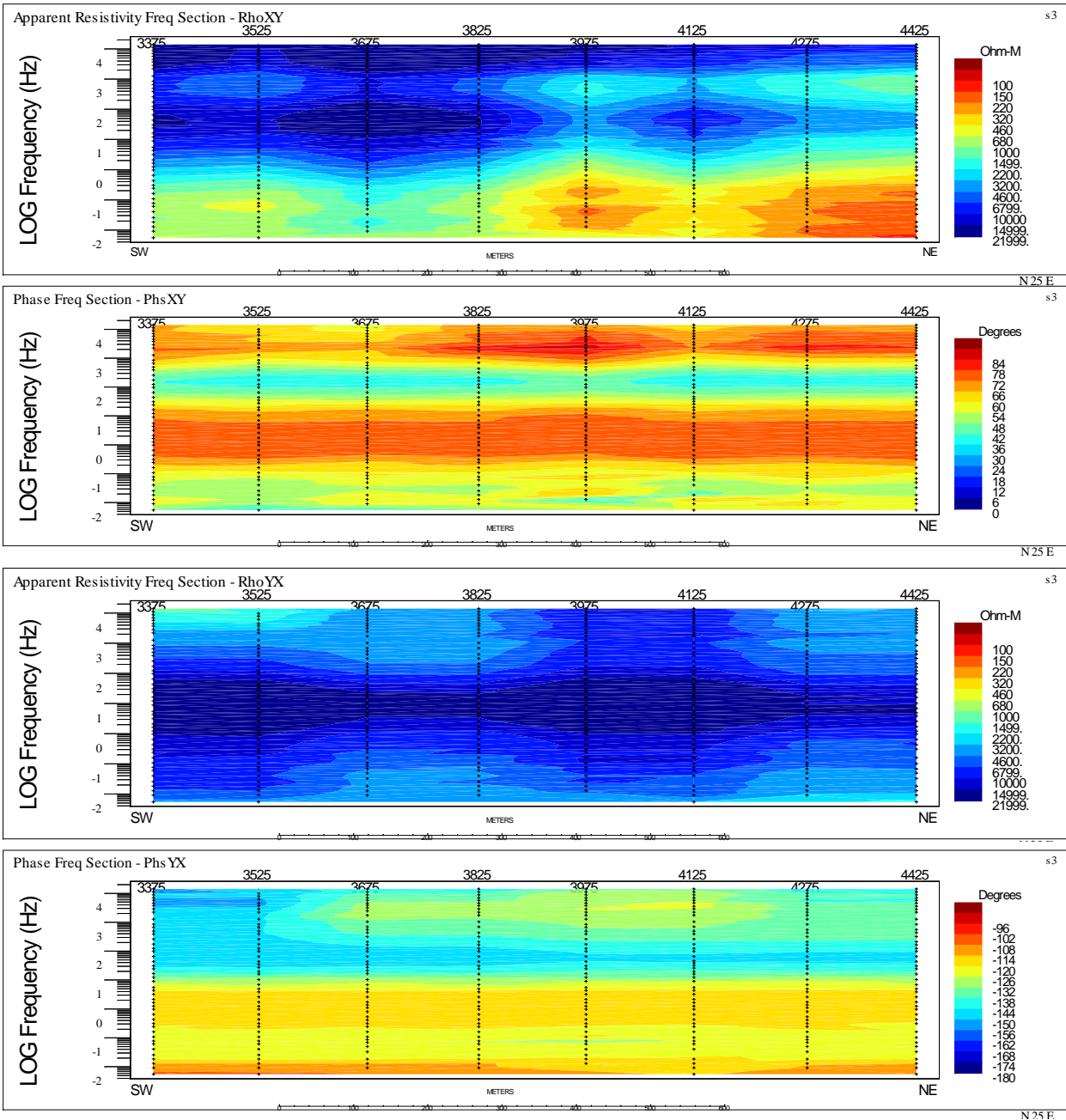
D.2 SPREAD 2 WITH X @ 38°



Spread 2 – Apparent Resistivity and Phase (XY & YX) Pseudo-Section.

STRIP 1 (TOP): RHO XY – STRIP 2: PHASE XY – STRIP 3: RHO YX – STRIP 4 (BOTTOM): PHASE YX
WHERE XY DENOTES ELECTRICAL (EX) FIELD AND ORTHOGONAL MAGNETIC (HY) FIELD (=EX/HY)
AND YX DENOTES ELECTRICAL (EY) FIELD AND ORTHOGONAL MAGNETIC (HX) FIELD (=EY/HX)

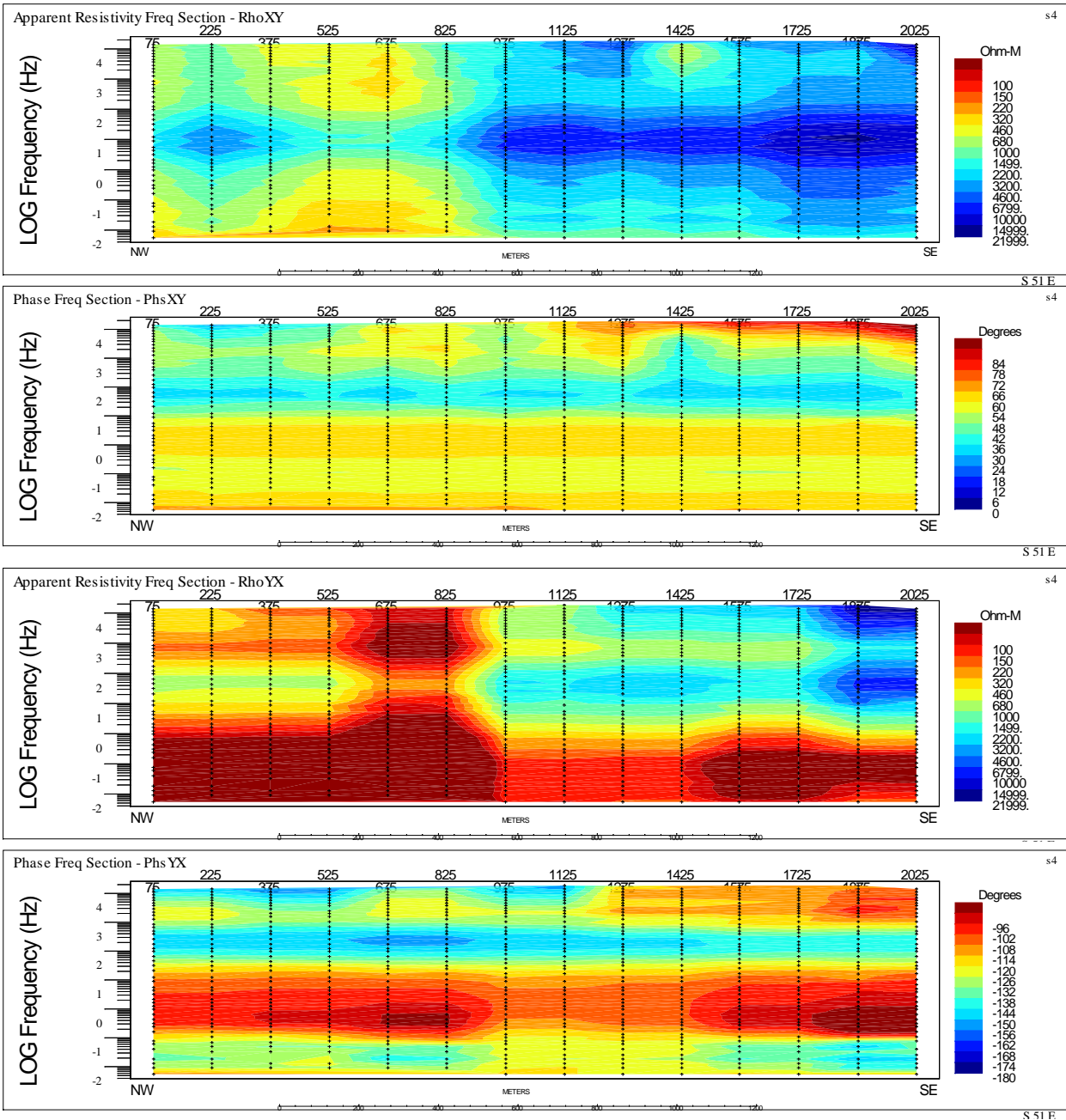
D.3 SPREAD 3 WITH X @ 23°



Spread 3 – Apparent Resistivity and Phase (XY & YX) Pseudo-Section.

STRIP 1 (TOP): RHO XY – STRIP 2: PHASE XY – STRIP 3: RHO YX – STRIP 4 (BOTTOM): PHASE YX
WHERE XY DENOTES ELECTRICAL (Ex) FIELD AND ORTHOGONAL MAGNETIC (Hy) FIELD (=Ex/Hy)
AND YX DENOTES ELECTRICAL (Ey) FIELD AND ORTHOGONAL MAGNETIC (Hx) FIELD (=Ey/Hx)

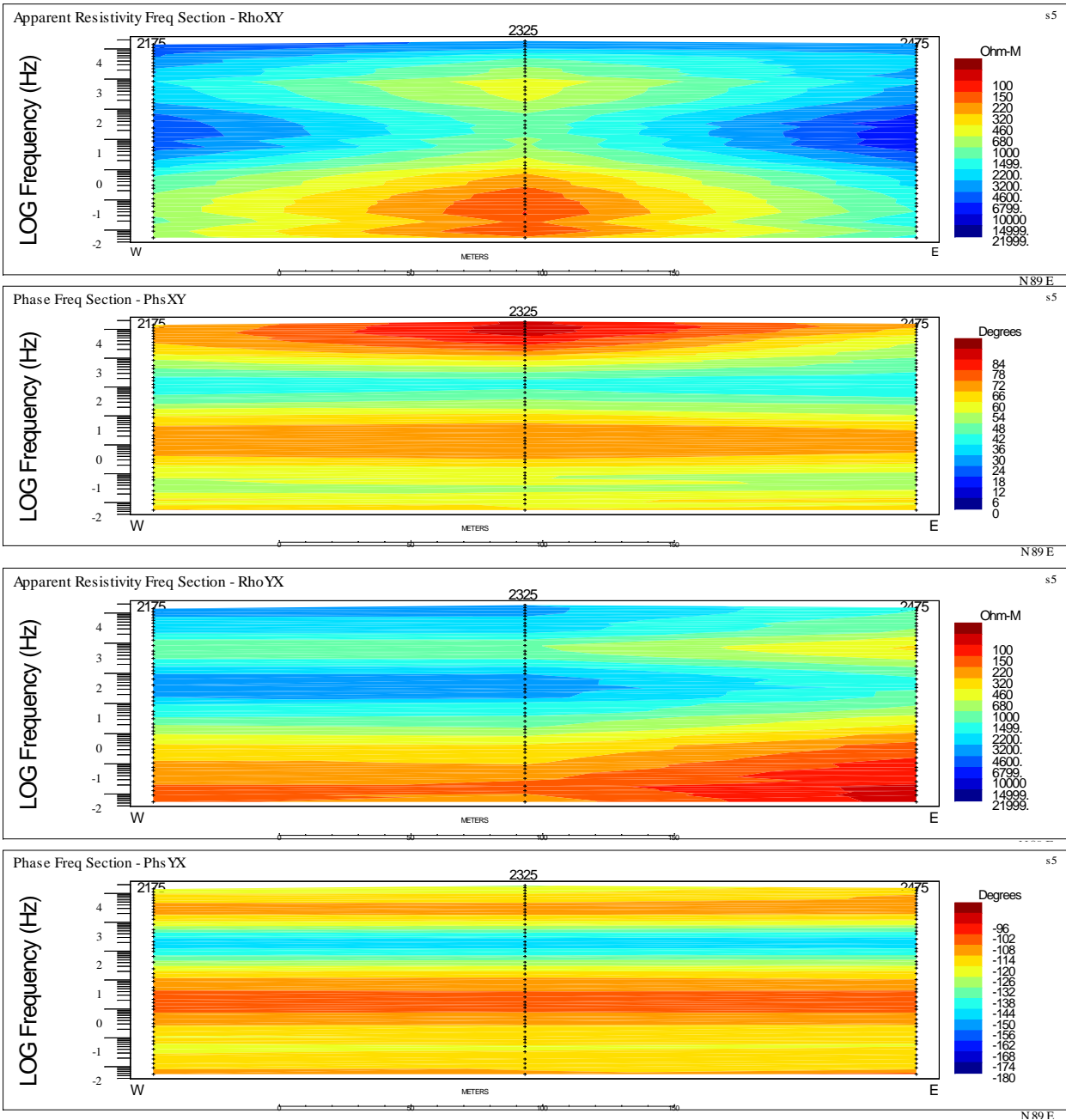
D.4 SPREAD 4 WITH X @ 130°



Spread 4 – Apparent Resistivity and Phase (XY & YX) Pseudo-Section.

STRIP 1 (TOP): RHO XY – STRIP 2: PHASE XY – STRIP 3: RHO YX – STRIP 4 (BOTTOM): PHASE YX
WHERE XY DENOTES ELECTRICAL (Ex) FIELD AND ORTHOGONAL MAGNETIC (Hy) FIELD (=Ex/Hy)
AND YX DENOTES ELECTRICAL (Ey) FIELD AND ORTHOGONAL MAGNETIC (Hx) FIELD (=Ey/Hx)

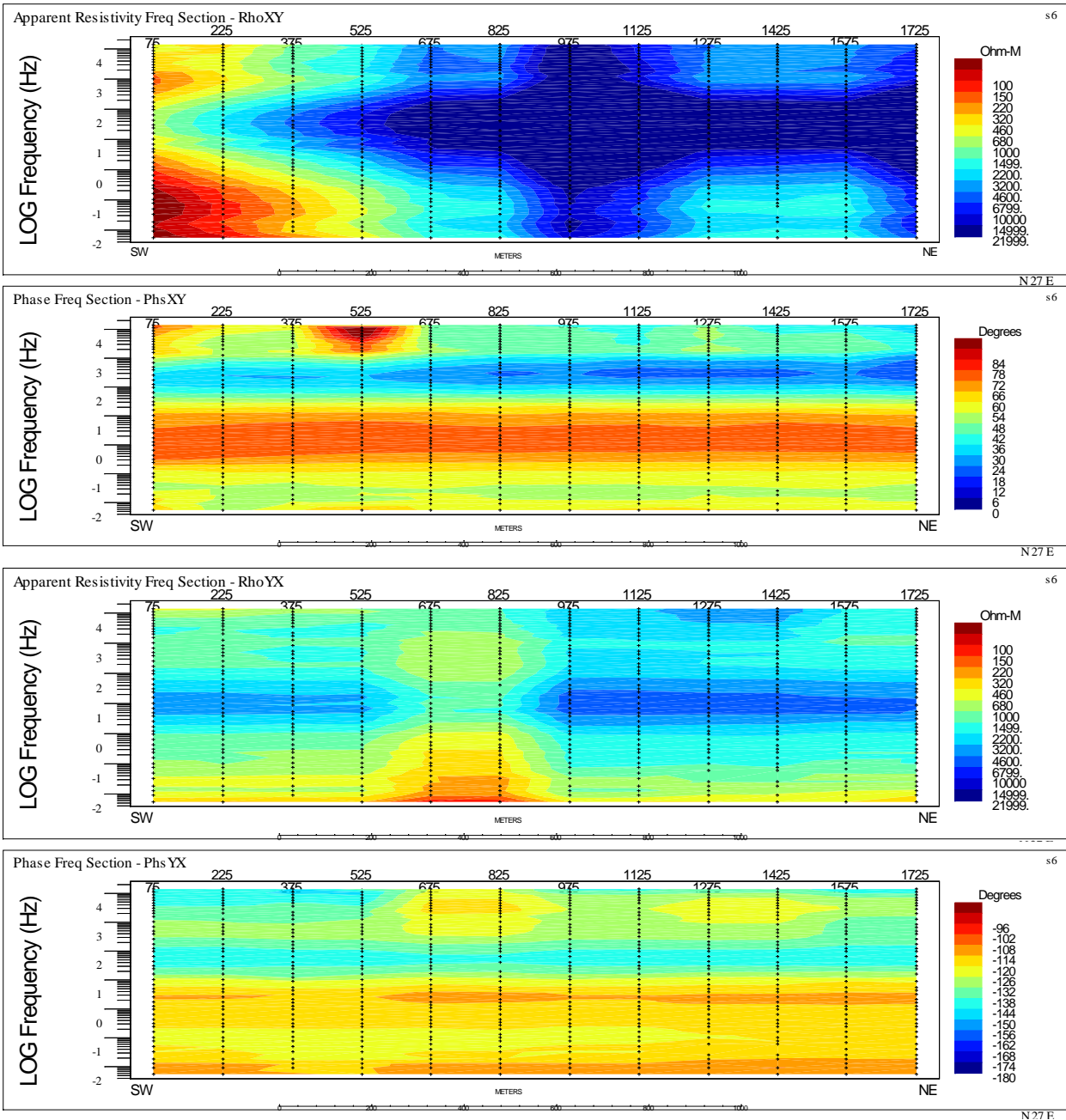
D.5 SPREAD 5 WITH X @ 93°



Spread 5 – Apparent Resistivity and Phase (XY & YX) Pseudo-Section.

STRIP 1 (TOP): RHO XY – STRIP 2: PHASE XY – STRIP 3: RHO YX – STRIP 4 (BOTTOM): PHASE YX
WHERE XY DENOTES ELECTRICAL (Ex) FIELD AND ORTHOGONAL MAGNETIC (Hy) FIELD (=Ex/Hy)
AND YX DENOTES ELECTRICAL (Ey) FIELD AND ORTHOGONAL MAGNETIC (Hx) FIELD (=Ey/Hx)

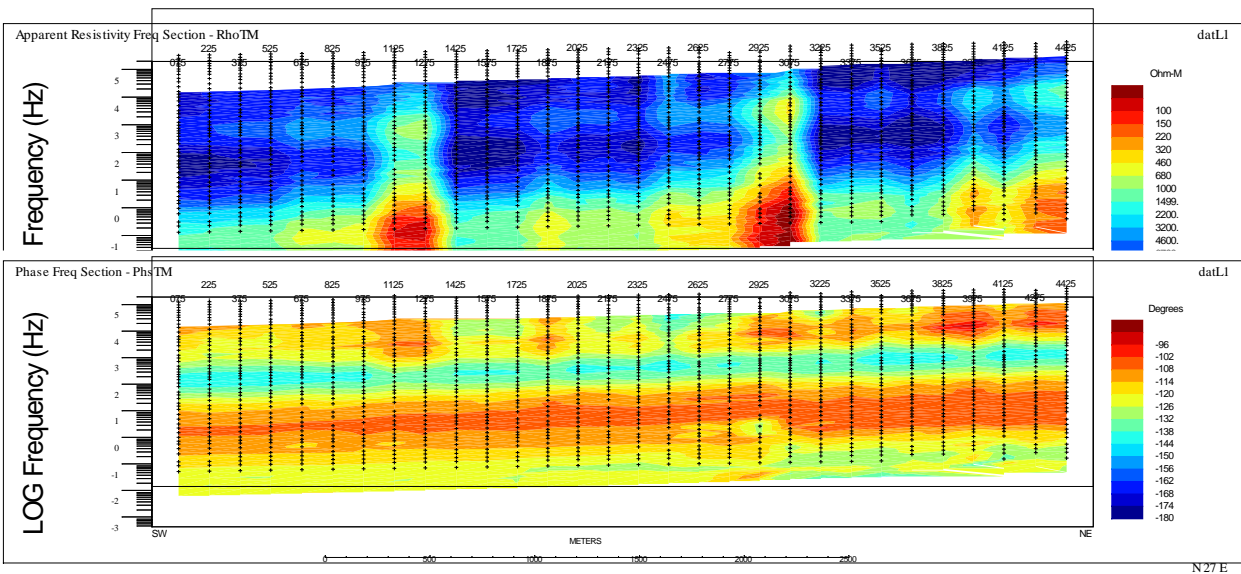
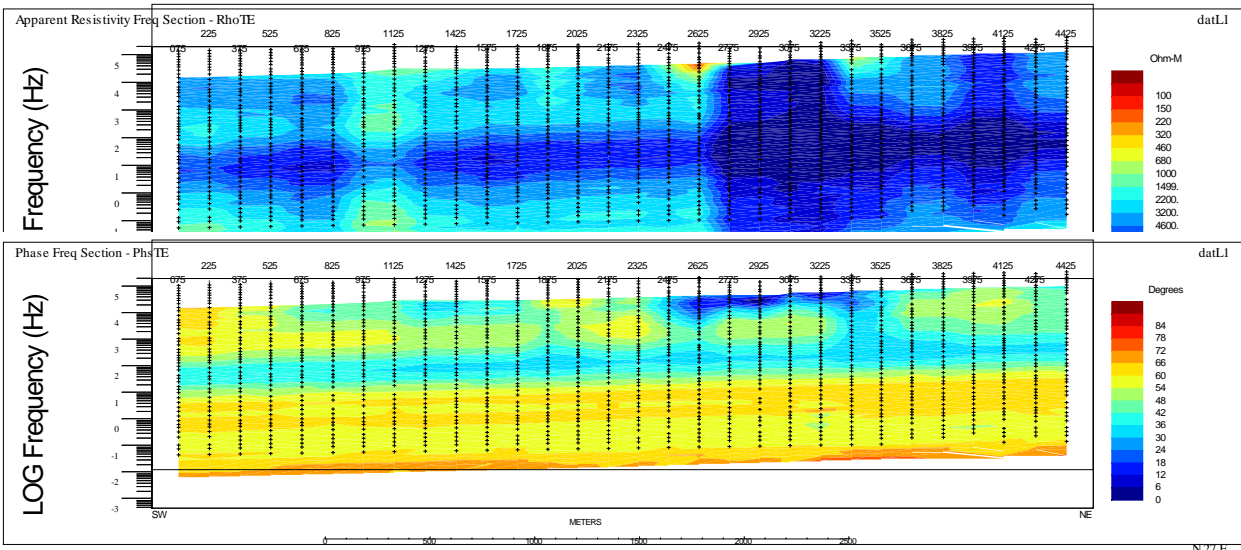
D.6 SPREAD 6 WITH X @ 26°



Spread 6 – Apparent Resistivity and Phase (XY & YX) Pseudo-Section.

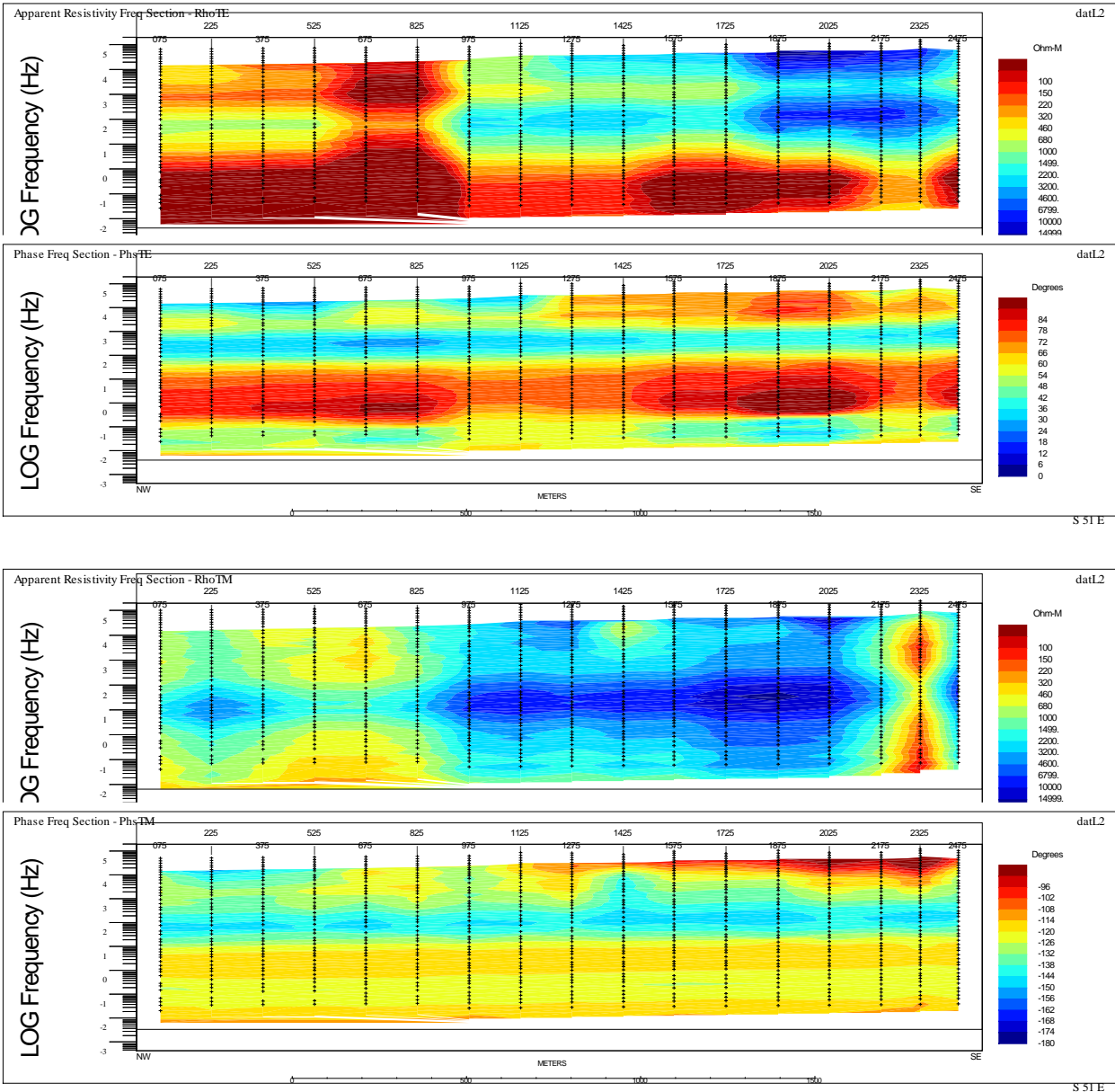
STRIP 1 (TOP): RHO XY – STRIP 2: PHASE XY – STRIP 3: RHO YX – STRIP 4 (BOTTOM): PHASE YX
WHERE XY DENOTES ELECTRICAL (EX) FIELD AND ORTHOGONAL MAGNETIC (HY) FIELD (=EX/HY)
AND YX DENOTES ELECTRICAL (EY) FIELD AND ORTHOGONAL MAGNETIC (HX) FIELD (=EY/HX)

E.1 LINE L100 WITH X @ -63° (TE = XY)



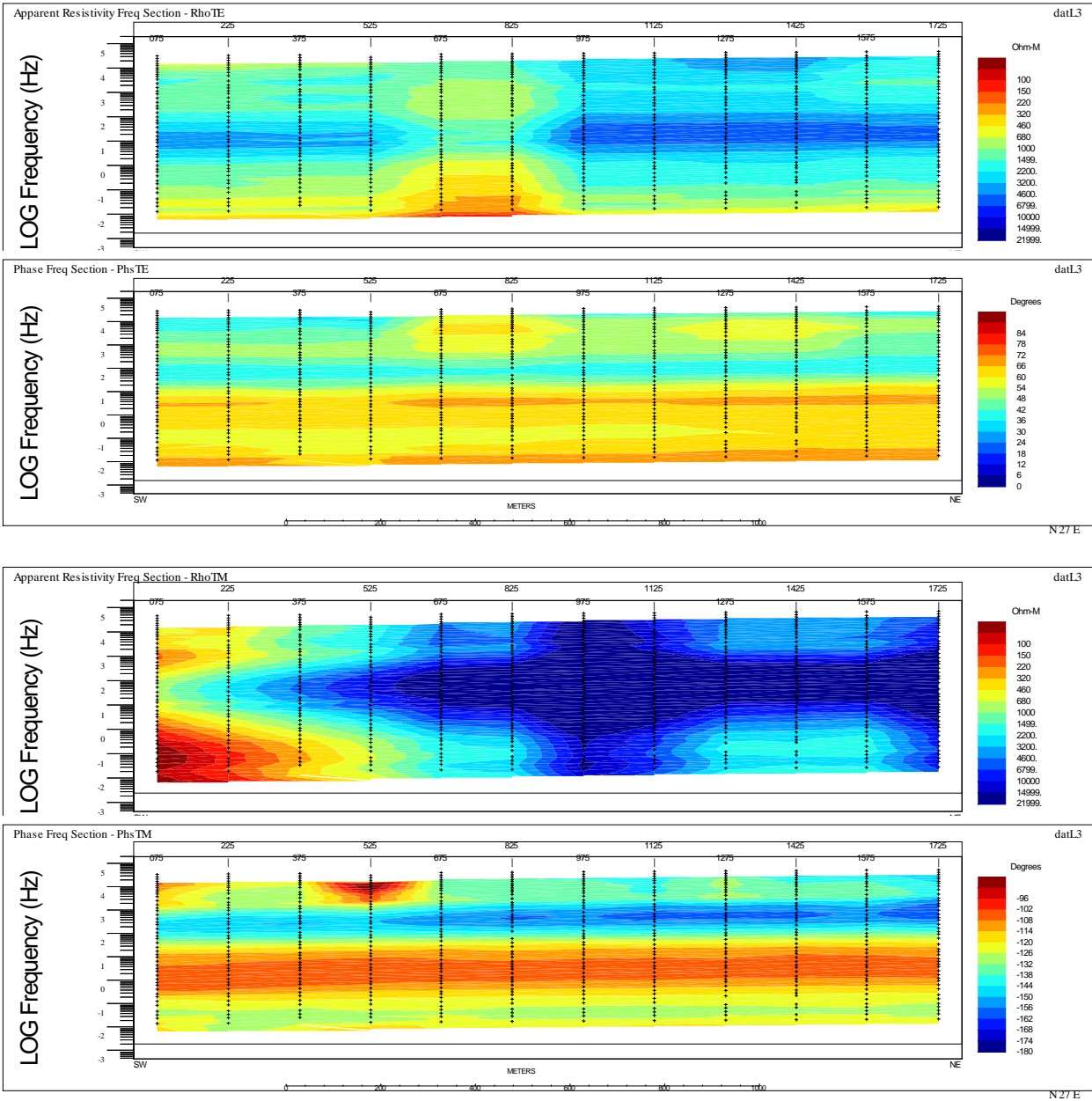
STRIP 1 (TOP): RHO TE – STRIP 2: PHASE TE – STRIP 3: RHO TM – STRIP 4 (BOTTOM): PHASE TM
WHERE TE = XY DENOTES ELECTRICAL (Ex) FIELD AND ORTHOGONAL MAGNETIC (Hy) FIELD (=Ex/Hy)
AND TM = YX DENOTES ELECTRICAL (Ey) FIELD AND ORTHOGONAL MAGNETIC (Hx) FIELD (=Ey/Hx)

E.2 LINE L200 WITH X @ +39° (TE = XY)



STRIP 1 (TOP): RHO TE – STRIP 2: PHASE TE – STRIP 3: RHO TM – STRIP 4 (BOTTOM): PHASE TM
WHERE TE = XY DENOTES ELECTRICAL (EX) FIELD AND ORTHOGONAL MAGNETIC (HY) FIELD (=EX/HY)
AND TM = YX DENOTES ELECTRICAL (EY) FIELD AND ORTHOGONAL MAGNETIC (HX) FIELD (=EY/HX)

E.3 LINE L300 WITH X @ -63° (TE = XY)



STRIP 1 (TOP): RHO TE – STRIP 2: PHASE TE – STRIP 3: RHO TM – STRIP 4 (BOTTOM): PHASE TM
WHERE TE = XY DENOTES ELECTRICAL (EX) FIELD AND ORTHOGONAL MAGNETIC (HY) FIELD (=EX/HY)
AND TM = YX DENOTES ELECTRICAL (EY) FIELD AND ORTHOGONAL MAGNETIC (HX) FIELD (=EY/HX)

F PARALLEL SENSOR TEST

Project CA00927T
Date: February 24th - 25th, 2012
Report by: Mojtaba Daneshvar
Staff: Wade lee
Mike Belben
Joey Plouff

QuickLay Version 4.00.10
Common folder V1.54
Datum: UTM WGS 84 / Zone 17T
Station: 405804mE / 5160727mN
Coil Azimuth: 0° true
Magnetic Declination 11° W

Results:

GHF-1071: Weak performance. Poor PSD, amplitude and phase.
P50-3130: Weak coherency

F.1 LOW FREQUENCY COILS

Available Coils.

TS Strip	Manufacture	Serial #	Task for
1	Phoenix	P50-3120	Spare
2	Phoenix	P50-3130	Spare
3	Phoenix	P50-3106	Remote Hx
4	Phoenix	P50-3107	Remote Hy
5	Phoenix	P50-3108	Line Hx
6	Phoenix	P50-3113	Line Hy
7	Phoenix	P50-3125	Line Hx
8	Phoenix	P50-3129	Line Hy

Processing Parameters.

Parameters	Values
PSD Method	Welch
Window	Hanning
Window Length	4096
Segment Overlap	50%

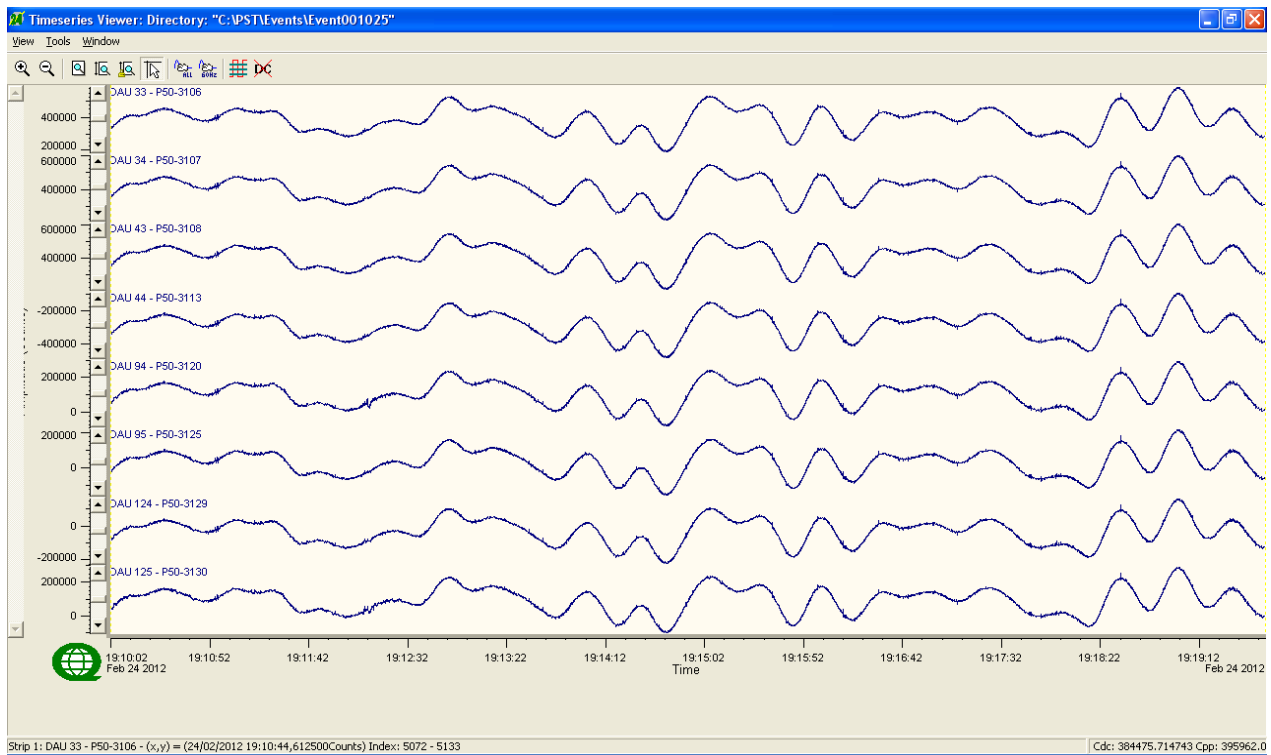
F.1.1 TEST RESULTS: 120SPS

NetEvent: 9036.001025
Sample Rate: 120sps
TS Length: 70,000 samples (~9min 43s)

Results:

P50-3130: lower coherency

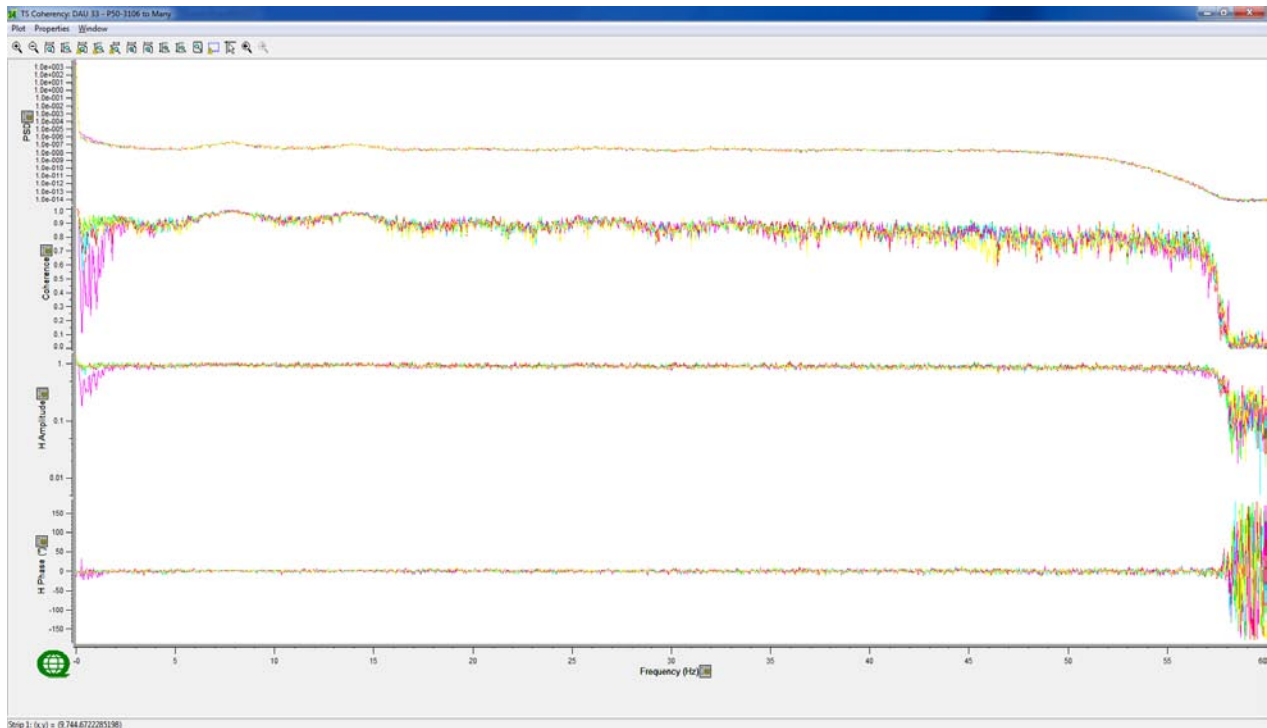
Time Series



Complete time series @ 120sps.

Low Frequency Coil Results:

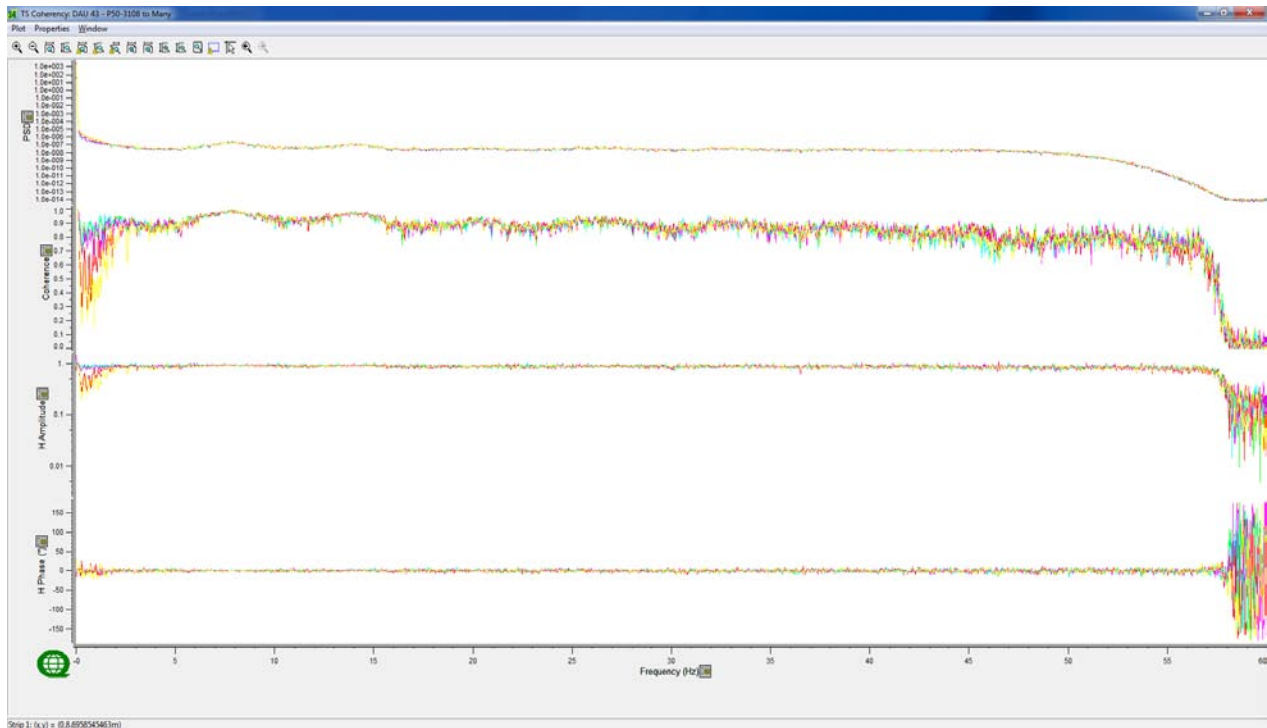
PSD of channels (strip 1), Coherency (strip 2) and Response Function (strips 3&4; Amplitude and Phase) compared to **Reference Channel P50-3106 (blue)** – *Linear frequency scale*.



Colour	Channel	Notes
Blue	P50-3106	
Green	P50-3107	
Red	P50-3108	
Cyan	P50-3113	
Magenta	P50-3120	
Yellow	P50-3125	This coil shows slightly lower coherency

Low Frequency Coil Results (continued):

PSD of channels (strip 1), Coherency (strip 2) and Response Function (strips 3&4; Amplitude and Phase) compared to **Reference Channel P50-3108 (blue)** – *Linear frequency scale*.

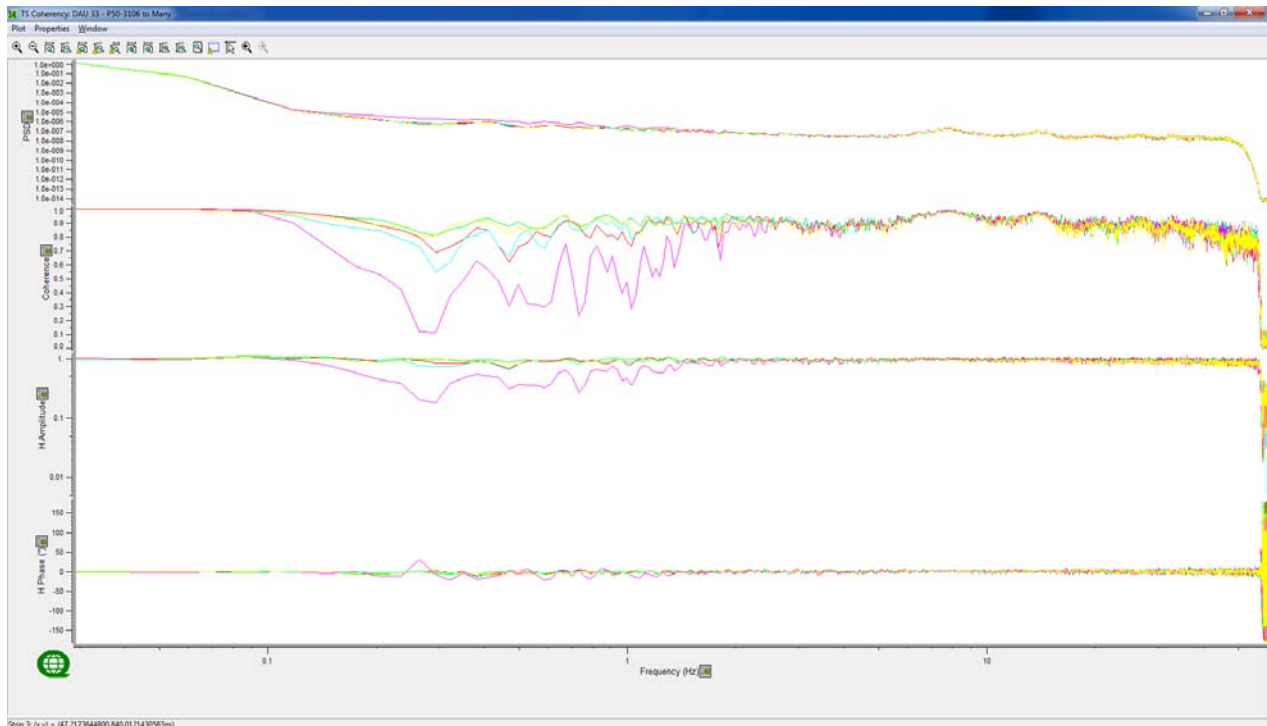


Strip 1: (x,y) = (0.8,0.05045463m)

Colour	Channel	Notes
Blue	P50-3108	
Green	P50-3113	
Red	P50-3120	Less coherent at lower frequencies
Cyan	P50-3125	
Magenta	P50-3129	
Yellow	P50-3130	Less coherent at lower frequencies

Low Frequency Coil Results (continued):

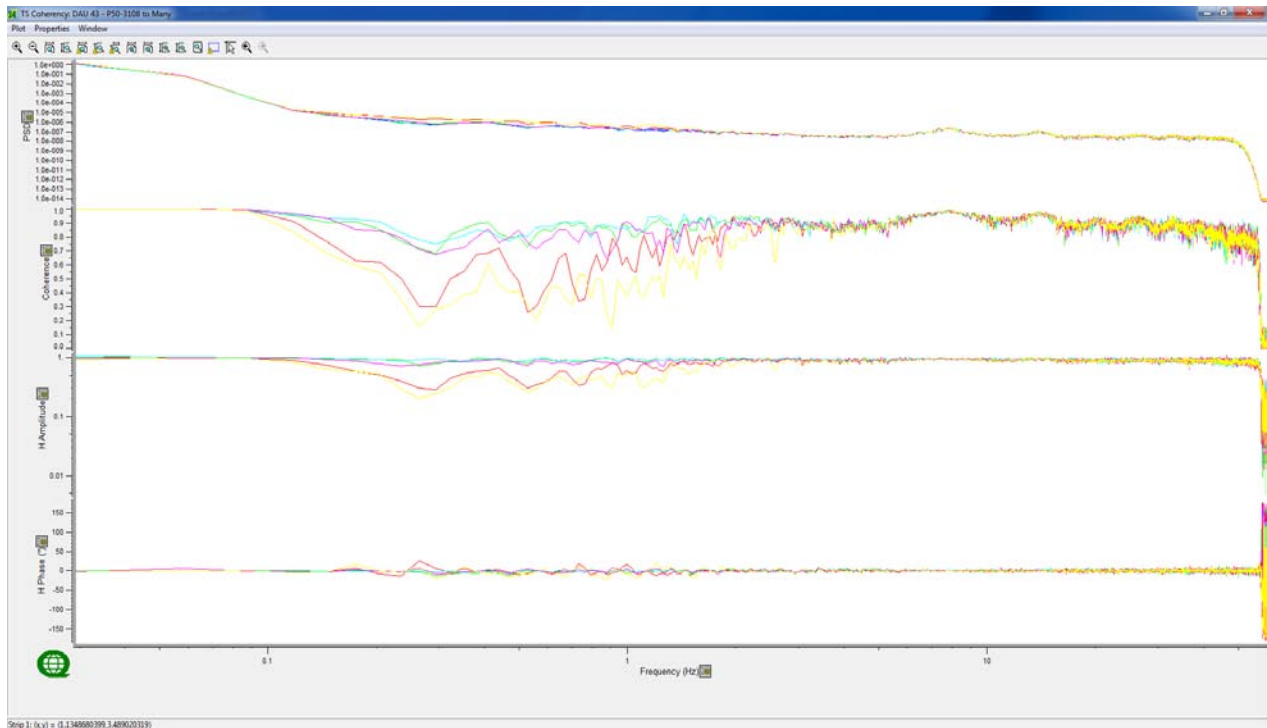
PSD of channels (strip 1), Coherency (strip 2) and Response Function (strips 3&4; Amplitude and Phase) compared to **Reference Channel P50-3106 (Blue)** – *Logarithmic frequency scale.*



Colour	Channel	Notes
Blue	P50-3106	
Green	P50-3107	
Red	P50-3108	
Cyan	P50-3113	
Magenta	P50-3120	Coil has low coherency
Yellow	P50-3125	

Low Frequency Coil Results (continued):

PSD of channels (strip 1), Coherency (strip 2) and Response Function (strips 3&4; Amplitude and Phase) compared to **Reference Channel P50-3108 (Blue)** – *Logarithmic frequency scale.*



Colour	Channel	Notes
Blue	P50-3108	
Green	P50-3113	
Red	P50-3120	weak coherency
Cyan	P50-3125	
Magenta	P50-3129	
Yellow	P50-3130	Weak coherency

F.2 HIGH FREQUENCY COILS

Available Coils.

TS Strip	Manufacture	Serial #	Task for
1	Geometrics	GHF-1071	Spare
2	Geometrics	GHF-1065	Spare
3	Geometrics	GHF-1044	Remote Hx
4	Geometrics	GHF-1048	Remote Hy
5	Geometrics	GHF-1052	Line Hx
6	Geometrics	GHF-1053	Line Hy
7	Geometrics	GHF-1068	Line Hx
8	Geometrics	GHF-1074	Line Hy

Processing Parameters.

Parameters	Values
PSD Method	Welch
Window	Hanning
Window Length	4096
Segment Overlap	50%

F.2.1 TEST RESULTS: 48KSPS

NetEvent: 9036.001043 & 9036.001049

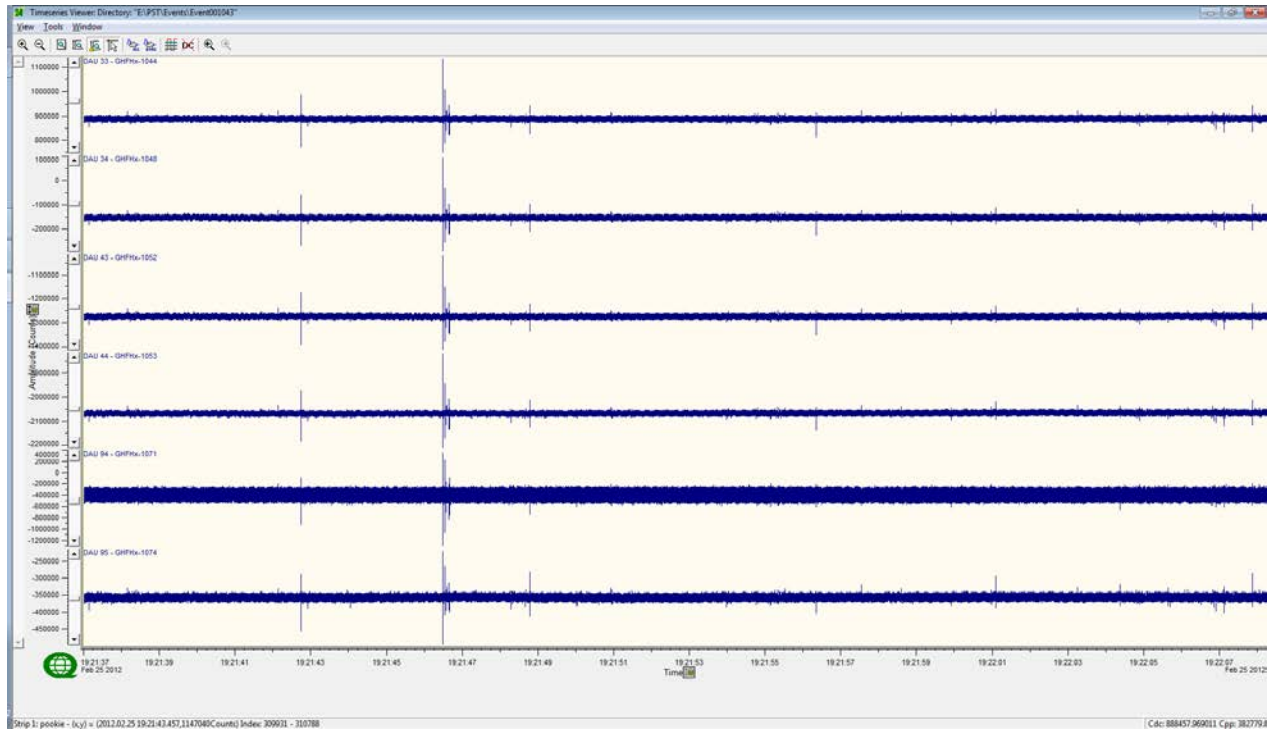
Sample Rate: 48ksps

TS Length: 1,500,000 samples (~31s)

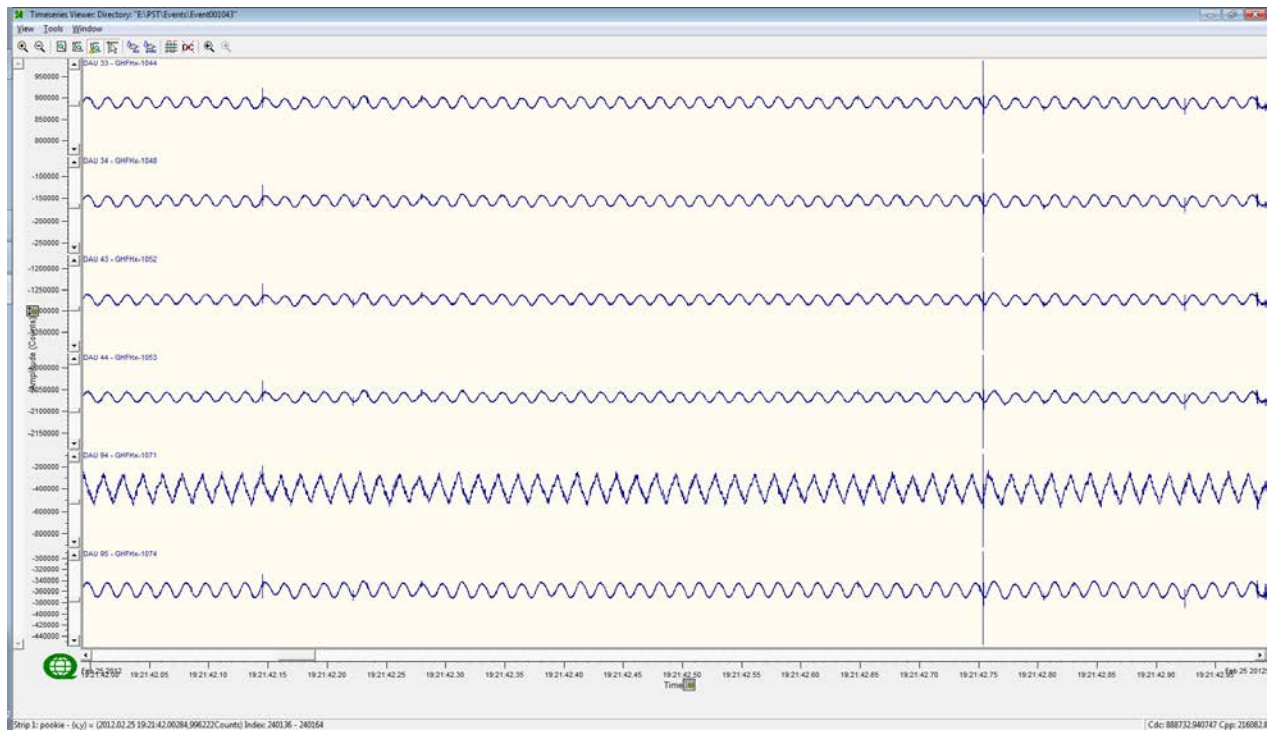
Results:

GHF-1071 This coil show very weak PSD, amplitude and phase.

Time Series

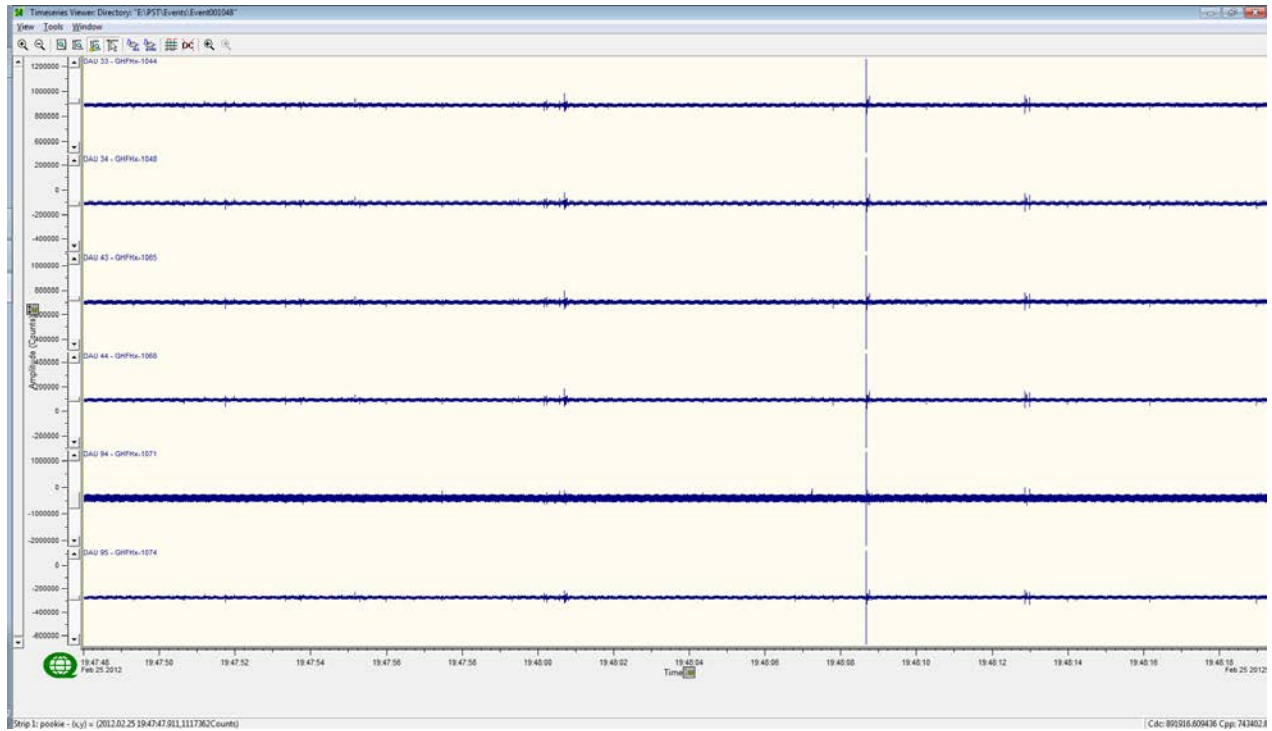


NetEvent9036.001043 Complete time series at 48kps.

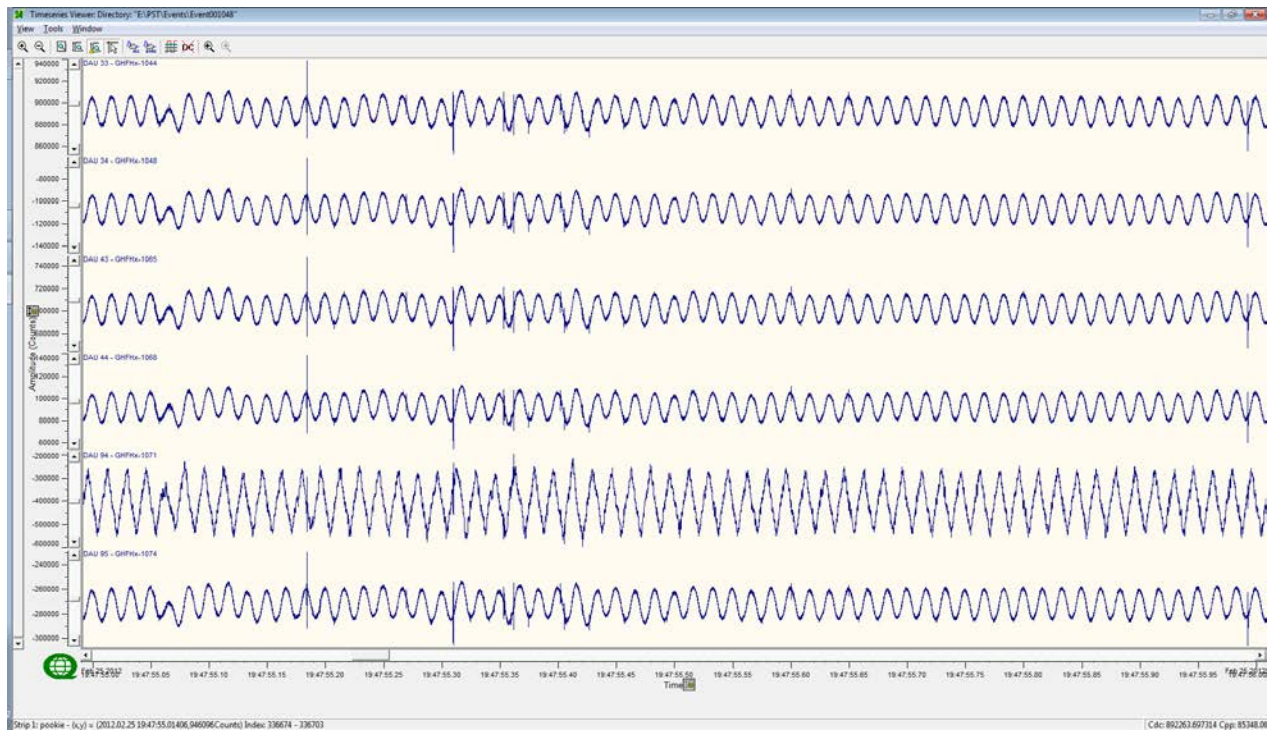


NetEvent9036.001043 Time series focused in on ~1s at 48kps.

Time Series



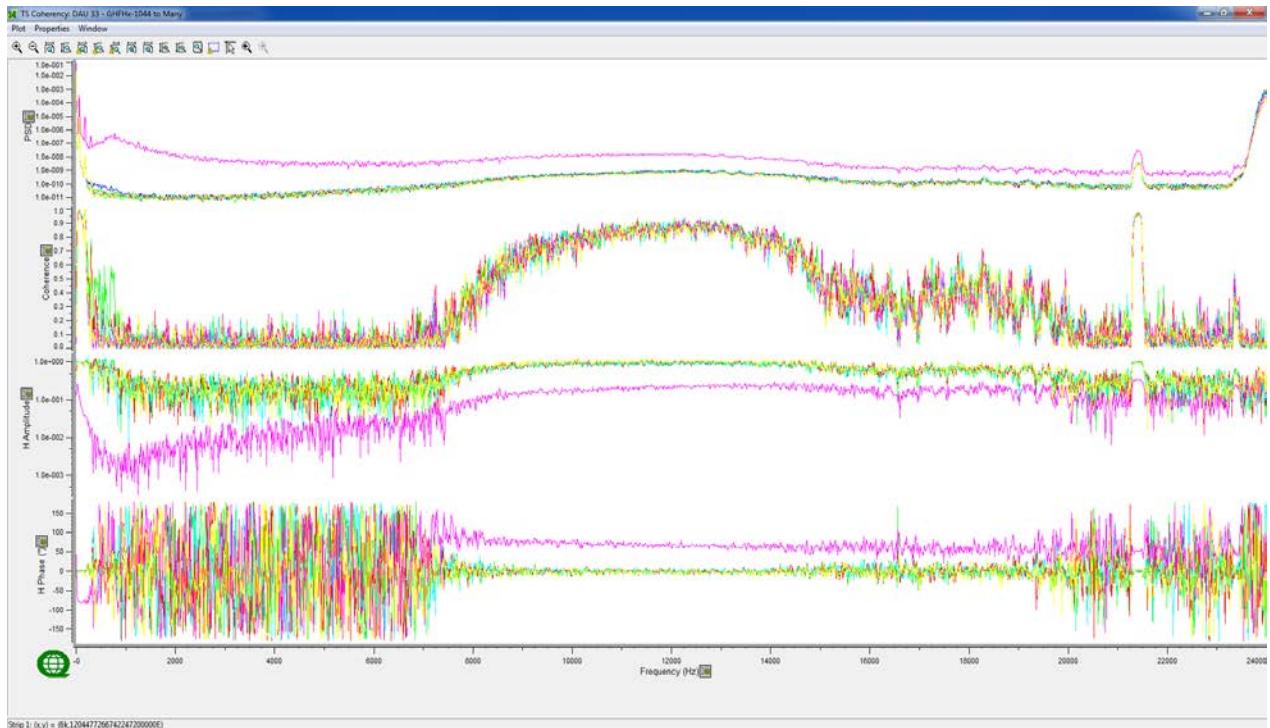
NetEvent9036.001048 Complete time series at 48kps.



NetEvent9036.001048 Time series focused in on ~1s at 48kps.

High Frequency (48k) Coil Results:

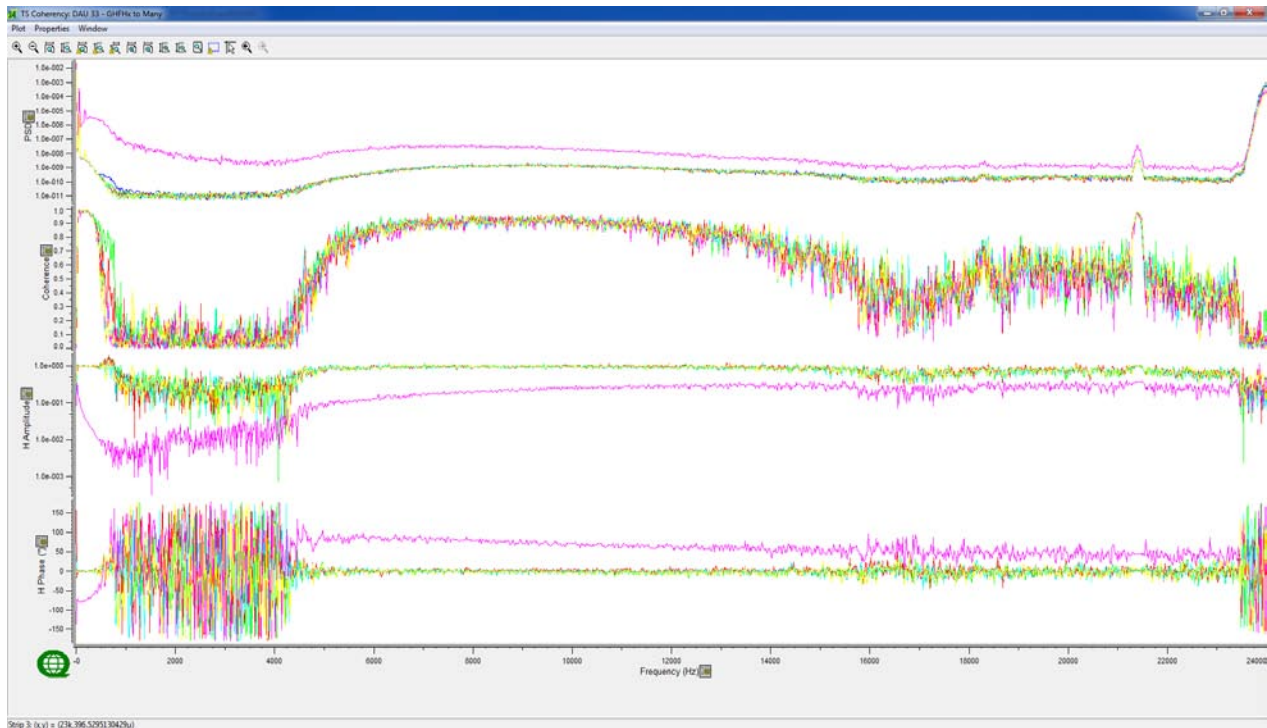
PSD of channels (strip 1), Coherency (strip 2) and Response Function (strips 3&4; Amplitude and Phase) compared to **Reference Channel GHF-1044 (Blue)** – *Linear frequency scale.*



Colour	Channel	Notes
Blue	GHF-1044	
Green	GHF-1048	
Red	GHF-1052	
Cyan	GHF-1053	
Magenta	GHF-1071	Weak PSD , amplitude and phase
Yellow	GHF-1074	

High Frequency (48k) Coil Results (continued):

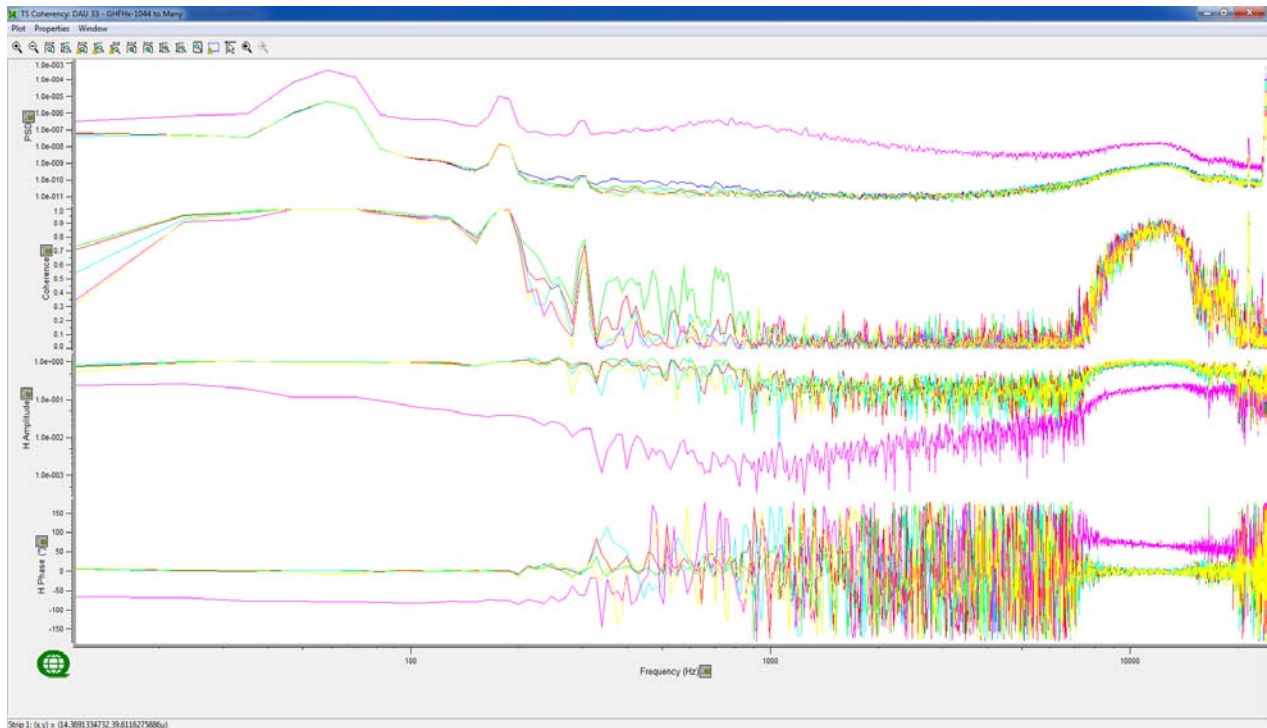
PSD of channels (strip 1), Coherency (strip 2) and Response Function (strips 3&4; Amplitude and Phase) compared to **Reference Channel GHF-1044 (Blue)** – *Linear frequency scale.*



Colour	Channel	Notes
Blue	GHF-1044	
Green	GHF-1048	
Red	GHF-1065	
Cyan	GHF-1068	
Magenta	GHF-1071	Weak PSD , amplitude and phase
Yellow	GHF-1074	

High Frequency (48k) Coil Results (continued):

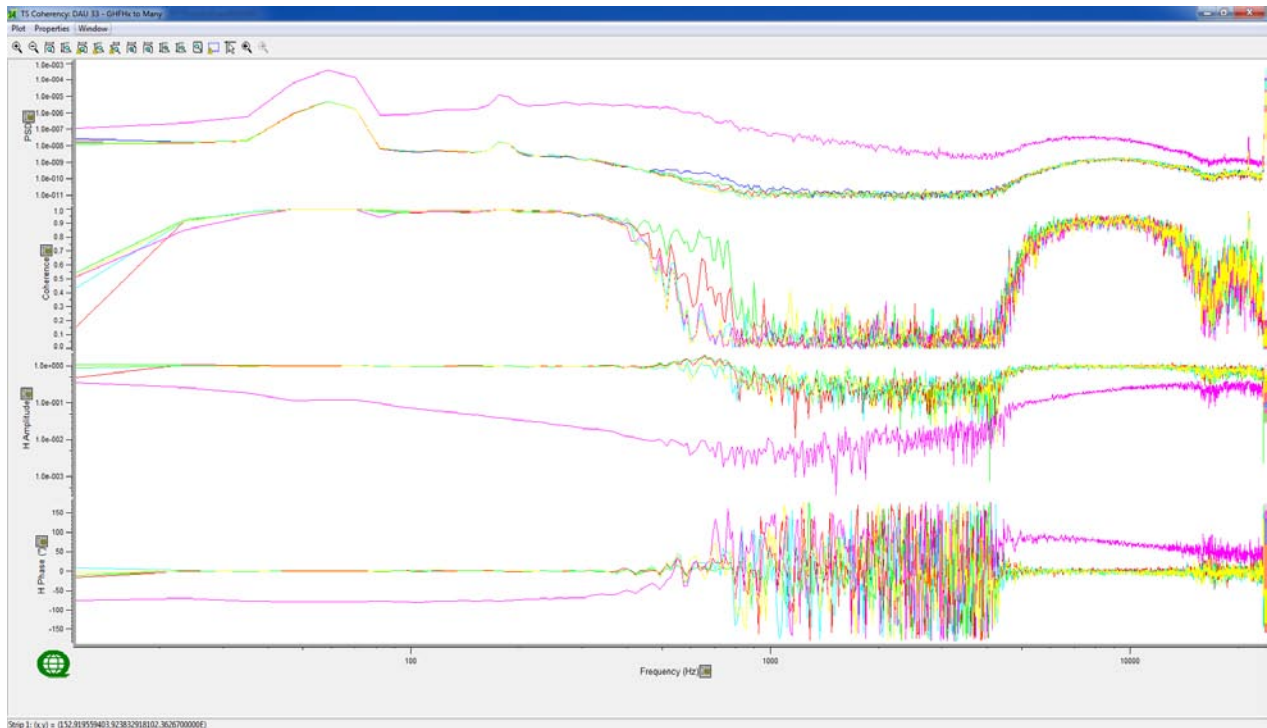
PSD of channels (strip 1), Coherency (strip 2) and Response Function (strips 3&4; Amplitude and Phase) compared to **Reference Channel GHF-1044(Blue)** – *Logarithmic frequency scale.*



Colour	Channel	Notes
Blue	GHF-1044	
Green	GHF-1048	
Red	GHF-1052	
Cyan	GHF-1053	
Magenta	GHF-1071	Weak PSD , amplitude and phase
Yellow	GHF-1074	

High Frequency (48k) Coil Results (continued):

PSD of channels (strip 1), Coherency (strip 2) and Response Function (strips 3&4; Amplitude and Phase) compared to **Reference Channel GHF-1044 (Blue)** – *Logarithmic frequency scale.*



Colour	Channel	Notes
Blue	GHF-1044	
Green	GHF-1048	
Red	GHF-1065	
Cyan	GHF-1068	
Magenta	GHF-1071	Weak PSD , amplitude and phase
Yellow	GHF-1074	

F.2.2 TEST RESULTS: 12KSPS

NetEvent: 9036.001044 & 9036.001050

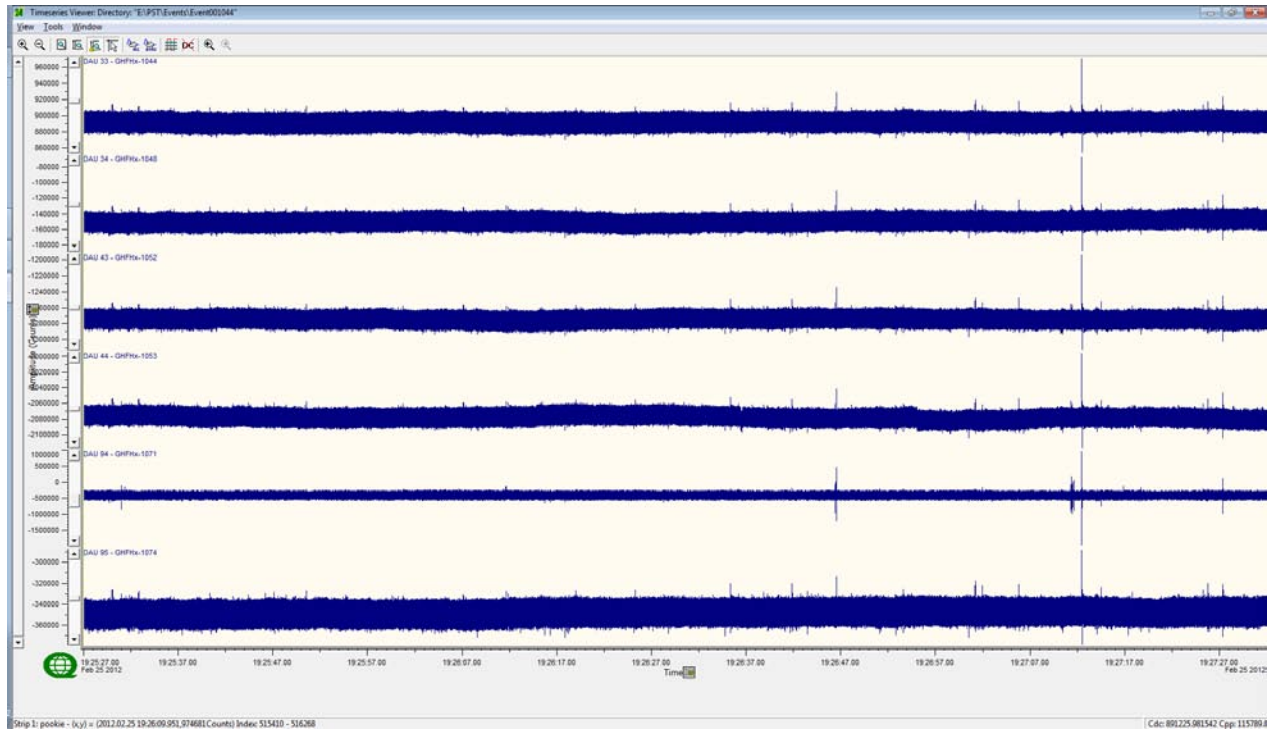
Sample Rate: 12ksps

TS Length: 1,500,000 samples (~2min)

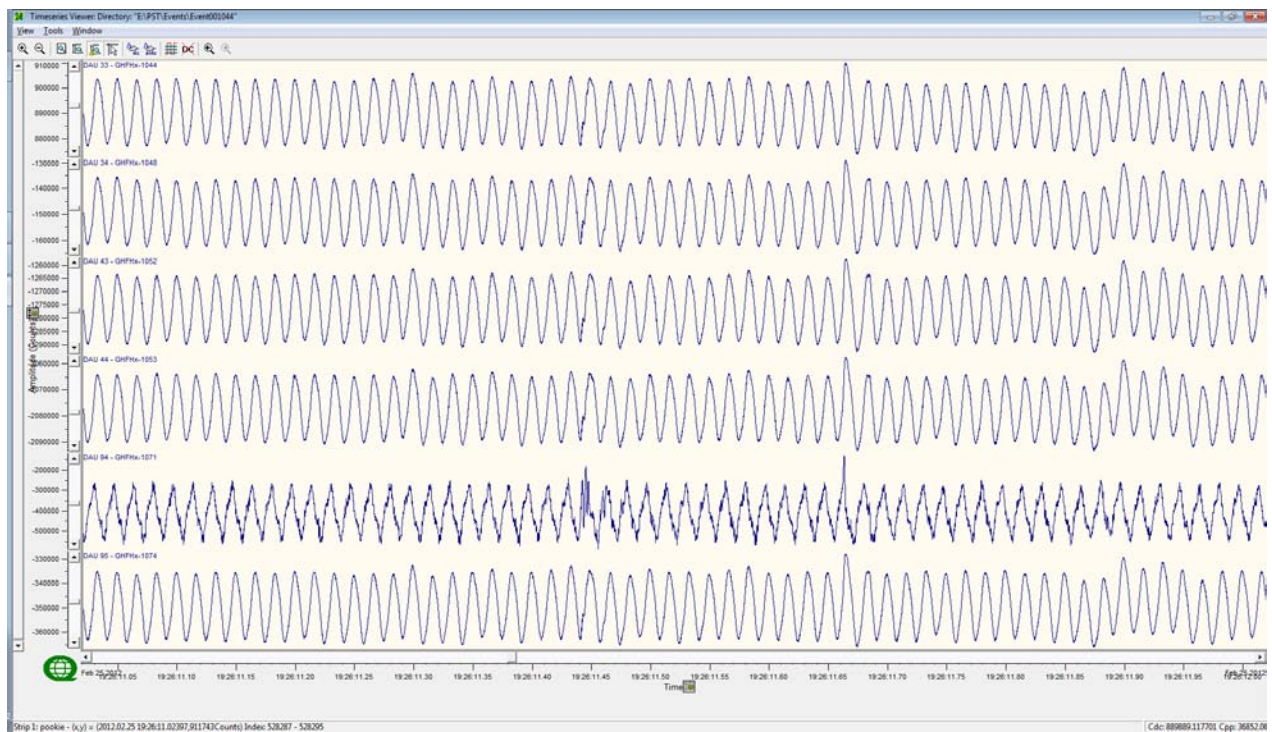
Results:

GHF-1071 This coil shows weak performance Weak PSD, amplitude and H phase.

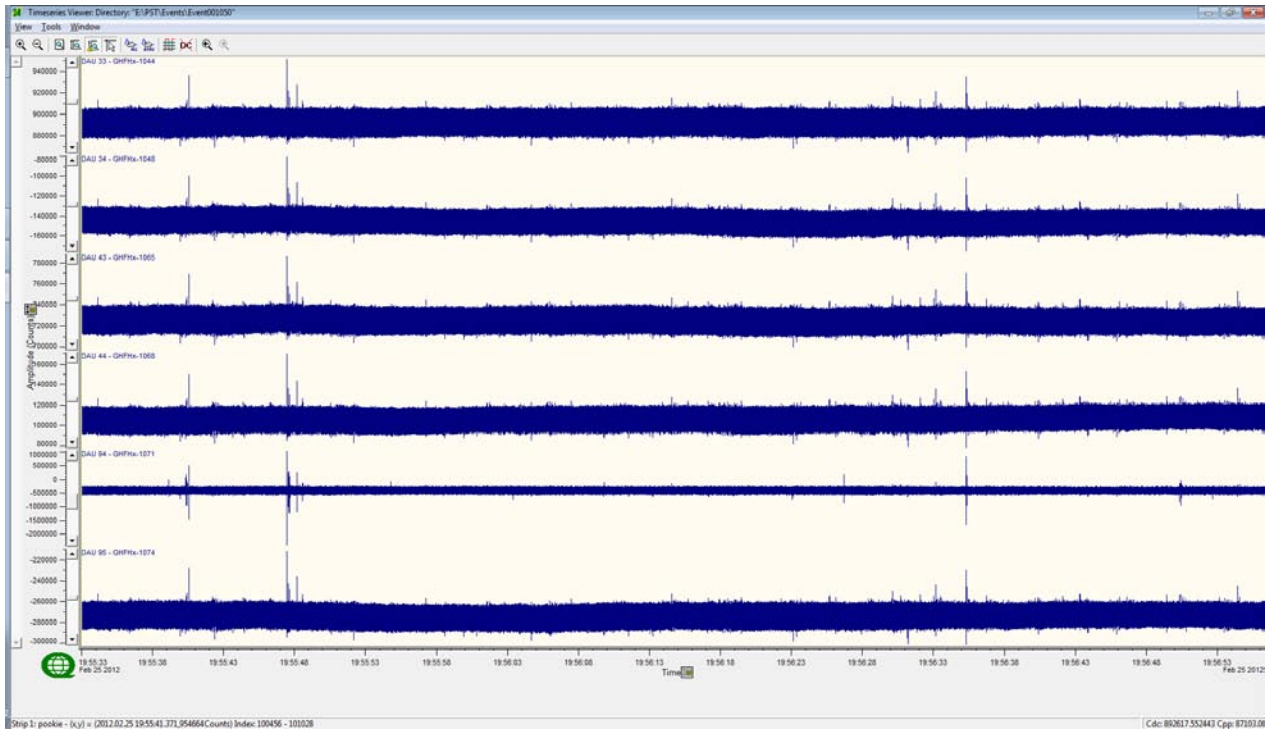
Time Series



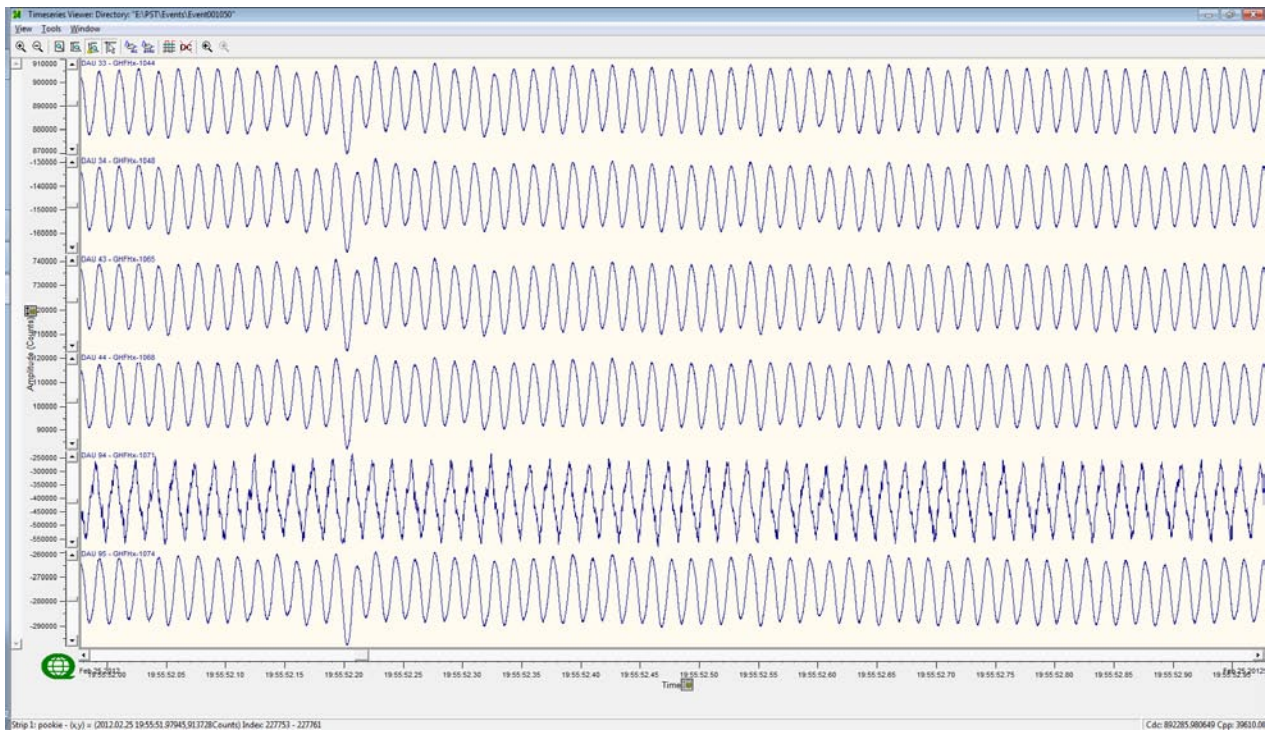
NetEvent9036.001044 Complete time series 12ksp.



NetEvent9036.001044 Focus on 1s of the time series 12ksp.



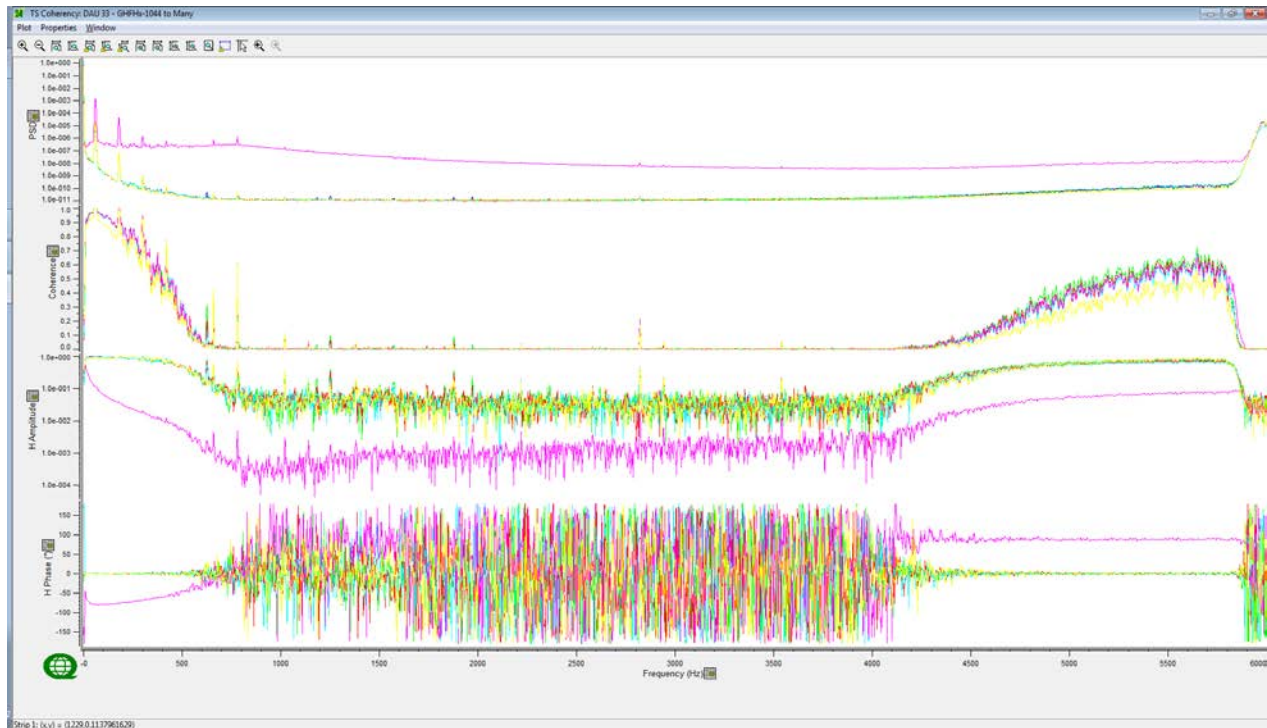
NetEvent9036.001050 Complete time series 12ksp.



NetEvent9036.001050 Focus on 1s of the time series 12ksp.

High Frequency (12k) Coil Results:

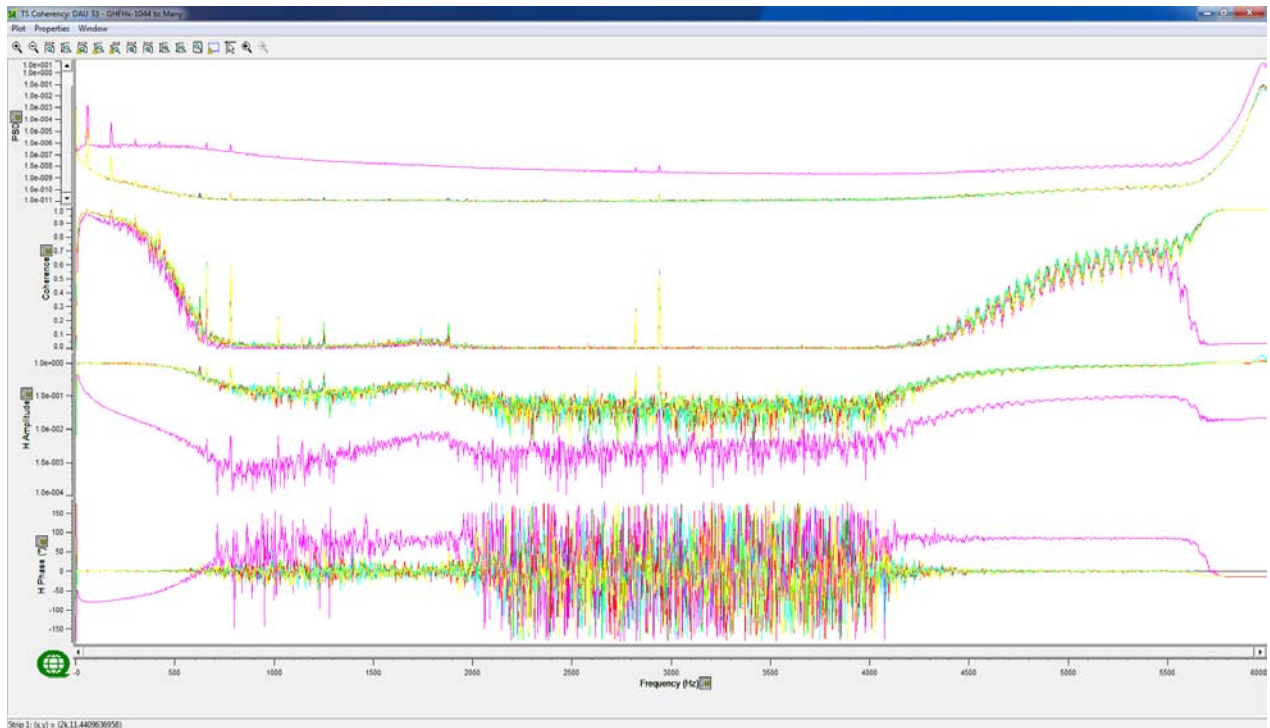
PSD of channels (strip 1), Coherency (strip 2) and Response Function (strips 3&4; Amplitude and Phase) compared to **Reference Channel GHF-1044 (blue)** – *Linear frequency scale*.



Colour	Channel	Notes
Blue	GHF-1044	
Green	GHF-1048	
Red	GHF-1052	
Cyan	GHF-1053	
Magenta	GHF-1071	Weak PSD , amplitude and phase
Yellow	GHF-1074	

High Frequency (12k) Coil Results (continued):

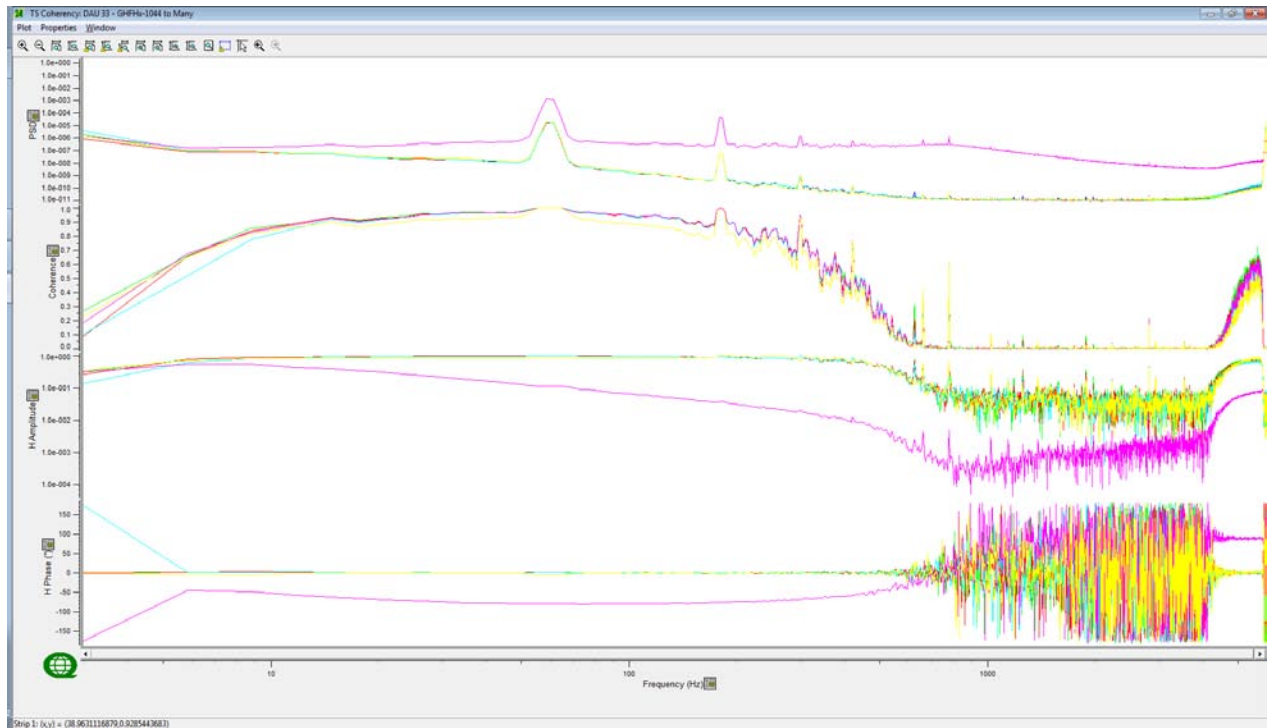
PSD of channels (strip 1), Coherency (strip 2) and Response Function (strips 3&4; Amplitude and Phase) compared to **Reference Channel GHF-1044 (blue)** – *Linear frequency scale*.



Colour	Channel	Notes
Blue	GHF-1044	
Green	GHF-1048	
Red	GHF-1065	
Cyan	GHF-1068	
Magenta	GHF-1071	Weak PSD , amplitude and phase
Yellow	GHF-1074	

High Frequency (12k) Coil Results (continued):

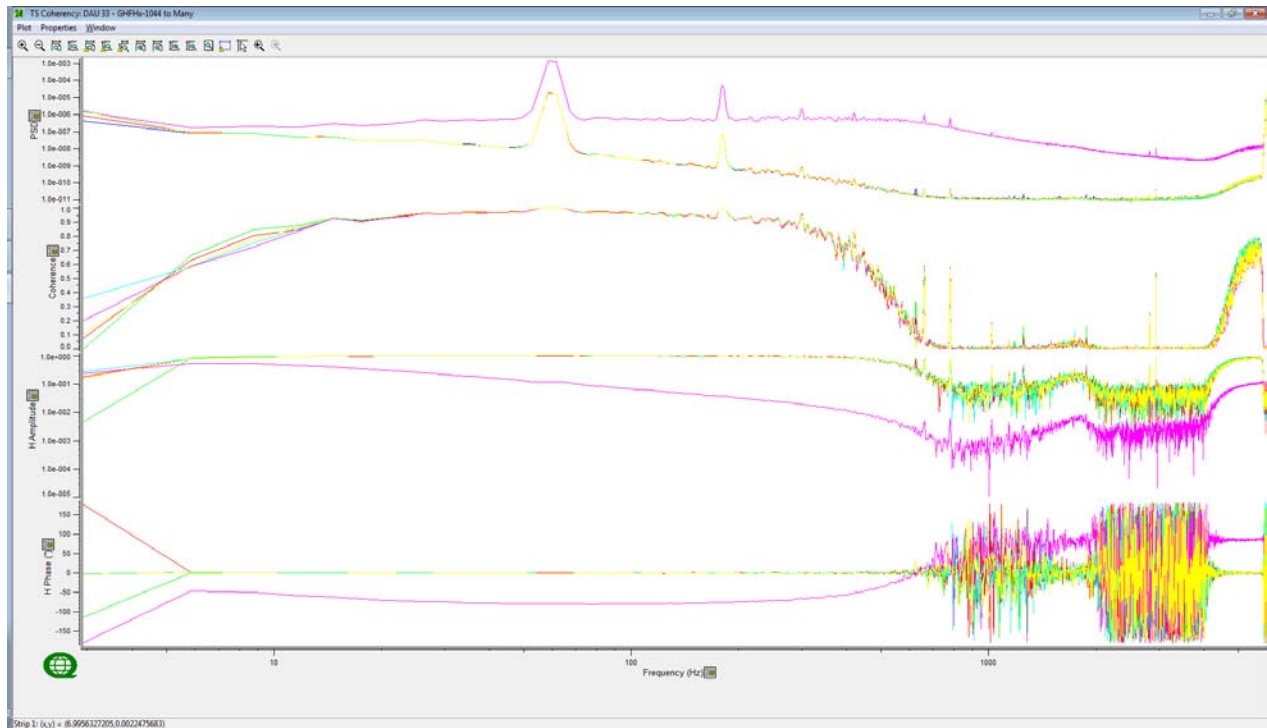
PSD of channels (strip 1), Coherency (strip 2) and Response Function (strips 3&4; Amplitude and Phase) compared to **Reference Channel GHF-1044(Blue)** – *Logarithmic frequency scale.*



Colour	Channel	Notes
Blue	GHF-1044	
Green	GHF-1048	
Red	GHF-1052	
Cyan	GHF-1053	
Magenta	GHF-1071	Weak PSD , amplitude and phase
Yellow	GHF-1074	

High Frequency (12k) Coil Results (continued):

PSD of channels (strip 1), Coherency (strip 2) and Response Function (strips 3&4; Amplitude and Phase) compared to Reference Channel **GHF-1044 (Blue)** – *Logarithmic frequency scale.*



Colour	Channel	Notes
Blue	GHF-1044	
Green	GHF-1048	
Red	GHF-1065	
Cyan	GHF-1068	
Magenta	GHF-1071	Weak performance. Weak PSD, amplitude and Phase.
Yellow	GHF-1074	

G MT REMOTE TEST – UNREFERENCED DATA

Project CA00972T
Date: February 24th, 2012
Report by: Mojtaba Daneshvar
QuickLay Version 4.00.10
Common folder V1.54
Remote Location: 405804mE / 5160727mN (WGS84/Zone17T)

Magnetic Declination: 11°West
Sensor Azimuth: **Ex** 17° North dipole = 100m
Ey 287° West dipole = 100m
Hx 17° North
Hy 287° West

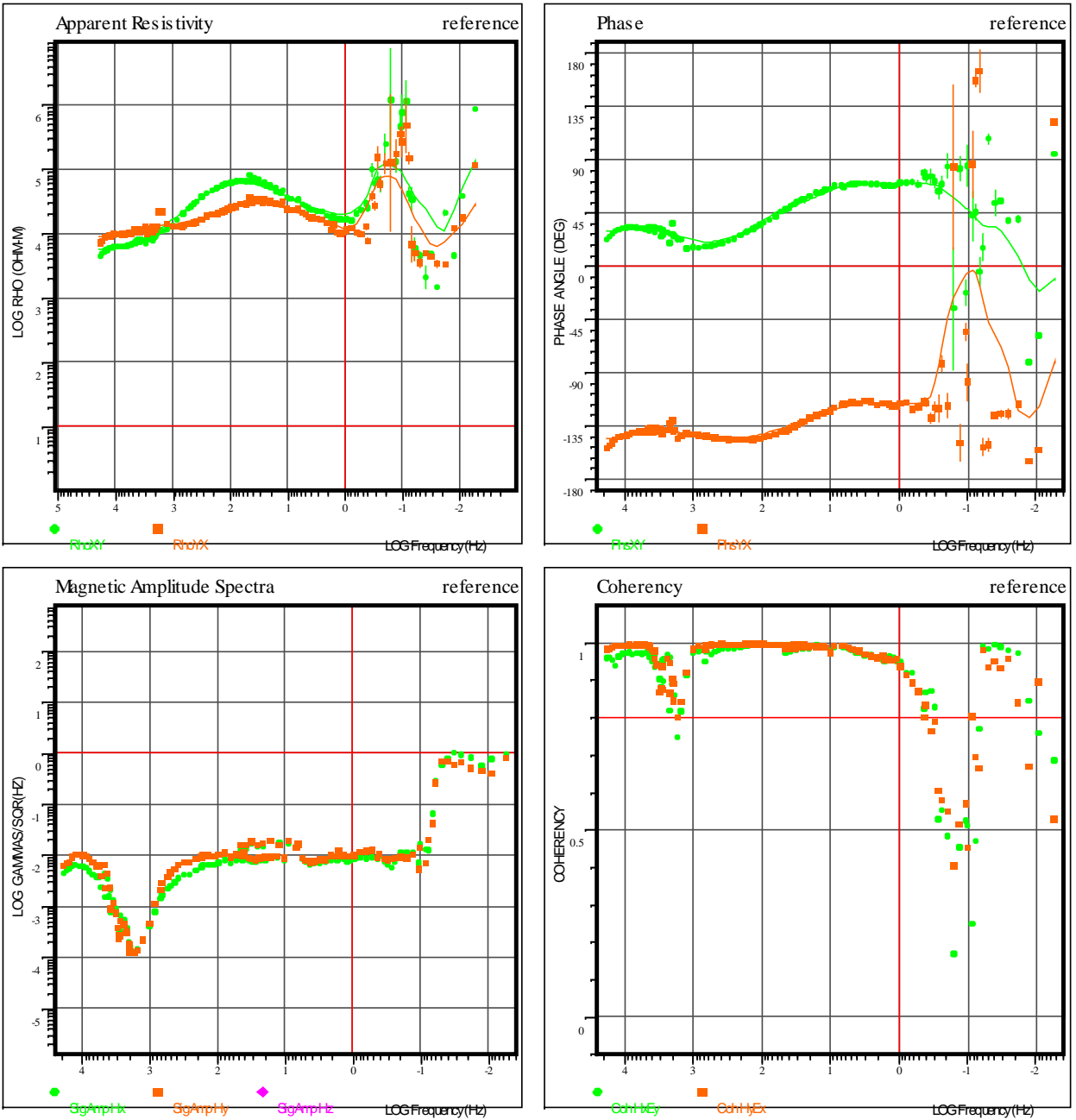
Screenshot of AU Info:

AU ID	Disabled	Net Position	AM	Site ID	Sensor ID	Battery	Impedance	Gain
9036		A0	CRU			11.6		
0033		B1	AM2-0007	P50-3106	P50-3105	12.4	97 (ohms)	3 (x16)
0034		B2	AM2-0007	P50-3107	P50-3107	12.2	96 (ohms)	3 (x16)
0043		B3	AM2-0012	G-1044	BF6-0012	12.4	53 (ohms)	3 (x16)
0044		B4	AM2-0012	G-1048	BF6-0013	12.1	52 (ohms)	3 (x16)
0094		B5	AM2-0027	RmEx		12.5	19829 (ohms)	3 (x16)
0095		B6	AM2-0027	RmEy		12.5	28563 (ohms)	3 (x16)

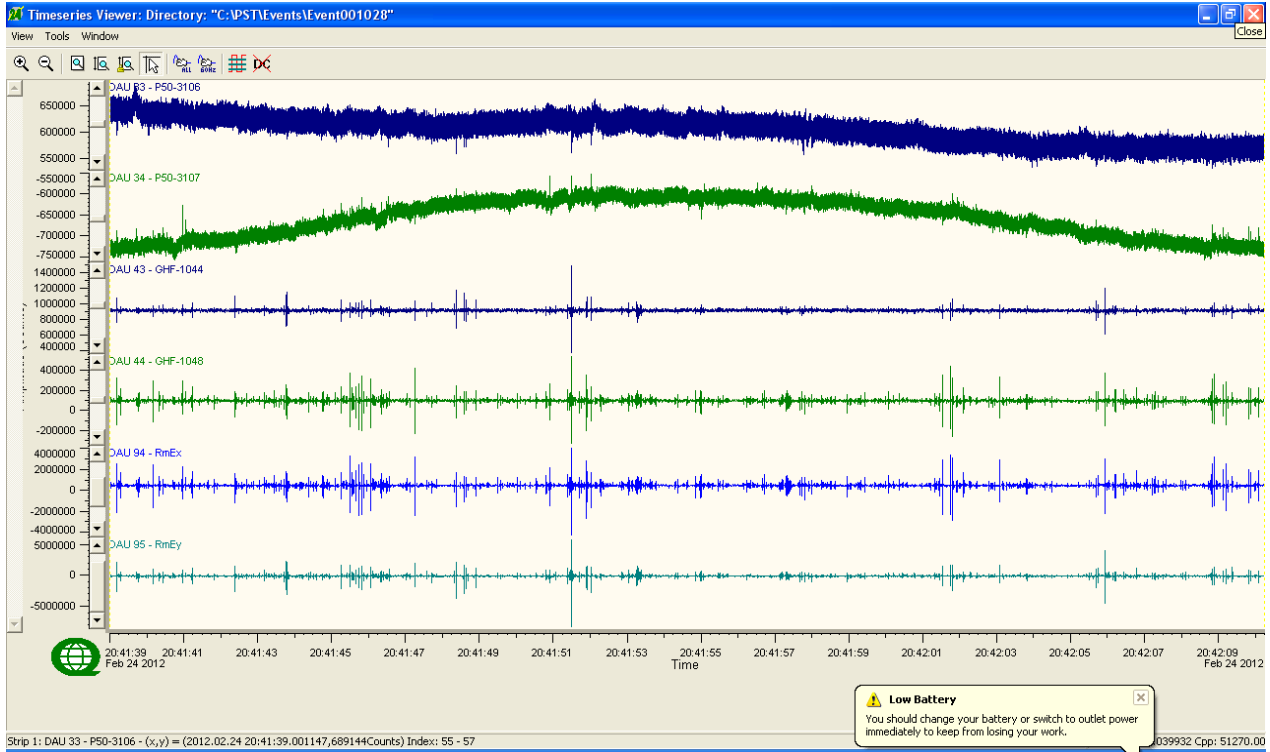
Culture: N/A

Details below ALL the data used and processed for the test:

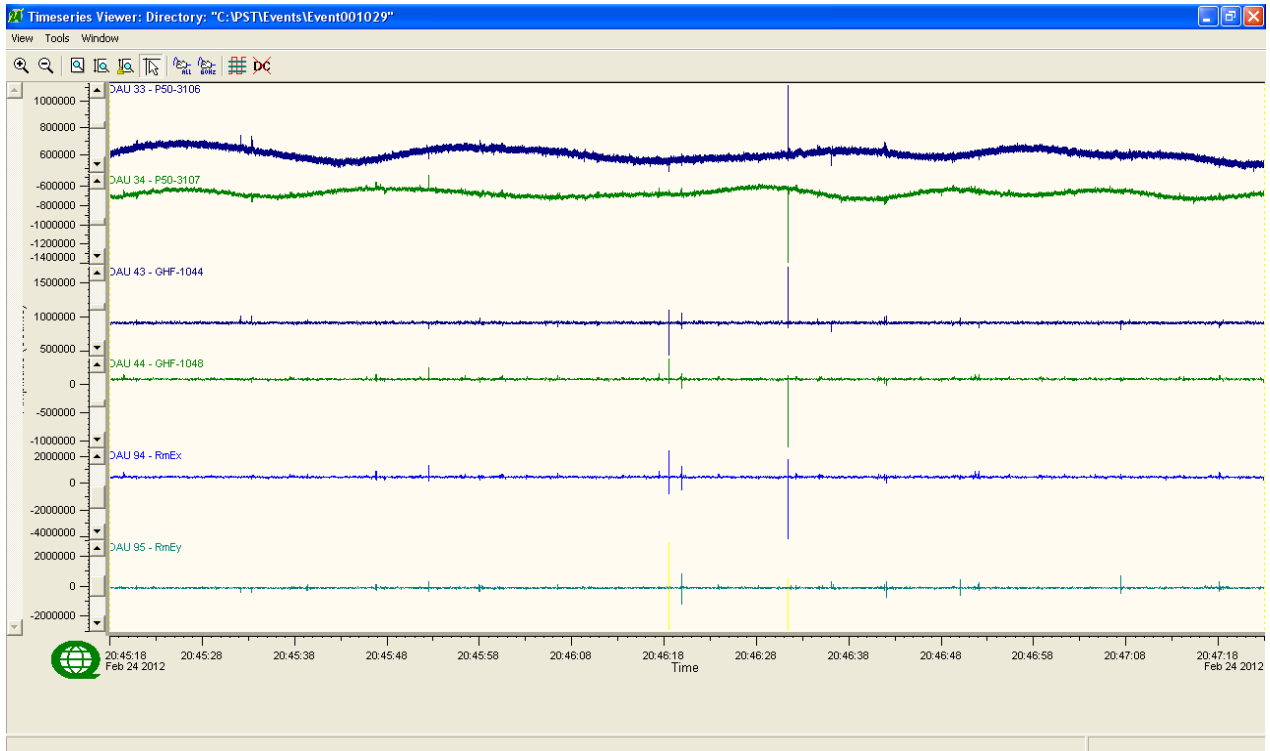
Sample Rate	Net Events	TS Length	Observations
48kps	9036.001028	~31s	N/A
12kps	9036.001029	~2min	N/A
120sps	9036.001027	~9min 43s	N/A



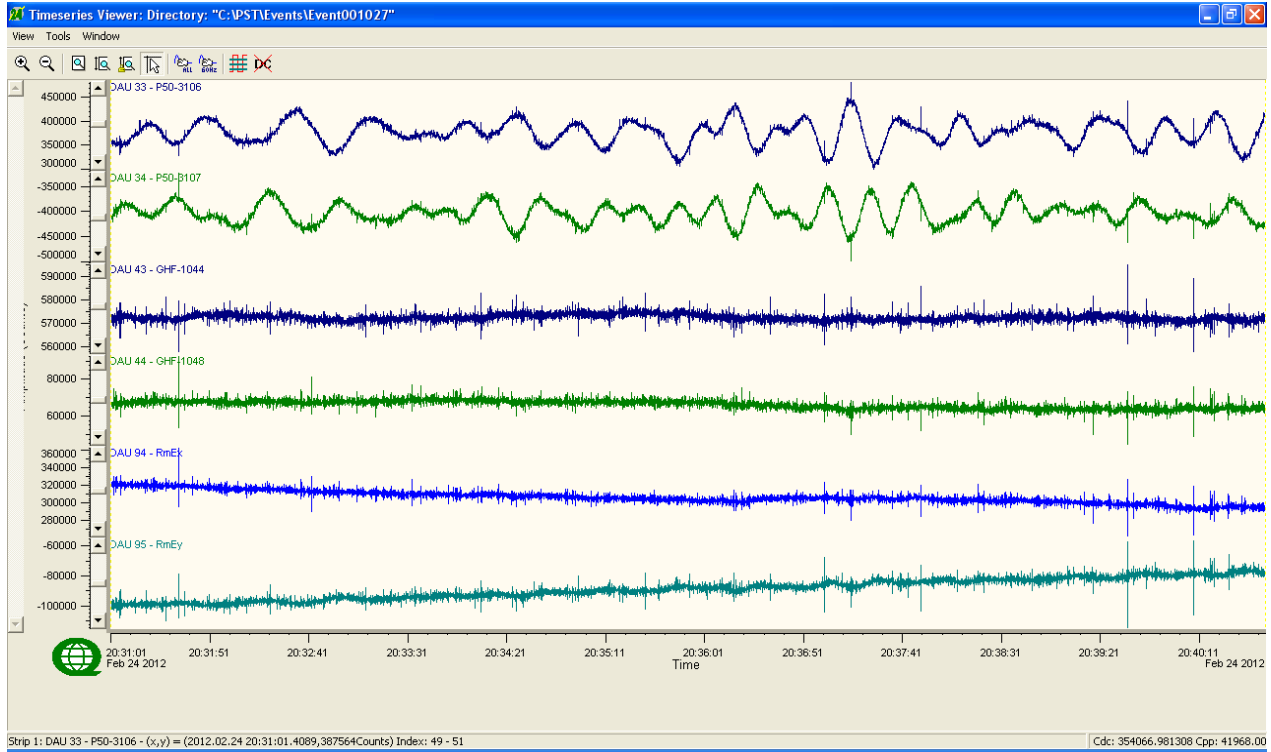
Apparent resistivity, phases, magnetic signal amplitude and off-diagonal coherences of the MT remote, data processed unreferenced.



Screen Capture of MT time series, sample rate at 48kps.



Screen Capture of MT time series, sample rate at 12kps.



Screen Capture of MT time series, sample rate at 120sps.

H INSTRUMENTS SPECIFICATIONS

H.1 REF TEK – 120 DATA ACQUISITION SYSTEM

Refraction Technology Inc. – Plano, Texas

Specifications:

Specification	Description
Physical	
Size:	267 x 248 x 184 mm 10.5 x 9.75 x 7.25 in.
Weight:	3.7kg 305 g 8 lbs (2-Channels maximum weight)
Temperature:	-40°C to 60°C operating range.
Environmental:	Operates in 1m of water without leaking for 48 hours. Airtight to 1.0 psi.
Shock:	Remains operational after 1m drop (any corner) onto cement floor.
Connectors	
Line A & Line B:	A pair of identical 10 pin U77/U style connectors. Each connector provides 3 pairs of lines (+): A (+)/B (-) Receive telemetry data and/or commands C (+)/D (-) Transmit telemetry data and/or commands E (+)/F (-) Sync
Power:	PTO7A12-8S style connector. Provides input +12 VDC supplied from battery.
Sensor:	PU283/U style connector. Provides for a direct connection from the AM to the sensor.
Power Requirements	
Battery:	Two 12 volt lead acid battery (7 Ah).
Signal Input	
Input Impedance:	10 megohms, 330pF, differential
Broadband Dynamic Range:	130dB (noise power ratio test @ 125 sample per second [sps])
ADC Type:	Delta-sigma modulation
Sample Rate:	Multiple 50 to 48,000
Gain Settings:	Four – programmable for 1, 4, 16 and 64.

Specification	Description				
Sensor Input Signal Range:		24-Bit High Speed A/D		24-Bit Low Speed A/D	
	Gain	Actual	Reported	Actual	Reported
	1	1.192 μ V	78.12mV	1.907 μ V	125.0mV
	4	298.0nV	19.53mV	476.8nV	31.25mV
	16	74.51nV	4.883mV	119.2nV	7.812mV
	64	18.63nV	1.221mV	29.80nV	1.953mV
Data Storage					
Data Size:	32-bit two's compliment.				
Base Memory:	128K EPROM 6.5Mb SRAM				
Base Capacity:	Better than 1.5 million samples or approximately 3 hours 10 minutes continuous data @ 125 sps.				
AM Telemetry					
Protocol:	Full duplex synchronous data link control (SDLC).				
Error Correction:	Packet acknowledge with modulo 8 sliding window.				
Speed	3.072Mb/second				
Encoding:	Bi-phase pulse = 1, missing pulse = 0				
Line Impedance:	100 Ohm				
Synchronization					
Timing:	Each AM on-line is timed and synchronized for simultaneous sampling within + 1.50 μ second.				
Protection					
Electrical Protection:	Line A and Line B signals circuits are protect by: - A surge arrestor located on the RT514 board (SS1-14). - A line isolation transformer located on the RT514 board (T1-6) with over-voltage diodes (D1-4) on both sides of each secondary windings				
State-of-Health					
Information Provided:	The AM reports information on battery status, clock setting, gain setting, calibration mode and the communications link.				

Acquisition Parameters

Acquisition parameters include the sample rate, transmitter frequency and number of samples desired. The operator can also determine whether the AMs calibration signal is activated during data collection.

In typical use, the acquisition parameters are set according to the specific application configuration and event type. For each event type, several recording sessions are made, each at a different transmitter frequency and sample rate. The recording period is set based on event type and transmitter frequency.

The listing below shows several examples of event type, typical transmitter frequency (Hz), sample rates (with applicable ADC resolution) and the corresponding number of samples (record period).

Event Type	Transmit Frequency	Sample Rate	ADC Resolution	Number of Sample
Geophysical Response	375 Hz	48,000	24	124,032
Gain Test	375	48,000	24	65,536
Geophysical Response	75	9,600	24	130,176
Gain Test	75	9,600	24	65,536
Geophysical Response	25/8	3,200	24	139,264
Gain Test	25/8	3,200	24	32,768
Sensor Impedance	N/A	1,600	24	8,704
Ambient Noise	N/A	1,600	24	8,192
Geophysical Response	25/128	800	24	147,456
Gain Test	25/128	800	24	16,384
Geophysical Response	25/2048	100	24	212,992
Gain Test	25/256	100	24	4,096
Gain Test	N/A	50	24	4,096
Geophysical Response	N/A	50	24	65,536

Sensor Calibration

The AM can source a 12.5Hz, 50µA signal to the sensor input for measuring the source impedance of the attached sensor. The user can also specify frequency in amplitude of calibration signal.

Telemetry Cable

The telemetry cable is a *Category V* specification cable and is supplied by the customer.

Sample Rates

The following table shows all available sample rates, based on a 12.288 Mhz oscillator. A 24-bit resolution ADC is used for sample rates 48000 through 4800 and a 24-bit resolution ADC is used for

sample rates 3200 and below. The correct ADC is selected automatically by the AM, based on the sample rate.

Typically, different sample rates and transmitter frequencies are used in 50 Hz and 60 Hz power environments to minimize AC power effects on the data. In the table, the shaded areas indicate the sample rates typically used in a 60 Hz power environment. A few rates are typically used in both environments.

Sample Rate	Power Line
48000	50 & 60
24000	50 & 60
19200	60
16000	50
12000	50 & 60
9600	50 & 60
6400	50
4800	60
3200	50
1920	60
1600	50
960	60
800	50
480	60
400	50
240	60
200	50
120	60
100	50
60	60
50	50
60/2	60
50/2	50
60/4	60
50/4	50
60/8	60
50/8	50
60/16	60
50/16	50
60/32	60
50/32	50

H.2 MTC 50 (P50) SERIES MAGNETIC SENSORS

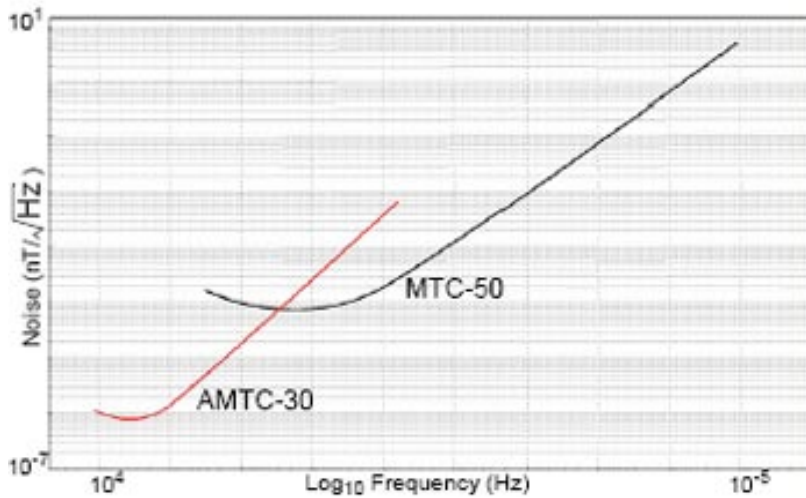
Phoenix Geophysics Ltd

MTC-50 magnetic sensor coils weigh just over 10 kg, and measure only 141 cm. They provide magnetotelluric data at frequencies between 400 Hz to 0.00002 Hz.



Technical Specifications

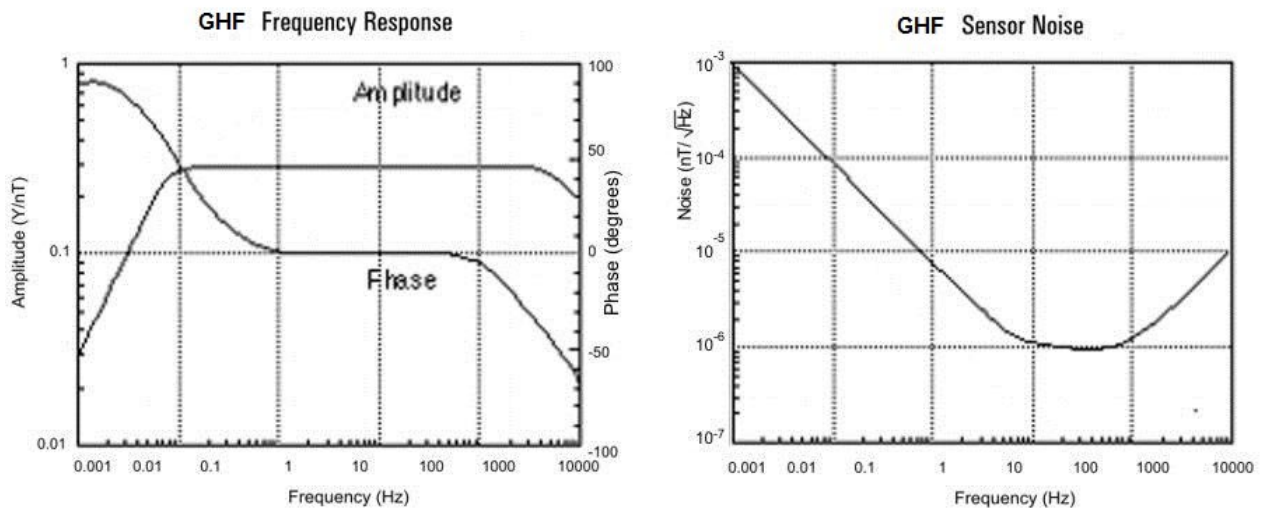
Overall Length : 141 cm
 Outside Diameter : 6.0 cm
 Weight : 10.5 kg
 Frequency Range (for MT) :
 400 Hz to 0.00002 Hz



H.3 GHF MAGNETIC FIELD INDUCTION SENSOR

Geometrics

The GHF sensor utilizes a magnetic feedback design to provide a stable flat response over several decades of frequency. The sensors respond as a B field detector over the flat band regions. Both the amplitude and phase responses are highly stable with variations of less than 0.1dB in amplitude and +/- one degree in phase between sensors. For the frequencies below the flat response region, the sensor response is proportional to signal frequency so that the sensor acts as a dB/dt detector. The coil is potted with epoxy and housed inside a rugged impact-resistant ABS tube. A matched low noise preamplifier is connected to the coil in a waterproof case and powered by an external +/- 12V power supply.



Features

- High sensitivity
- Very low noise
- Magnetic feedback design
- Ruggedized and waterproof
- Light weight and compact
- Low power consumption (210 mW)
- Stable phase response

Performance

- Frequency Range: 1 Hz to -100 kHz or 1 Hz to 25 kHz
- 3 dB frequency corners: 10 Hz, 25 kHz or 10 Hz, 100 kHz
- Sensitivity (flat region): 0.3 V/nT (standard)
- Power consumption: 9mA at +/-12V

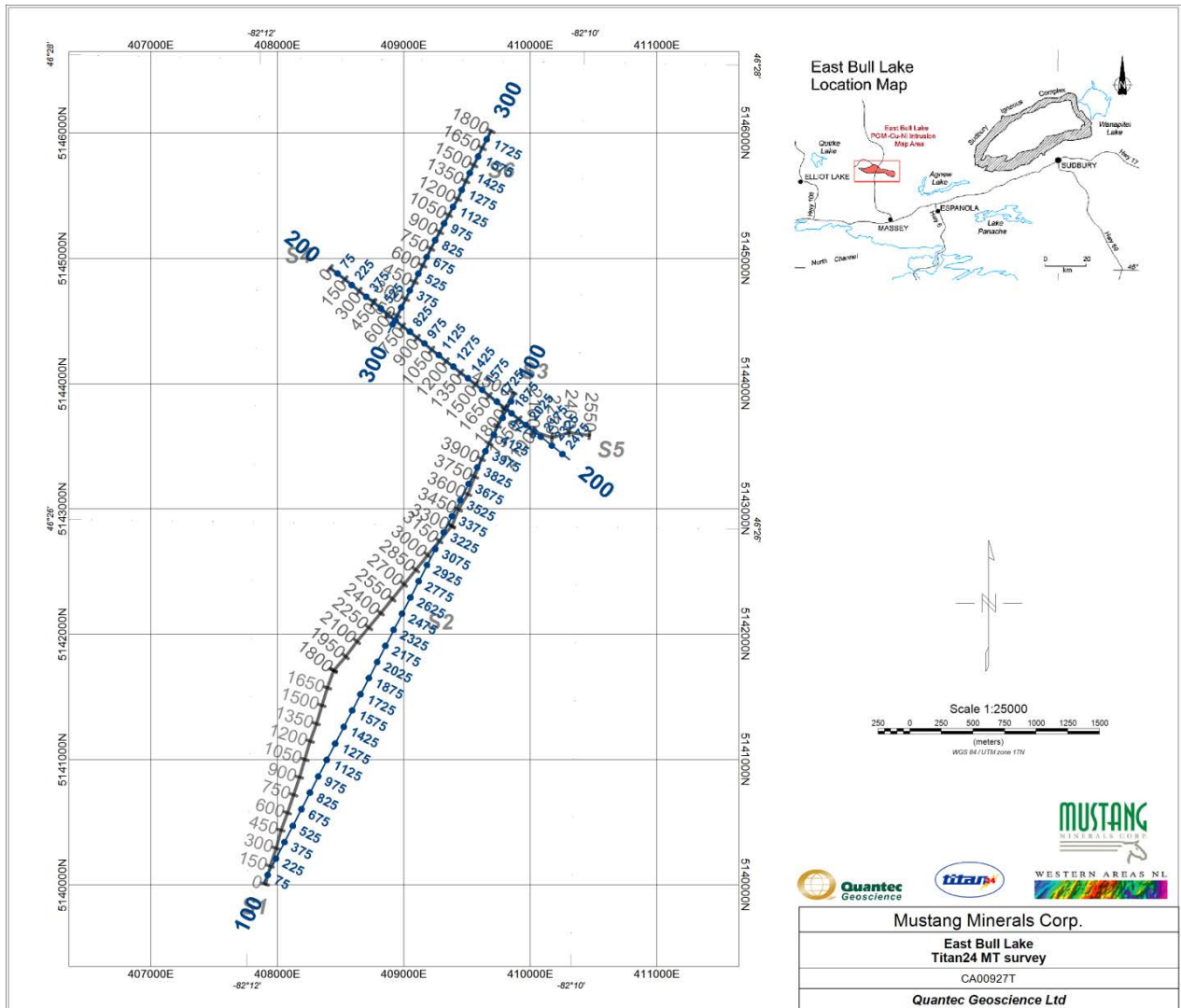
Applications

- Magnetotellurics
- Audiomagnetotellurics
- Controlled-source electromagnetics
- Magnetometric resistivity
- Time domain electromagnetics

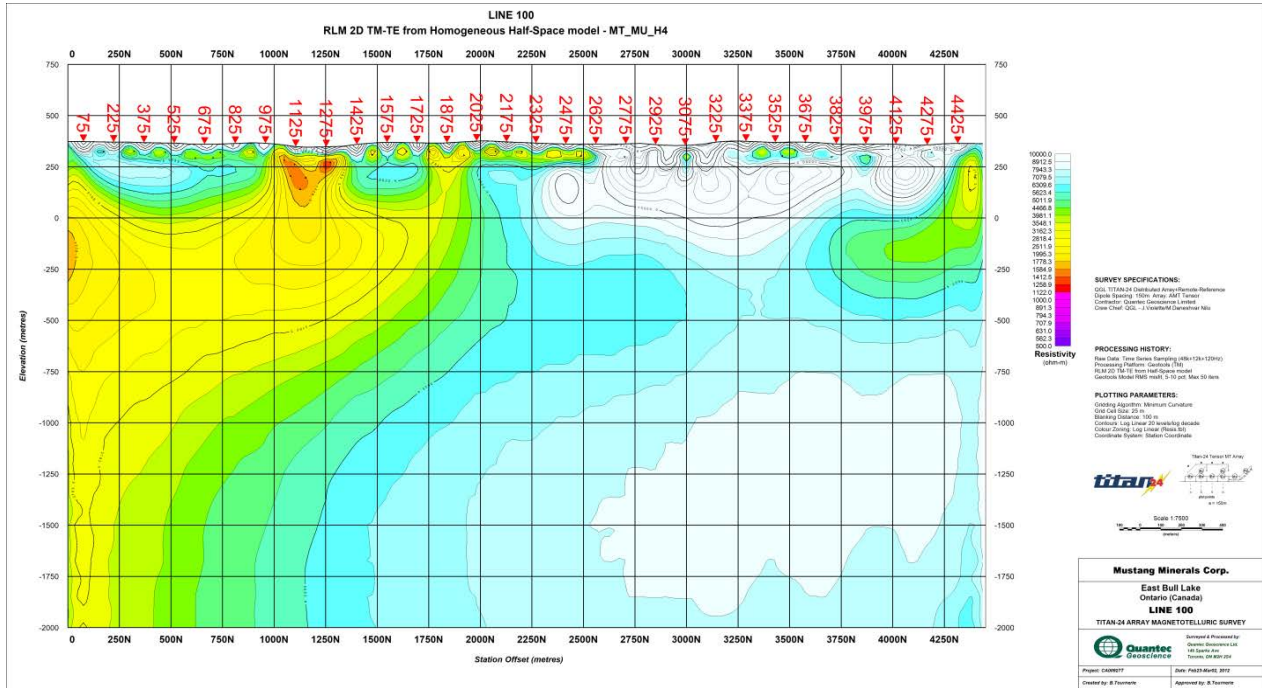
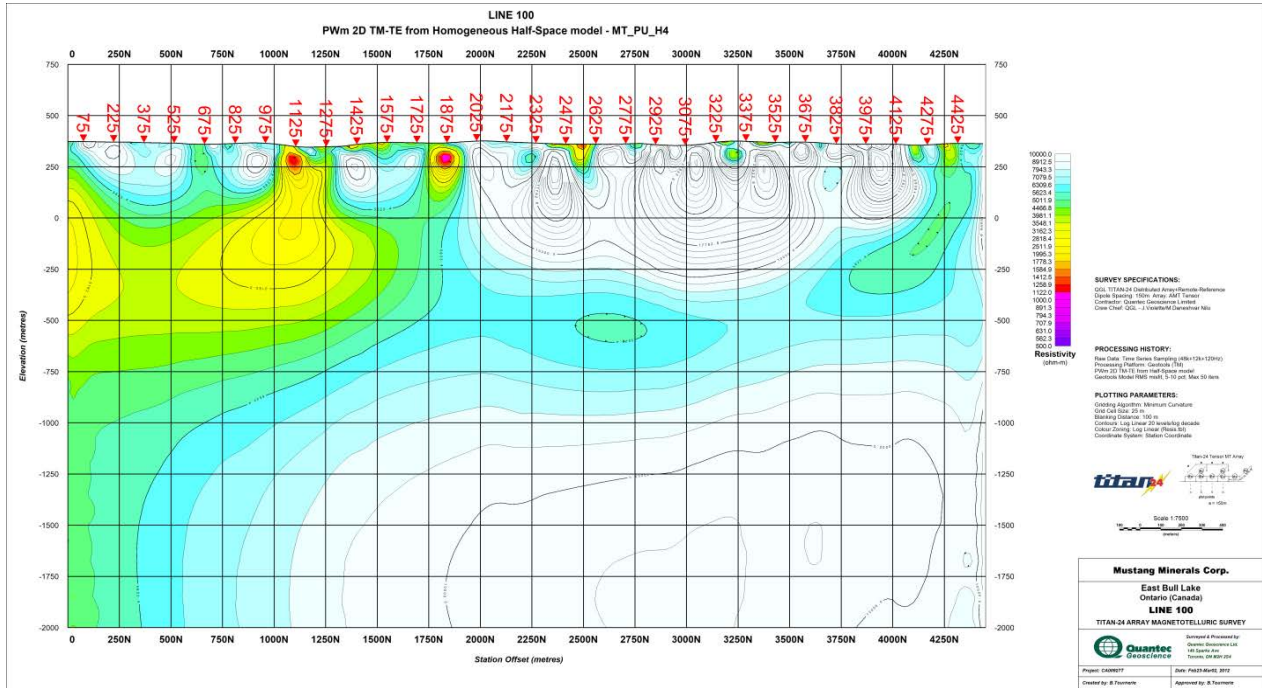
Physical

- Housing: High Impact ABS Straight Tube
- Length: 73 cm (29 inches)
- Diameter: 5 cm (2 inches)
- Weight: 1.7 kg (3.7 lbs)
- Connector: 8-pin Tajimi

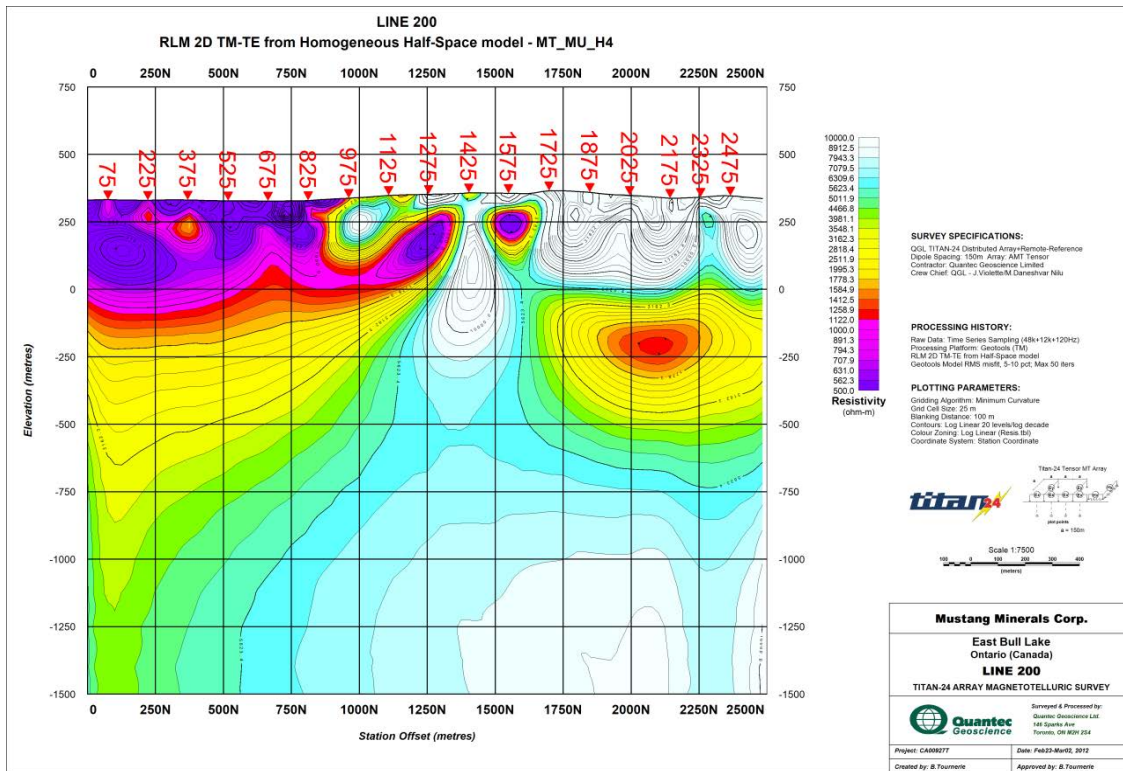
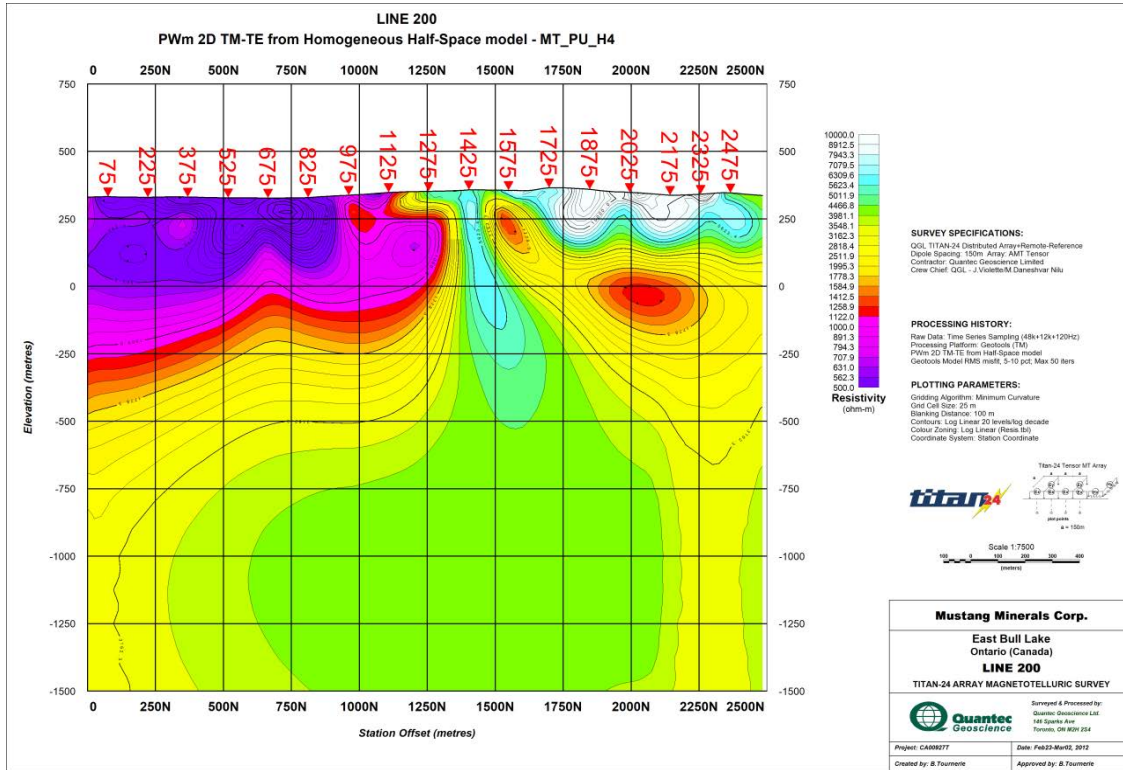
I GEOSOFT SECTIONS



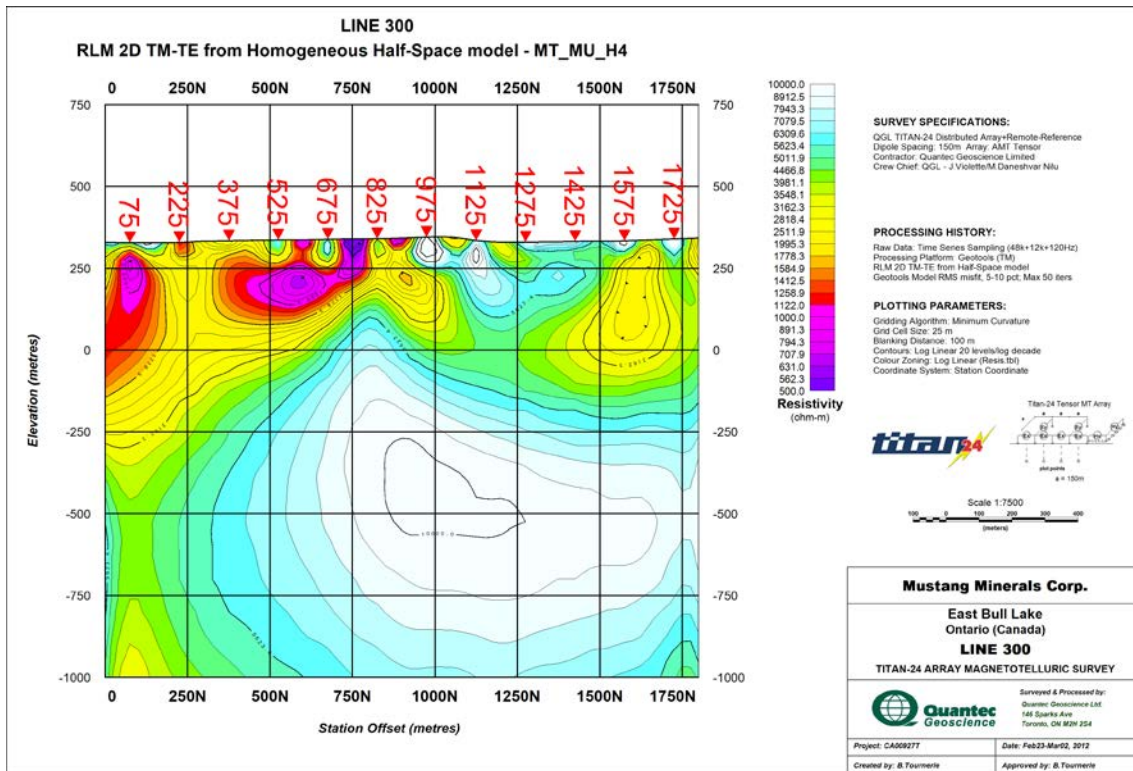
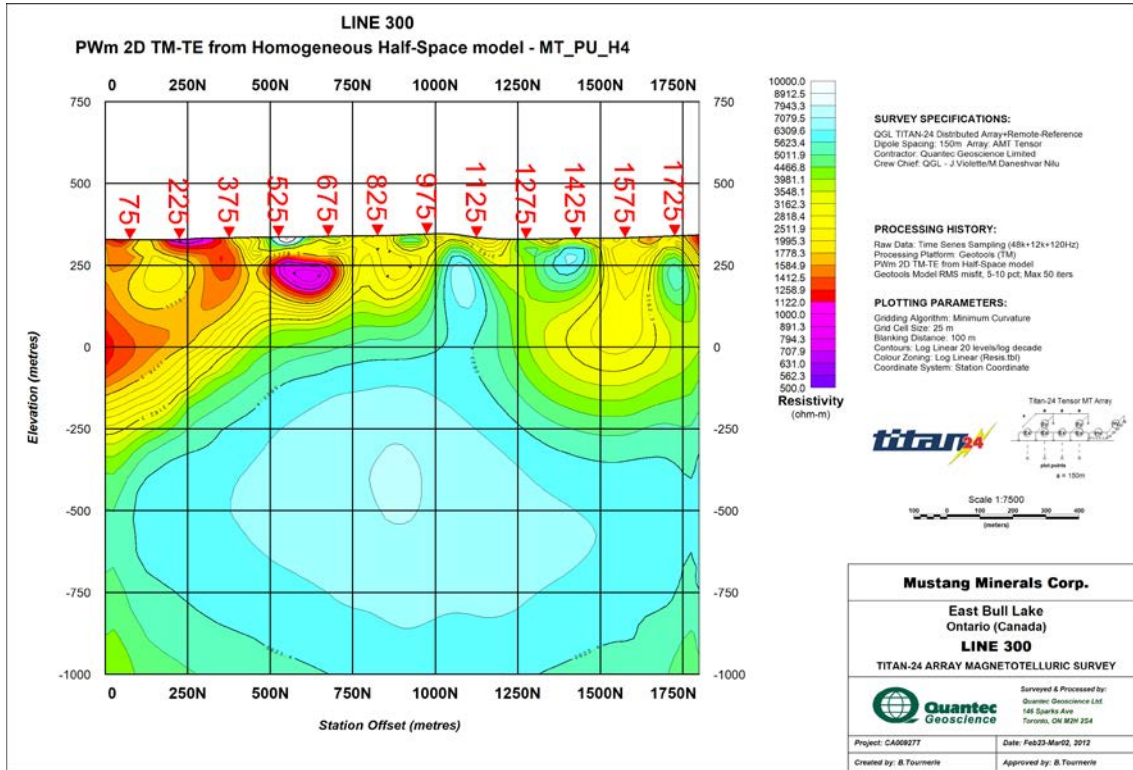
I.1 LINE L100



I.2 LINE L200



I.3 LINE L300



J INTRODUCTION TO THE MAGNETOTELLURIC METHOD

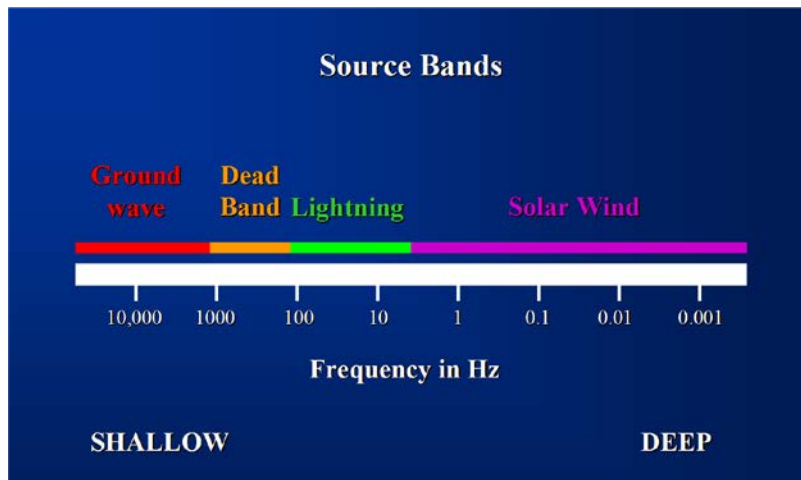
J.1 INTRODUCTION

The magnetotelluric (MT) method utilizes time-variations in the Earth’s natural electric (E) and magnetic (H) fields to image the resistivity of the subsurface structure. The natural electromagnetic (EM) signals are assumed to be of plane-wave source over the frequency range with which the MT surveys are usually carried out. The plane-wave source is simpler to model compared with the complex transmitter geometries and signals used in the other EM methods. It makes the MT responses easier to understand and interpret with respect to the subsurface resistivity variations.

The E and H fields are measured over a broad range of frequencies. Typically, the frequencies can range from above 10 kHz to below 0.001Hz. Considering the conductivity of the Earth’s materials and the frequency range over which the MT data are measured, the EM fields propagate in a diffusive regime. High frequency signals are attenuated more rapidly in the subsurface. Therefore, high frequency data are indicative of shallow resistivity structure while low frequency data are indicative of deep resistivity structure.

At frequencies below 1Hz the EM signal source is due to oscillations of the Earth’s ionosphere as it interacts with the solar wind. At frequencies above 1Hz the signal source is due to worldwide lightning activities. There is a lack of natural signal around 1Hz, often referred to as the “hole”. Modern 24-bit recording hardware and signal processing techniques, however, have largely eliminated the data quality degradations that have been traditionally seen around the 1Hz signal hole.

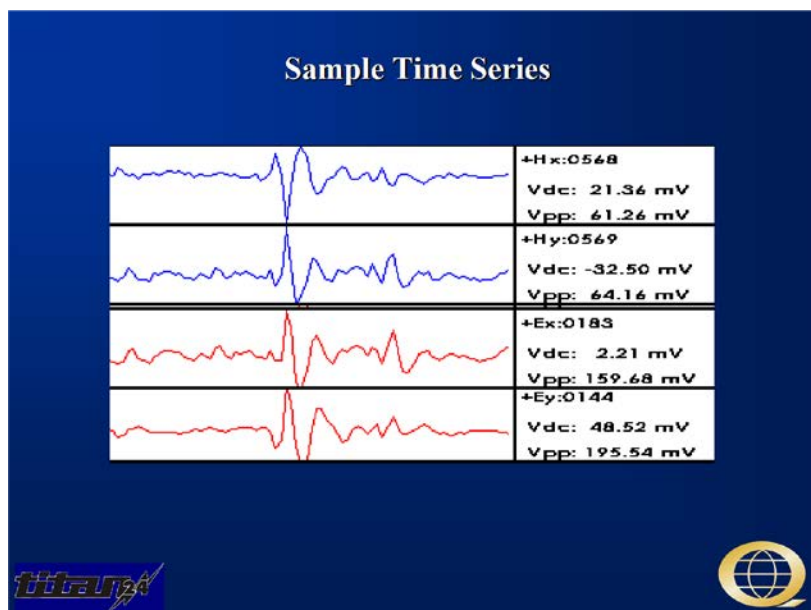
Between about 8Hz and 300Hz the signal from worldwide lightning activity propagates in a “resonant” cavity (the resistive atmosphere) between the conductive ionosphere and the conductive Earth’s surface. Above 3 kHz the signal propagates as a ground wave. Between 300Hz and 3 kHz there is a “dead-band” where the signal does not propagate well. Despite hardware and signal processing improvements this dead-band remains problematic. When signal (atmospheric activity) is present within several hundreds of miles of the survey area the data quality improves. When no signal is being generated in the vicinity of the survey area the data quality is poor.



J.2 MEASUREMENTS

Both the electric and magnetic fields are measured at each site. The measured field strengths depend on the ionosphere and lightning activities and are essentially of random nature. While the E and H field strengths are random the ratio of these two fields depends on the frequency and the subsurface resistivity structure. For a homogeneous and a 1D earth resistivity structures, the magnetic field is perpendicular to the electric field. However, it is possible for a complex subsurface resistivity structure to rotate the fields. Therefore, full tensor data, including two perpendicular electric and two perpendicular magnetic fields, are usually measured.

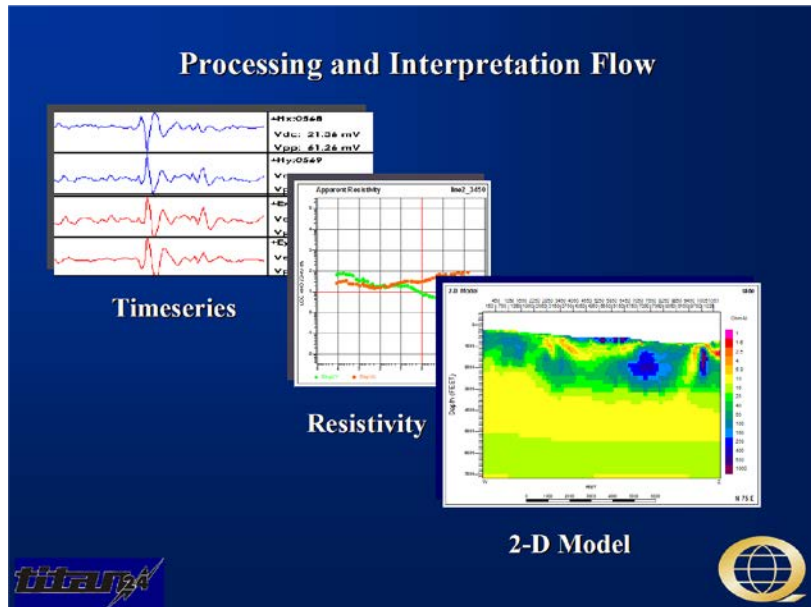
In the field surveys, the electric and magnetic fields are measured as a function of time. The electric field is measured using two orthogonal grounded dipoles. The magnetic field is also measured using induction coils parallel to the electric dipoles.



J.3 DATA PROCESSING

Extracting the subsurface resistivity structure from the measured magnetic and electric fields is a multi-step process. First, time series are transformed into frequency domain and sophisticated processing techniques are used to estimate the MT impedance tensor from the electric and magnetic fields. The impedance tensor is then used to calculate the apparent resistivity and phase data. In interpretation stage, inversion techniques are used to invert the apparent resistivity and phase data in to the subsurface true resistivity image. Finally, the resistivity image must be interpreted in terms of geologic units.

In time series processing, the measured magnetic and electric fields are Fourier transformed into the frequency domain. Calibration curves are applied to the measured fields to remove the acquisition system response. The Fourier coefficients represent the amplitude and phase of the electric and magnetic fields as a function of frequency.



A variety of complex signal processing techniques are used to minimize noise and bias in the estimation of geophysical parameters from the measured fields. The approaches include:

- Spatial isolation of noise. A remote reference magnetic station is used to separate signal from local noise in the magnetic field data;
- Coherency sieves to find coherent signal. First the local and remote magnetic field measurements are compared and coherent signal are kept. Then the local magnetic and electric fields are compared for coherency;
- Frequency isolation of noise. Long Fourier transforms are used to provide extremely sharp isolation of noise in frequency;
- Time isolation of noise. Short Fourier transforms are used to remove noise that is isolated in time (noise spikes, or noise that is randomly turning off and on);
- Robust statistics that minimize biasing effects of a few isolated measurements.

The geophysical parameters are estimated after the processing is completed. In frequency domain, the ratio between the two measured components (E and H) is called electrical impedance (Z) and is defined as $|Z| = |E/H|$. The primary geophysical parameters are usually represented as plots of the apparent resistivity versus frequency and the phase versus frequency. The impedance values are used to calculate apparent resistivity and phase data as follows:

$$\rho_a(\Omega m) = \frac{1}{\mu\omega} |Z|^2 \quad \text{and} \quad \varphi = \arg(Z)$$

The apparent resistivity is a function of the frequency. The apparent resistivity can be considered as a volumetric weighted average of the resistivity and thickness of the rocks being sampled. Consequently, it is a smoothly varying function of the frequency. It can be shown theoretically that on a log-log plot of the apparent resistivity vs. frequency the curve cannot exceed a slope of +/- 45 degrees for a layered earth model. For a homogenous half-space or a one-dimensional (1D) earth the phase is related to the apparent resistivity through the Hilbert transform. This association does not exist for the 2D and the 3D earth models.

J.4 INTERPRETATION

Plots of apparent resistivity and phase data versus frequency in a log-log scale are a conventional way of looking at the data before interpretation. If the survey involves several MT sites located along a line pseudo-sections of the apparent resistivities and phases in both components provides a first impression of the resistivity variation of the subsurface along the survey line.

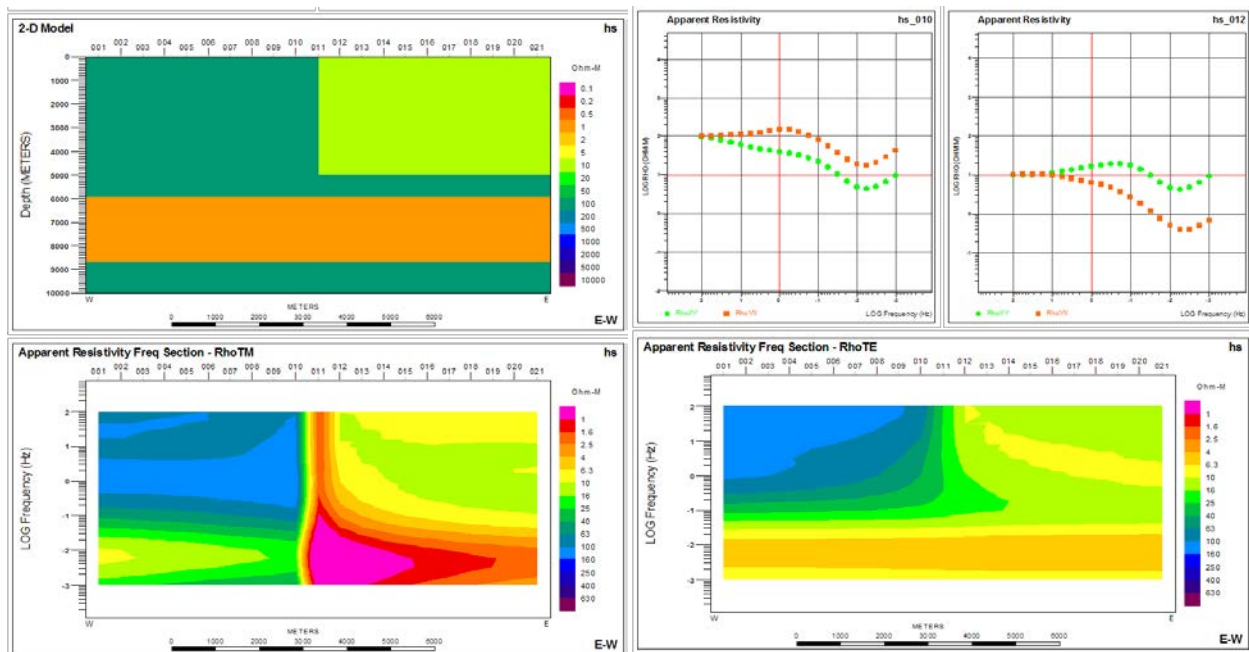
The depth of penetration of the EM signal depends on the frequency of the data and the resistivity of the subsurface. The depth at which the signal amplitude attenuates to 37% (1/e) of its initial value is called the electromagnetic skin depth (δ) and is defined as:

$$\delta(m) = \sqrt{\frac{2}{\mu\omega\sigma}} = 503 \left(\sqrt{\frac{\rho}{f}} \right)$$

where δ (m) is the skin depth, μ the magnetic permeability, σ (S/m) the conductivity (1/resistivity), ω the angular frequency ($=2\pi f$), f (Hz) the frequency, and ρ (Ωm) the resistivity (1/conductivity)

The skin depth concept provides an estimation of the maximum depth of investigation of the MT data.

The following plots illustrate example of the apparent resistivity curves for two MT sites as well as the apparent resistivity cross-sections along a MT line over a simple geological model.



Interpretation of the MT data is performed using the maps of true resistivity of the subsurface. Inversion algorithms in one-dimension (1D), two-dimension (2D), and three-dimension (3D) are used to invert the apparent resistivity and phase data in to the maps of true resistivity of the subsurface. A simple layered subsurface structure generally can adequately be reproduced using the 1D inversion. In the case of more complex 2D or 3D structures, the MT response will be affected by lateral variations in resistivity. Consequently, a 2D or 3D inversion algorithm is required to allow the lateral resistivity variations.

In 1D earth assumption, off-diagonal elements of the impedance tensor are equal and of opposite signs and the diagonal elements are zero. The 1D inversion of the MT data produces a resistivity-depth profile

for each MT site. The results represent a first order approximation of the resistivity variations with depth using a layered-earth model.

If there are lateral variations in the resistivity of the subsurface along one direction only (perpendicular to the strike) then a 2D inversion and interpretation is required. In this case, for a data rotated to the strike direction, off-diagonal elements of the impedance tensor are of opposite signs but not equal and the diagonal elements are zero. Because the electrical conductivity is constant along the strike direction (for example x-direction) all derivatives with respect to x will be zero. Therefore, Maxwell's equations are simplified and can be separated into two distinct modes so-called Transverse Electric (TE) and Transverse Magnetic (TM). The TE-mode represents the condition where the electric field is parallel to the strike direction while the TM-mode represents the condition where the magnetic field is parallel to the strike direction.

A cross-section of the true resistivity variations perpendicular to the assumed strike direction is created in the 2D inversion and is used in interpretation. For more complex geological structures a 3D inversion is essential to adequately describe the resistivity variation of the subsurface. In this case, none of the elements in the impedance tensor are equal or zero.

One of the factors that can affect the multi-dimensional MT data and interpretation is "static shift". The apparent resistivity curves can be biased (shifted up or down) by lateral resistivity contrasts with dimensions smaller than the minimum wavelength of the EM fields. These small features cannot be resolved by the MT data and they introduce a DC shift on the log-log apparent resistivity plots. This effect can be recognized by examining the sounding resistivity curves from the neighbouring MT sites and must be treated before the interpretation. Note that there are no static shift effects in the phase data.

K REFERENCES

A.1 TITAN-24 METHOD AND APPLICATION

- Donohue, J.G., and Sheard, S.N., 2001. Geophysics in North West Queensland – Improving the use of electrical geophysics. AIG Journal Paper 2001-01.
- Garner, S., and Webb, D., 2000. Broadband MT and IP electrical property mapping with MIMDAS. SEG Technical Program Expanded Abstracts, 1085-1088.
- Goldie, M., 2007. A comparison between conventional and distributed acquisition induced polarization surveys for gold exploration in Nevada. *The Leading Edge*, 26 (2), 180-183.
- Hollyer, G, and Hearst, R., 2009. Deep exploration technologies for discovery in the shadow of head frames. *First Break*, 27 (July), 99-105.
- Kingman, J., and Garner, S., 2003. Benefits of large channel capacity systems in electrical geophysics. ASEG 16th Geophysical Conference and Exhibition, Adelaide.
- Legault, J., Carriere, D., and Petrie, L., 2008. Synthetic model testing and distributed acquisition dc resistivity results over an unconformity uranium target from the Athabasca Basin, northern Saskatchewan. *The Leading Edge*, 27 (1), 46-51.
- Sheard, N., 1998. MIMDAS: A new direction in geophysics. Proceedings of the ASEG 13th International Conference, Hobart, Tasmania.
- White, M., and Gordon, R., 2003. Deep imaging: New technology lowers cost of discovery. *Canadian Mining Journal*, April, 27-28.

K.1 MAGNETOTELLURIC (MT) METHOD

- Bahr, K., and Simpson, F., 2005, *Practical Magnetotellurics*, Cambridge University Press.
- Berdichevsky, M.N., Dmitriev, V.I., Pozdnjakova, E.E., 1998. On two-dimensional interpretation of magnetotelluric soundings. *Geophys. J. Int.* 133, 585–606.
- Constable, S.C., Parker, R.L., and Constable, C.G., 1987. Occam’s inversion - A practical algorithm for generating smooth models from electromagnetic sounding data. *Geophysics*, 52 (3), 289-300.
- de Lugao, P.P., and Wannamaker, P.E., 1996. Calculating the two-dimensional magnetotelluric Jacobian in finite elements using reciprocity. *Geophysical Journal International*, 127, 806-810.
- Marquardt, D.W., 1963. An algorithm for least-squares estimation of non-linear parameters. *J. Sot. Ind. Appl. Math.*, 11, 431–441.
- Nabighian, M.N., 1987. *Electromagnetic Methods in Applied Geophysics, Volume 2: Application (Parts A and B)*. Society of Exploration Geophysicists (SEG), Tulsa.
- Orange, A.S., 1989. Magnetotelluric exploration for hydrocarbons. *Proceedings of the IEEE*, 77, 287-317.
- Rodi, W., and Mackie, R.L., 2001. Nonlinear conjugate gradients algorithm for 2D magnetotelluric inversions. *Geophysics*, 66, 174-187.
- Siripunvaraporn, W., Egbert, G., Lenbury, Y., and Uyeshima, M., 2005. Three-Dimensional Magnetotelluric: Data Space Method. *Physics of the Earth and Planetary Interiors*, 150, 3-14.

Vozoff, K., 1972. The Magnetotelluric method in the Exploration of Sedimentary basins. *Geophysics*, 37, 98-141.

Wannamaker, P., Hohmann, G., Ward, S., 1984. Magnetotelluric response of three-dimensional bodies in layered earth. *Geophysics* 49, 1517–1534.

Wannamaker, P.E., Stodt, J.A., and Rijo, L., 1987. A stable finite-element solution for two-dimensional magnetotelluric modeling. *Geophysical Journal of the Royal Astronomical Society*, 88, 277-296.

Wight, D.E., 1987. MT/EMAP Data Interchange Standard, Revision 1.0. Society of Exploration Geophysicists (SEG). (Document available at the SEG web site: www.seg.org).

K.2 GEOLOGY AND TECHNICAL REPORTS

Easton, R.M., Josey, S.D., Murphy, E.I. and James, R.S. 2011. Geological compilation, East Bull Lake and Agnew intrusions; Ontario Geological Survey, Preliminary Map P.3596, scale 1:50 000.

Dyer, R.D. 2008. East Bull Lake Intrusion Copper-Nickel-Platinum Group Element Dispersion Case Study, Northeastern Ontario; *in* Summary of Field Work and Other Activities 2008, Ontario Geological Survey, Open File Report 6226, p.27-1 to 27-7.

SUMMARY TABLE

SUMMARY TABLE	
CLIENT	
Client / Company Name	Mustang Minerals Corp.
Client Main Location	(Ontario, Canada)
Client Representative	David B. Stevenson
Phone Number	(416) 955 4773
Fax Number	(416) 955 4771
Email Contact (if available)	dbs@mustangminerals.com
PROJECT	
Project Grid Name	East Bull Lake Project
Project Grid Location	(Ontario, Canada)
Survey Type	Titan-24 MT
Survey Period (YY/MM/DD to YY/MM/DD)	2012/02/23 to 2012/03/01
Quantec Project Number	CA00927T
Geophysicist(s) in charge	<u>Data QAQC:</u> Mojtaba Daneshvar Nilu <u>Inversion & Interpretation:</u> Benoît Tournerie
REPORT	
Signed by	Benoît Tournerie, DSc, PGeo
Report Date	03/04/2012